

Comenius University in Bratislava
Faculty of Mathematics, Physics and Informatics



Approaches of near stars to the Sun

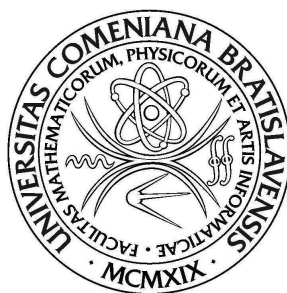
Master Thesis

Bratislava 2011

Bc. Jorge Luis Cayao Díaz

Comenius University in Bratislava
Faculty of Mathematics, Physics and Informatics

Reference number: 5a178088-2127-4be8-90ad-c41906d8c9ed



Approaches of near stars to the Sun

Master Thesis

Department of Astronomy, Physics of the Earth and Meteorology

Branch of study: Physics

Study programme: 4.1.7 Astronomy and 4.1.8 Astrophysics

Thesis Supervisor: Doc. RNDr. Jozef Klačka, PhD.

Bratislava 2011

Bc. Jorge Luis Cayao Díaz



Univerzita Komenského v Bratislave
Fakulta matematiky, fyziky a informatiky

ZADANIE ZÁVEREČNEJ PRÁCE

Meno a priezvisko študenta: Bc. Jorge Luis Cayao Díaz
Študijný program: astronómia a astrofyzika (Jednoodborové štúdium, magisterský II. st., denná forma)
Študijný odbor: 4.1.1. fyzika
Typ záverečnej práce: diplomová
Jazyk záverečnej práce: anglický
Sekundárny jazyk: slovenský

Názov : Approaches of Near Stars to the Sun

Cieľ : Calculate perihelion distances of close stars.

Vedúci : doc. RNDr. Jozef Klačka, PhD.

Spôsob sprístupnenia elektronickej verzie práce:
dočasne neprístupná, po uplynutí bez obmedzenia

Dátum zadania: 26.10.2009

Dátum schválenia: 20.10.2010

prof. RNDr. Branislav Sitár, DrSc.
garant študijného programu

.....
študent

.....
vedúci práce

Dátum potvrdenia finálnej verzie práce, súhlas s jej odovzdaním (vrátane spôsobu sprístupnenia)

.....
vedúci práce

Approaches of near stars to the Sun

by

Jorge Luis Cayao Díaz

Submitted to the Department of Astronomy, Physics of the Earth and
Meteorology

in partial fulfillment of the requirements for the degree of

Master in Physics, Specialization: Astronomy and Astrophysics

at the

COMENIUS UNIVERSITY IN BRATISLAVA
FACULTY OF MATHEMATICS, PHYSICS AND INFORMATICS

June 2011

© Jorge Luis Cayao Díaz, MMXI. All rights reserved.

The author hereby grants to UNIBA-FMFI permission to reproduce
and to distribute copies of this thesis document in whole or in part.

Author
Department of Astronomy, Physics of the Earth and Meteorology
May 6, 2011

Certified by
Jozef Klačka
Assoc. Professor of Physics
Department of Astronomy, Physics of the Earth and Meteorology
Thesis Supervisor

I declare that the submitted work is my own under the careful supervision of my adviser and that I have not used any other than permitted reference sources or materials nor engaged in any plagiarism. All references and other sources used by me have been appropriately acknowledged in the work.

Jorge Luis Cayao Díaz

Approaches of near stars to the Sun

by

Jorge Luis Cayao Díaz

Submitted to the Department of Astronomy, Physics of the Earth and Meteorology
on May 6, 2011, in partial fulfillment of the
requirements for the degree of
Master in Physics, Specialization: Astronomy and Astrophysics

Abstract

In this thesis, we investigate aspects of computing the perihelion distances and impact parameters for near stars to the Sun, and, we analyze the solar motion. The perihelion distances and impact parameters are studied for three different analytical approaches. First, we focus on the non-interacting system based on the object's motion with respect to the Sun along a straight line. We show that this approach gives results which are in agreement with those published in the literature [2] for Barnard's, Gl 217.1, Gl 729 and GJ 2046 stars. Second, we consider the two-body problem. As we expected, in this case we obtain less perihelion distances than for the non-interacting system. Third, we propose a simple model to describe the relative motion Sun-object, where in addition to the gravitational effects of the Galaxy, we consider oscillations (including anharmonic) of the Sun and the object with respect to the galactic equatorial plane. Equation of motion for these anharmonic oscillations is solved analytically. We show that some computed perihelion distances in this case are greater (totally different) than those given in literature, what is possible since anharmonic oscillations are not considered in the literature [2, 18]. However, for stars Gl 729, Gl 54.1 and LP 816-60 this simple model gives reasonable values in comparison with the literature. Finally, we focus on the solar motion (motion of the Sun with respect to the Local Standard of Rest), where the reference frame is given by the nearest stars. We develop a new method for determining the solar motion taking into account also stellar proper motions and radial velocities. The results are compared with other solutions given by approximation methods, where some of the observational parameters are neglected. The direct method is the best method in determining the solar motion. However, the motion of the Sun with respect to the surrounding interstellar gas and dust yields significantly different values for the solar motion. The only consistency between the results of stars and the interstellar gas and dust is the value of solar motion velocity component normal to the galactic equatorial plane Z_S . Relevance of the solar motion, in direction perpendicular to the Galactic equator, for evolution of the orbits of the comets of the Oort cloud, and, in directions lying in the Galactic equator, for the values of the Oort constants and the shape of the rotation curve and the essence of the dark matter is pointed out.

Keywords: perihelion distance, impact parameter, Oort cloud, solar motion

Thesis Supervisor: Jozef Klačka

Title: Assoc. Professor of Physics

Department of Astronomy, Physics of the Earth and Meteorology

Priblíženia blízkyh hviezd k Slnku

Jorge Luis Cayao Díaz

Odovzdané na Katedru astronómie, fyziky Zeme a meteorológie
6. mája 2011, v čiastočnom splnení
požiadavok na získanie titulu
Magister v odbore Fyzika, špecializácia: Astronómia a astrofyzika

Abstrakt

V tejto práci sme skúmali metódy na počítanie perihéliových vzdialeností a zámerné vzdialenosti pre vybrané blízke hviezdy a analyzovali sme pohyb Slnka. Perihéliové vzdialenosti azámerné vzdialenosti sme skúmali analyticky ztroch rôznych pohľadov. V prvom sme sa sústredili na neinterakčný systém založený na pohybe objektu po priamke určenej počiatočnou polohou a rýchlosťou hviezdy vzhľadom na Slnko. Výsledky, ktoré sme dosiahli, boli v súlade s literatúrou [2] pre Barnardovu hviezdu a pre hviezdy Gl 217.1, Gl 729 a GJ 2046. V druhom prípade sme sa sústredili na problém dvoch telies, keď sa uvažovala gravitčná interakcia medzi hviezdou a Slnkom. V tomto prípade, ako sme očakávali, sme dosiahli menšie perihélné vzdialenosti ako pre neinterakčný systém. V treťom spôsobe sme navrhli jednoduchý model popisujúci relatívny pohyb hviezdy vzhľadom na Slnko, kde sme uvažovali gravitačné efekty Galaxie vo forme oscilácie Slnka a hviezdy vzhľadom na galaktický rovník a aj anharmonické oscilácie v tomto smere. Pohybová rovnica týchto anharmonických oscilácií sa tiež rieši analyticky. Ukázali sme, že v tomto prípade sú niektoré vypočítané perihéliové vzdialenosti väčšie (úplne odlišné) od tých uvádzaných v literatúre. Toto môže byť spôsobené neuvažovaním (anharmonických) oscilácií vich použitých metódach [2, 18]. Napriek tomu, pre hviezdy Gl 729, Gl 54.1 and LP 816-60 tento jednoduchý model nám dáva rozumné hodnoty v porovnaní s literatúrou. Nakoniec sme sa sústredili na pohyb Slnka (pohyb vzhľadom na miestny štandard pokoja), kde sme za náš referenčný systém zvolili najbližšie hviezdy. Vyvinuli sme novú metódu na určovanie pohybu Slnka, kde sme uvažovali aj vlastné pohyby hviezd a radiálne rýchlosti. Výsledky sme porovnávali sostatnými riešeniami získanými z aproximáčnych metód, pri ktorých boli niektoré z pozorovaných parametrov zanedbané. Z výsledkov nám vyplynulo, že priama metóda je najlepšia pri určovaní pohybu Slnka. Avšak, pohyb Slnka, ak berieme do úvahy okolitý medzihviezdny plyn aprach, dáva signifikantne odlišné hodnoty pre solárny pohyb. Jediná spojitost medzi výsledkom pre hviezdy amedzihviezdny plyn aprach je hodnota rýchlosti solárneho pohybu vsmere normály na galaktickú rovníkovú rovinu Z_S . Dôležitosť pohybu Slnka, v smere kolmom na Galaktický rovník sa zdôrazuje hlavne pri evolúcii orbít komét Oort-ovho oblaku. Zistenie solárneho pohybu, v smere rovnobežnom s galaktickým rovníkom je dôležité pre zistenie hodnôt Oortových konštánt, tvaru rotačnej krivky a podstaty tmavej hmoty.

Kľúčové slová: perihéliová vzdialenosť, impakt parameter – zámerná vzdialenosť, Oortov oblak, pohyb Slnka

Školiteľ: Jozef Klačka

Titul: Docent fyziky, Katedra astronómie, fyziky Zeme a meteorológie

Aproximaciones de estrellas cercanas al Sol

Jorge Luis Cayao Díaz

Entregado al departamento de Astronomía, Física de la tierra y Meteorología el
6 de Mayo de 2011, en cumplimiento parcial de los
requerimientos para obtener el título de
Master en Física, Especialidad: Astronomía y Astrofísica

Resumen

En esta tesis se investigan aspectos del cálculo de las distancias del perihelio y los parámetros de impacto para estrellas cercanas, y, se analiza el movimiento solar. Las distancias del perihelio y los parámetros de impacto se estudian siguiendo tres enfoques diferentes. En primer lugar, nos centramos en un sistema sin interacción basado en el movimiento del objeto con respecto al Sol a lo largo de una línea recta. Se demuestra que este método da resultados de acuerdo con [2] para las estrellas Barnard, Gl 217.1, Gl 729 y GJ 2046. En segundo lugar, consideramos el problema de los dos cuerpos. Como era de esperar, en este caso se obtienen distancias más cortas que para el sistema sin interacción. En tercer lugar, proponemos un modelo simple para describir el movimiento relativo Sol-objeto, donde en adición a los efectos gravitacionales de la Galaxia, consideramos oscilaciones (incluyendo anarmónicas) del Sol y del Objeto con respecto al plano galáctico ecuatorial. La ecuación de movimiento de estas oscilaciones anarmónicas se resuelve analíticamente. Se demuestra, que algunas distancias calculadas en este caso son mayores (totalmente diferentes) a las que figuran en la literatura, lo que es posible, ya que oscilaciones anarmónicas no se consideran en la literatura [2, 18]. Sin embargo, para Gl 729, Gl 54.1 y LP 816-60 este modelo da valores razonables en comparación con [2, 18]. Por último, nos centramos en el movimiento solar (movimiento del Sol con respecto al Lugar de reposo estándar), donde se toma como marco de referencia las estrellas más cercanas. Se desarrolla un nuevo método para la determinación del solar movimiento teniendo en cuenta también los movimientos propios estelares y velocidades radiales. Los resultados se comparan con otras soluciones dadas por métodos de aproximación, cuando algunos de los parámetros de observación no se toman en cuenta. El método directo es el mejor método para determinar el movimiento solar. Sin embargo, el movimiento del Sol con respecto al gas y polvo interestelar circundante da valores significativamente diferentes para el movimiento solar. La consistencia sólo entre los resultados de las estrellas y el gas y el polvo interestelar es el valor de la componente de la velocidad de movimiento solar normal al plano ecuatorial galáctico Z_S . Se indica la relevancia del movimiento solar en dirección perpendicular al ecuador galáctico para la evolución de las órbitas de cometas de la nube de Oort, y en direcciones situadas en el ecuador galáctico para los valores de las constantes de Oort, la forma de la curva de rotación y la esencia de la materia oscura.

Palabras clave: Distancia del perihelio, parámetro de impacto, nube de Oort, movimiento solar.

Supervisor de tesis: Jozef Klačka, Profesor Asociado de física, Departamento de Astronomía, Física de la Tierra y Meteorología

Acknowledgments

I gratefully acknowledge financial support from the National Scholarship Programme of the Slovak Republic. I was not alone on my journey to finishing this Master thesis. First, my thanks go to my parents gave me their love, support and freedom. Second, I would like to express my gratitude to Doc. Jozef Klačka Ph.D. for his invaluable help and support. Without his continual assistance this work would not get much farther than to this page.

Contents

0	Introduction	16
0.1	Outline and Summary of Results	18
1	The impact parameter and the perihelion position vector	20
2	Non-interacting system	22
3	The two-body problem	24
3.1	Impact parameter	25
3.2	Trajectory	27
4	Galactic tide	35
4.1	Model of Galaxy	35
4.1.1	Motion in Galaxy near to the galactic equator	36
4.1.2	Solar oscillations along the z -axis	39
4.2	Simple model	43
4.2.1	Star's oscillation along the z -axis	44
4.2.2	Initial conditions for the motion along the z -axis ($u = 0$)	45
4.2.3	Initial conditions for the object's motion along x , y and z direc- tions ($u \neq 0$)	47
4.2.4	The perihelion position vector	52
4.3	The Equatorial and galactic Coordinates	54
4.3.1	The conversion from (α, δ) to (l, b)	56
4.3.2	Proper motions	56
5	Summary of main equations	58
5.1	Observational data	58

5.2	Non-interacting system	59
5.3	The two-body problem	60
5.3.1	Choosing the right angle	61
5.4	Galactic tide	62
6	Applications	66
6.1	Non-interacting calculations	68
6.2	Two-body calculations	69
6.3	Simple model	70
7	The solar motion	72
7.1	The solar motion	72
7.1.1	Determining \mathbf{V}_S by direct calculation	73
7.1.2	Determining \mathbf{V}_S by Least square method	74
7.2	Results	78
7.2.1	For $r_i < 100 \text{ pc}$	78
7.2.2	For $r_i < 40 \text{ pc}$	79
7.2.3	For $r_i < 15 \text{ pc}$	79
7.2.4	The solution of Eqs. (7.7) for different distances	80
7.3	Application	81
7.3.1	The solar oscillation – simple access	82
7.3.2	The solar oscillation – improved access	82
7.3.3	The Oort constants	83
7.3.4	Oort cloud of comets	85
7.4	Discussion	86
7.4.1	More on the Least square method	88
7.4.2	More on the real motion of the Sun	90
8	Zhrnutie diplomovej práce	93
8.1	Systém bez interakcie	93
8.2	Problém dvoch telies	93
8.3	Galaktické slapy	94
8.3.1	Oscilácie Slnka a hviezdy	94
8.3.2	Jednoduchý model	94

8.4	Pohyb Slnka	94
A	Equations deduced from the Least square method	96

List of Figures

3-1	Path of the studied object in the field of the Sun.	25
3-2	Geometric representation of the object's momentum.	26
7-1	The relation between the velocity components of the solar motion and radius of the solar neighborhood.	81
7-2	Evolution of eccentricity under the action of gravity of the Sun and Galaxy. The model by [19] is used. Two values of Z_S are used: the dotted line holds for $Z_S = 6.14 \text{ km/s}$, the solid line holds for $Z_S = 7.70 \text{ km/s}$	86
7-3	Evolution of eccentricity under the action of gravity of the Sun and Galaxy. The model by Klačka (2009) is used. Two values of Z_S are used: the dotted line holds for $Z_S = 6.14 \text{ km/s}$, the solid line holds for $Z_S = 7.70 \text{ km/s}$	92

List of Tables

3.1	Choosing the right angle.	33
5.1	Choosing the right angle	62
6.1	Computed perihelion distances by Dybczyński ($ \mathbf{q} $)[2]	66
6.2	Parameters of some nearest stars studied in this thesis.	67
6.3	Computed galactic coordinates	67
6.4	Computed impact parameters and perihelion position vectors for the non-interacting system	68
6.5	Computed impact parameters and perihelion distances for the non-interacting system in parsecs, respectively. r_0 represents the initial distance of the object with respect to the Sun.	68
6.6	Computed impact parameters, perihelion position vectors and dispersion angles for the two-body system	69
6.7	Computed impact parameters, perihelion distances (in parsecs) and dispersion angles for the two-body system	70
6.8	Computed perihelion distances (in parsecs) for our proposed simple model ($u = 0$)	70
6.9	Computed perihelion distances (in parsecs) for our proposed simple model ($u \neq 0$)	71
7.1	The solar motion in the galactic coordinates for our sample of stars with $r_i < 100$ pc calculated using the direct method (Eqs. (7.7)) and the Least square method (Eqs. (A.2)-(A.6)).	78
7.2	The solar motion in the galactic coordinates for our set of stars with $r_i < 40$ pc calculated using the direct method (Eqs. (7.7)) and the Least square method (Eqs. (A.2)-(A.6)).	79

7.3	The solar motion in the galactic coordinates for our set of stars with $r_i < 15 \text{ pc}$ calculated using the direct method (Eqs. (7.7)) and the Least square method (Eqs. (A.2)-(A.6)).	79
7.4	The solar motion calculated by direct method (Eqs. (7.7)) for different distances. Velocity components are given in galactic coordinates.	80
7.5	Amplitude z_{max} and periods of the solar oscillations with the initial position $z(t = 0) = 30 \text{ pc}$. Various initial velocities Z_S and constant mass density are used.	82
7.6	Amplitude z_{max} and periods of the solar oscillations with the initial position $z(t = 0) = 30 \text{ pc}$. Various initial velocities Z_S are used. Mass density as a function of z is considered.	83
7.7	The solar motion. SM1 corresponds to the standard motion presented by [8, 4]. SM2 corresponds to the basic motion presented by [8]. SM3 is presented by [29]. SM4 is presented by [17] and [1].	88
7.8	Velocity components of the Sun with respect to the surrounding interstellar gas and dust. Two values of the speed V_S are considered. The components are measured in galactic coordinates.	91

Chapter 0

Introduction

The outer part of the Solar System, known as the Oort cloud of comets, is under gravitational influence of both the Sun and the Galaxy. The effect of the Sun is described by the two-body problem. The effect of the Galaxy is equivalent to galactic tide and the physical model is given by Klacka (2009) [19]. However, besides the regular permanent action of the gravity of the Sun and the Galaxy, also random perturbations can play non-negligible role in the orbital evolution of the comets in the Oort cloud. These irregular random perturbations are also of gravitational origin. They are generated by *close* approaches of stars and interstellar clouds (consisting of gas and dust) to the Sun, or, more correctly, to the comets of the Oort cloud [14]. This Master Thesis deals with the problem of the *close* approach of a galactic object to the Sun. Hence, we want to find the minimal distance between the object and the Sun, i.e., the perihelion distance of the object. More generally, position vector of the perihelion. This Thesis presents several approaches to the problem of finding the perihelion distance of a galactic object. These approaches treat the problem from an analytical point of view. The first case assumes no interaction between the Sun and the Galactic object. The second case considers the two-body problem, i.e., gravitational interaction between the Sun and the object is taken into account. The third analytical approach considers oscillation of the Sun and the object with respect to the galactic equatorial plane. All three cases are treated in an analytical way and the obtained results for several stars are summarized in tables. By solving the equation of general motion given in Chapter 4, where gravity of the Sun and Galaxy are considered, our results may be improved.

These results are compared with those published in the literature. Since the oscilla-

tory motion of the Sun with respect to the galactic equatorial plane plays an important role in the evolution of the Oort cloud of comets, Chapter 7 of this thesis deals with the solar motion. The kinematics of stars near to the Sun has long been known to provide crucial information regarding both the structure and evolution of the Milky Way [29]. That is the reason why we calculate the solar motion in the reference frame connected with the nearest stars. We identify series of N stars with heliocentric distances less than 100, 40, 15 pc and then determine the velocity of the Sun relative to the mean velocity of these stars.

0.1 Outline and Summary of Results

We study approaches of near stars, objects, to the Sun. General motivation for this problem is its application to the evolution of the Oort cloud of comets situated at the borders of the Solar System. The object (a star or interstellar cloud of dust or gas) motion with respect to the Sun is calculated on the basis of gravitational forces acting both on the Sun and the comet. Effect of the Galaxy in the form of galactic tide is based on the observations. The flat rotation curve is considered together with the most probable values of the Oort constants. The effect of the galactic bulge is consistent with the mass distribution given by Maoz (2007) [7]. Moreover, motion of the Sun in the Galaxy is considered, too. We take into account not only the fact that the Sun revolves the center of the Galaxy, as it is conventionally done. We take into account also the oscillations of the Sun with respect to the galactic equatorial plane. This model is presented in Klačka (2009) [19]. Besides the fixed mass density used as an approximation to reality for the galactic bulge, we can take into account the decrease of the bulge mass density as a function of the distance from the galactic equatorial plane. The effect of this simple improvement will be treated. Great part of the Thesis will be devoted to the effect of close approaches of stars or interstellar clouds to the Solar System and to the study of the solar motion.

We will first calculate perihelion distance and impact parameter for a star with close approach to the Solar system. Better value of the perihelion will be found using the two-body problem (the star and the Sun). After the two-body consideration, we focus on the relative motion Sun-object in the field of the Galaxy (here, we consider that the Sun and star have a motion with respect to galactic equatorial plane), for which we propose a simple model for stars nearest to the Sun. How can these effects enhance the number of comets entering the inner part of the Solar System?

We also devote our reserach to analyze the solar motion.

We present the following steps of this thesis in the next six chapters. **Chapter 1: The impact parameter and the perihelion position vector** gives some definitions found in the literature for the impact parameter and for the perihelion position vector.

Chapter 2: The non-interacting system is based on the motion of an object (a star or an interstellar cloud which in reality perturb comets in the Oort cloud) which

does not interact with the Sun. Here, the object moves along a straight line in an inertial frame of reference (e.g., galactic)

Chapter 3: The two-body system analyzes the way to compute the path of an object (a star or an interstellar cloud) under the solar gravitation, and, finally the impact parameter and the position vector of the perihelion. It is a typical two-body problem.

Chapter 4: Galactic tide investigates the relative motion Sun-object, where in addition to the gravitational effects of the Galaxy, we consider anharmonic oscillations for the Sun and object. This simple model does not consider gravitational interaction between these two bodies, and it is based on the fact that the relative motion of the object with respect to the Sun depends linearly on time for x and y coordinates and takes into account anharmonic oscillations along the z -axis (for the Sun and for the Star, we suppose the same anharmonic motion). Equation of motion for this anharmonic motion is solved analytically.

Chapter 5: Summary of main equations summarizes the important equations found in previous Chapters. Chapter 6: Applications applies the results to compute the perihelion position vector and the impact parameter for stars, which are taken from the literature [2].

Chapter 7: The solar motion calculates the solar motion in the reference frame connected with the nearest stars. The reference frame is given by the nearest stars. We develop a new method for determining the solar motion taking account also stellar proper motions and radial velocities. The results are compared with other solutions given by approximation methods, where some of the observational parameters are neglected.

Finally, I summarize the thesis in Chapter ??, and discuss further research directions. Also, I summarize the thesis in Slovak in Chapter 8. Additional material can be found at the end of the thesis. Appendix A shows the equations deduced from the Least square method.

Chapter 1

The impact parameter and the perihelion position vector

We are interested in the nearest distance between an approaching star (or interstellar cloud consisting of dust and gas) and the Sun. This is given by the magnitude of the perihelion position vector.

The process of scattering is standardly described by the **impact parameter**. Let us present several definitions of the impact parameter:

1. “The distance of one of the scattering partners from the asymptote of the trajectory of the other scattering partner is the *impact parameter*.” [9, p. 189]
2. “The *impact parameter* b is defined as the perpendicular distance from the projectile’s incoming straight-line path to a parallel axis through the target’s center.” [27, p. 558].
3. Consider scattering of a projectile from a target particle. “The initial velocity of the projectile is \mathbf{v}_0 and it is assumed that in the absence of any interaction it would travel in a straight line and pass the target at a distance b , called the *impact parameter*.” [25, p. 362]

Thus, we can define the impact parameter b as the perpendicular distance between the straight-line of the initial velocity vector of an object (a star or an interstellar cloud) and the center of the field $U(r)$ created by the Sun that the object is approaching (see also [6, p. 35–66] and [26, p. 126–143]). **The perihelion** is the point in the solar orbit

of an object when it is nearest to the Sun. **The perihelion distance** is the distance between the object and the Sun at this point.

When a comet moves around the Sun, they interact and the motion of the comet is affected by the solar gravitation, by the galactic tide and other forces. Perturbations from near stars or interstellar clouds can be also important.

Chapter 2

Non-interacting system

In this Chapter we focus on the system where an object (a star or an interstellar cloud which in reality perturb comets in the Oort cloud) does not interact with the Sun. Here, the object moves along a straight line in an inertial frame of reference (e.g., galactic). The motion is given by the position vector \mathbf{r} in the inertial frame:

$$\mathbf{r} = \mathbf{r}_\odot + \mathbf{r}_0 + \mathbf{v}_0 t \quad \Rightarrow \quad \mathbf{r} - \mathbf{r}_\odot = \mathbf{r}_0 + \mathbf{v}_0 t, \quad (2.1)$$

where $\mathbf{r}_0 = (x_0, y_0, z_0)$ and $\mathbf{v}_0 = (v_{x,0}, v_{y,0}, v_{z,0})$ are the initial ($t = 0$) position and velocity vectors of the object with respect to the Sun, \mathbf{r}_\odot is the position vector of the Sun in the inertial frame of reference. To find the impact parameter we minimize the magnitude of the second equation in Eqs. (2.1)

$$b = \min_t |\mathbf{r} - \mathbf{r}_\odot| = \min_t |\mathbf{r}_0 + \mathbf{v}_0 t| \quad (2.2)$$

or

$$b = \min_t \sqrt{(x_0 + v_{x,0}t)^2 + (y_0 + v_{y,0}t)^2 + (z_0 + v_{z,0}t)^2}. \quad (2.3)$$

Minimizing the previous equation we find the condition

$$(x_0 + v_{x,0}t_b)v_{x,0} + (y_0 + v_{y,0}t_b)v_{y,0} + (z_0 + v_{z,0}t_b)v_{z,0} = 0,$$

from which

$$t_b = -\frac{x_0 v_{x,0} + y_0 v_{y,0} + z_0 v_{z,0}}{v_{x,0}^2 + v_{y,0}^2 + v_{z,0}^2} \quad (2.4)$$

Putting Eq. (2.4) into Eq. (2.3) we get

$$\begin{aligned}
b = \frac{1}{v_0^2} & \left\{ \left[x_0 (v_{y,0}^2 + v_{z,0}^2) - (y_0 v_{y,0} + z_0 v_{z,0}) v_{x,0} \right]^2 \right. \\
& + \left[y_0 (v_{x,0}^2 + v_{z,0}^2) - (x_0 v_{x,0} + z_0 v_{z,0}) v_{y,0} \right]^2 \\
& \left. + \left[z_0 (v_{x,0}^2 + v_{y,0}^2) - (x_0 v_{x,0} + y_0 v_{y,0}) v_{z,0} \right]^2 \right\}^{1/2}, \tag{2.5}
\end{aligned}$$

where $v_0^2 = v_{x,0}^2 + v_{y,0}^2 + v_{z,0}^2$.

Then, the vector of perihelion position is

$$\mathbf{q} = \mathbf{r}_b - \mathbf{r}_\odot = \mathbf{r}_0 + \mathbf{v}_0 t_b, \quad t_b = - \frac{x_0 v_{x,0} + y_0 v_{y,0} + z_0 v_{z,0}}{v_{x,0}^2 + v_{y,0}^2 + v_{z,0}^2}. \tag{2.6}$$

We treated non-interacting system. In this case the impact parameter fulfills the condition $b = |\mathbf{q}|$. The impact parameter equals to the perihelion distance.

Chapter 3

The two-body problem

The classical problem of celestial mechanics focus on the motion of one body with respect to another under the influence of their mutual gravitation [6, p. 34], [26, p. 184]. In its simplest form, this problem is little more than the generalization of the central force problem[26, p. 126], but in some cases the bodies are of finite size and are not spherical. This may complicate the problem enormously as the potential fields of the objects no longer vary as the inverse square of the distance. This causes orbits to precess and the objects themselves to undergo gyration motion [16, p. 71]. The masses need not be point masses - as long as they are spherically symmetric, they act gravitationally as if they were point masses [16, p. 71–80]. In this Chapter we compute the path of an object (a star or an interstellar cloud) under the solar gravitation, and, finally the impact parameter and the position vector of the perihelion. It is a typical two-body problem. Angular momentum is conserved. We show two ways how to find the impact parameter. For this, we use some important parameters as the reduced mass which we defined (as is given in the literature) in the form of $\mu = mM/(m + M)$ and the Universal Gravitational Constant G . The value of G is the same anywhere in the Universe, and it does not vary with time [13, 28]. Here, we adopt these assumptions, while noting that it is a legitimate cosmological question to consider what implications there may be if either of them is not so. G is among those fundamental constants whose numerical value has been determined with least precision. Its currently accepted value is $(6.67259 \pm 0.00085) \times 10^{-11} \text{ Nm}^2\text{kg}^{-2}$ [13, 28]. It is worth noting that, while the product GM for the Sun is known with very great precision, the mass of the Sun is not known to any higher degree of precision than that of the gravitational constant.

3.1 Impact parameter

Our problem is represented in Fig. 3-1. Conservation of the angular momentum yields

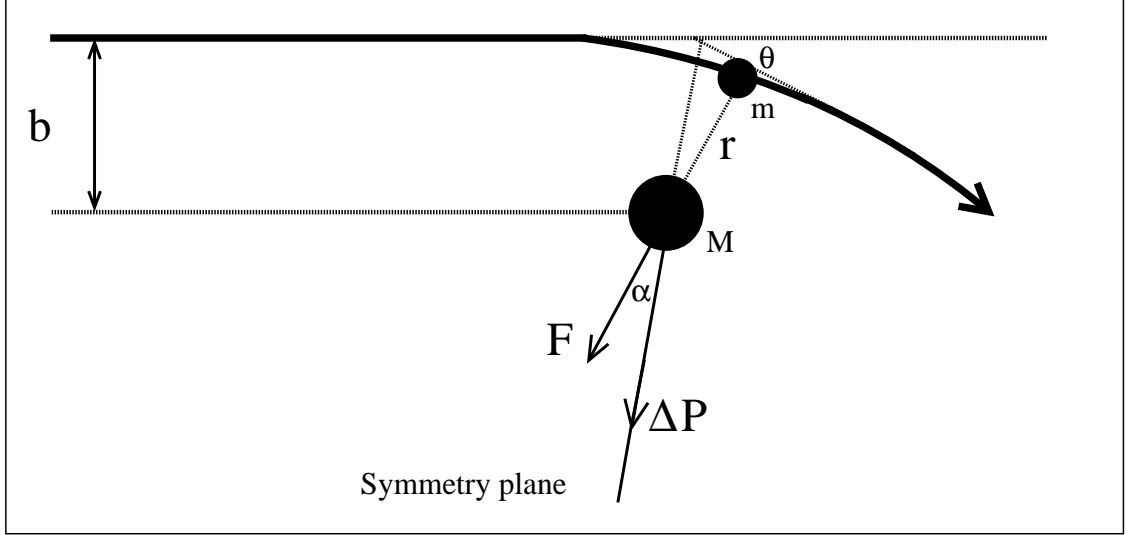


Figure 3-1: Path of the studied object in the field of the Sun.

$\mu v_{\infty} b = \mu r^2 \omega$ ($\omega = d\alpha/dt = v_{\infty} b/r^2$), where $v_{\infty} = |\mathbf{v}_{\infty}|$ is the magnitude of the velocity vector in the infinity \mathbf{v}_{∞} of the object with respect to the Sun, $v = |\mathbf{v}|$ is the magnitude of the velocity vector \mathbf{v} of the object with respect to the Sun at a given time t . We assume that the interaction between the object and the Sun can be neglected at the initial moment. Here, m is the mass of the object, \mathbf{r} is the object position vector at the time t , and, b is the impact parameter.

In accordance with a simple geometry, from Fig. 3-2, where $P = |\mathbf{P}_{out}| = |\mathbf{P}_{in}|$,

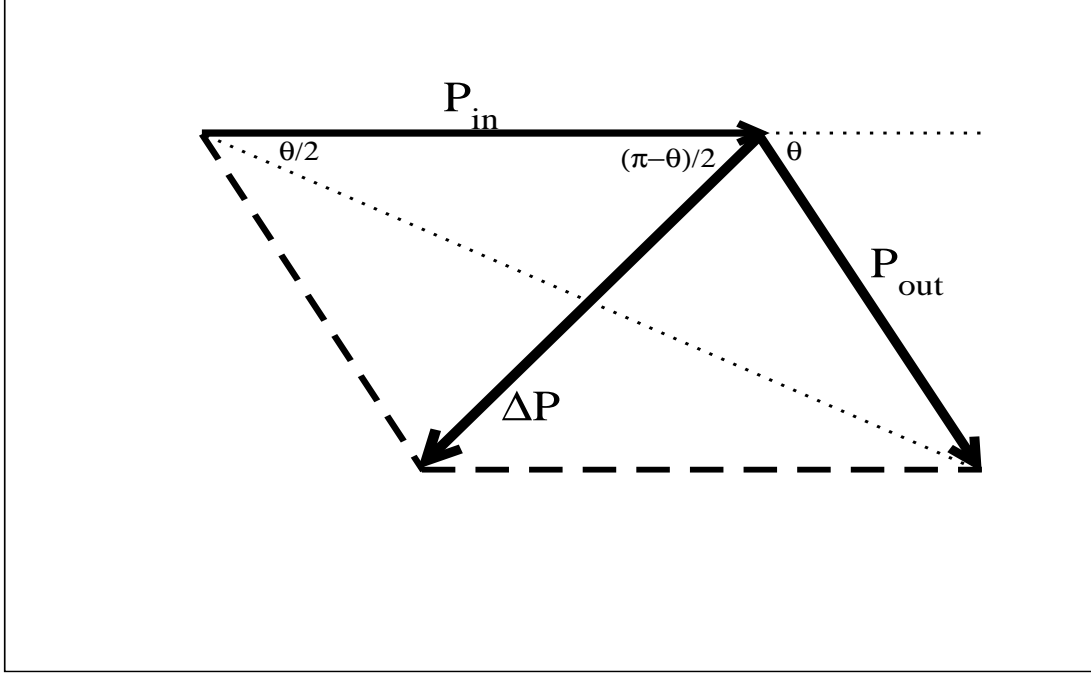


Figure 3-2: Geometric representation of the object's momentum.

we have $\Delta P = 2P \sin(\theta/2)$, and from the second Newton's law we get

$$\begin{aligned}
 \mathbf{F} &= \frac{d\mathbf{P}}{dt}, \\
 \Delta P &= \int F \cos \alpha \, dt \\
 &= \int \frac{GmM}{r^2} \cos \alpha \, dt = GmM \int \frac{\cos \alpha}{r^2} \frac{dt}{d\alpha} d\alpha \\
 &= GmM \int \frac{\cos \alpha}{r^2} \frac{r^2}{v_\infty b} d\alpha = \frac{GmM}{v_\infty b} \int_{-(\pi-\theta)/2}^{(\pi-\theta)/2} \cos \alpha \, d\alpha \\
 \Delta P &= \frac{GmM}{v_\infty b} 2 \cos(\theta/2), \tag{3.1}
 \end{aligned}$$

where $F \cos \alpha$ is the force projection onto $\Delta \mathbf{P}$. Doing an elementary comparison between the found relations for ΔP (from geometry and Newton's law) we find the impact parameter

$$b = \frac{GmM}{Pv_\infty} \cot(\theta/2), \tag{3.2}$$

since, in accordance with Fig. 2-2 and cosine theorem, $|\Delta \mathbf{P}|^2 = 2P^2(1 - \cos \theta)$, or

$$b = \frac{G(m+M)}{v_\infty^2} \cot(\theta/2), \tag{3.3}$$

since $P = \mu v_\infty$.

3.2 Trajectory

In this part, we study the motion of an object (e.g. a star) in a central field (solar gravitational field). We compute the impact parameter and the perihelion position vector. The mutual potential energy of two spherically symmetric distributed masses at a distance r apart, which is the work required to bring them to a distance r from an infinite initial separation, is

$$V(r) = \frac{k}{r} = -\frac{GMm}{r}.$$

$l = \mu v r \sin \varphi$ is the angular momentum. The position of m with respect to M , in polar coordinates, is given by

$$(x, y) = |\mathbf{r}|(\cos \varphi, \sin \varphi).$$

Notice that r and φ are time dependent. The kinetic energy is $T = \mu(\dot{r}^2 + r^2\dot{\varphi}^2)/2$. Therefore the Lagrangian in polar coordinates for this system is

$$L(r, \dot{r}, \varphi, \dot{\varphi}) = \frac{\mu}{2} (\dot{r}^2 + r^2\dot{\varphi}^2) - \frac{k}{r}, \quad (3.4)$$

from where the equations of motion are given by

$$\frac{d}{dt} \frac{\partial L}{\partial \dot{\varphi}} - \frac{\partial L}{\partial \varphi} = 0, \quad \frac{d}{dt} \frac{\partial L}{\partial \dot{r}} - \frac{\partial L}{\partial r} = 0. \quad (3.5)$$

If the Lagrangian does not contain a given coordinate, in this case φ , then the coordinate is said to be cyclic and the corresponding conjugate momentum is conserved. Such quantity is the angular momentum perpendicular to the plane of motion, i.e. $\mathbf{l} = \mathbf{r} \times \mathbf{p}$, then

$$l = \mu v r \sin \varphi = \mu v_0 b. \quad (3.6)$$

By using Eq. (3.5) we get

$$\frac{d}{dt} \frac{\partial L}{\partial \dot{\varphi}} = 0 \quad \Rightarrow \quad \frac{\partial L}{\partial \dot{\varphi}} = l \quad \Rightarrow \quad \dot{\varphi} = \frac{l}{\mu r^2}, \quad (3.7)$$

where l is a constant of motion; and for r :

$$\mu\ddot{r} - \frac{l}{\mu r^3} - \frac{k}{r^2} = 0. \quad (3.8)$$

The solution of the previous equation gives the orbit of a particle in a central field. To solve Eq. (3.8) we substitute $r = 1/u$. Applying the chain rule one can verify

$$\dot{r} = \dot{\varphi} \frac{dr}{du} \frac{du}{d\varphi} \Rightarrow \dot{r} = -\frac{l}{\mu} \frac{du}{d\varphi} \Rightarrow \ddot{r} = -\frac{l^2 u^2}{\mu^2} \frac{d^2 u}{d\varphi^2}. \quad (3.9)$$

Doing correct substitutions we find

$$\frac{d^2 u}{d\varphi^2} + u = -\frac{\mu k}{l^2}, \quad (3.10)$$

which is a nonhomogeneous second order linear equation. The solutions of this equation are of two types: along **unbound** orbits $r \rightarrow \infty$ and hence $u \rightarrow 0$, while on **bound** orbits r and u oscillate between finite limits. The general solution for this equation is

$$u(\varphi) = \alpha \sin \varphi + \beta \cos \varphi - \frac{\mu k}{l^2}, \quad (3.11)$$

where the constants α and β are given by the initial conditions. The initial incoming state (*in* state) is given (see Fig. 3-1 and polar coordinates of the object) by the condition $\varphi \rightarrow \pi$, $\dot{r} = -v_\infty$ (the minus sign represents the fact that the object comes from the left and approaches to the central field); the final outgoing state (*out* state) is given (see Fig. 3-1 and polar coordinates of the object) by the condition $\varphi \rightarrow 2\pi - \theta$, $r \rightarrow \infty$. Thus, *in* state yields

$$u(\varphi \rightarrow \pi) \rightarrow 0, \quad \beta \cos \pi - \frac{\mu k}{l^2} = 0 \Rightarrow \beta = -\mu k/l^2$$

Moreover, in accordance with (see Eq. (3.9))

$$\dot{r} = -\frac{l}{\mu} \frac{du}{d\varphi},$$

we obtain (for $\varphi \rightarrow \pi$), with $\dot{r} = -v_\infty$,

$$\alpha = -\frac{\mu v_\infty}{l} .$$

The *out* state yields

$$u(\varphi \rightarrow 2\pi - \theta) \rightarrow 0 , \quad -\alpha \sin \theta + \beta \cos \theta - \frac{\mu k}{l^2} = 0 ,$$

$$\frac{\mu v_0}{l} \sin \theta - \frac{\mu k}{l^2} \cos \theta - \frac{\mu k}{l^2} = 0 ,$$

therefore

$$\begin{aligned} 1 + \cos \theta &= \frac{v_\infty l}{k} \sin \theta , \\ &= \frac{v_\infty^2 \mu b}{GmM} \sin \theta , \\ &= \frac{v_\infty^2 b}{G(m+M)} \sin \theta . \end{aligned} \tag{3.12}$$

Then, for the impact parameter, we get

$$\begin{aligned} b &= \frac{G(M+m)}{v_\infty^2} \frac{1 + \cos \theta}{\sin \theta} , \\ &= \frac{G(m+M)}{v_\infty^2} \cot \left(\frac{\theta}{2} \right) . \end{aligned} \tag{3.13}$$

which is the same result as Eq. (3.3) found in the previous subsection. The velocity in the infinity v_∞ is found from conservation of energy in the infinity and in the time where are taken initial conditions, then the energy for initial conditions is given by

$$E_0 = \frac{\mu}{2} v_0^2 + \frac{k}{r_0} , \tag{3.14}$$

and in the infinity,

$$E_\infty = \frac{\mu}{2} v_\infty^2 . \tag{3.15}$$

Since the energy is conserved, $E_0 = E_\infty$, for the speed in the infinity we get

$$v_\infty = \sqrt{\frac{2}{\mu} \left(\frac{\mu}{2} v_0^2 + \frac{k}{r_0} \right)} . \quad (3.16)$$

From Eq. 3.3, or from Eq. 3.13, we cannot get b , cause we do not know neither b nor θ . For this reason it requires to use another equation. That equation is then given by the conservation of angular momentum, $\mu v_\infty b = \mu |\mathbf{r}_0 \times \mathbf{v}_0|$, from where we get

$$b = \frac{|\mathbf{r}_0 \times \mathbf{v}_0|}{v_\infty} , \quad (3.17)$$

where we assume that the velocity vector in the infinity is perpendicular to the impact parameter, then $|\mathbf{e}_r \times \mathbf{e}_t|_\infty = 1$. Hence, from previous equation we find b , and replacing in Eq. 3.3, or in Eq. 3.13 we are able to find the dispersion angle φ .

We write Eq. (3.11) in a better and more familiar form, or, we just seek for a general solution to Eq. (3.10) in the form of $u(\varphi) = D \cos(\varphi - \varphi_0) - \mu k / l^2$, where $D = \sqrt{\alpha^2 + \beta^2}$, $\cos \varphi_0 = \alpha / D$, and $\sin \varphi_0 = -\beta / D$. φ_0 can be computed by using Tab. 3.1 given below. Therefore,

$$r(\varphi) = \frac{p}{1 + \epsilon \cos(\varphi - \varphi_0)} , \quad (3.18)$$

where $p = |\mathbf{H}|^2 / (\mu k) = l^2 / (k \mu)$ is the parameter (known as semi-latus rectum), $\epsilon = -(l^2 / k \mu) A = \sqrt{1 + 2El^2 / (\mu k^2)}$ is the eccentricity, E is the energy of the system and the angle $\varphi - \varphi_0$ is known as the **true anomaly**. The energy of the system is given by

$$E = T + V = \frac{\mu \dot{r}^2}{2} + \frac{\mu}{2} r^2 \dot{\varphi}^2 + \frac{k}{r} ,$$

where the second and the third terms represent the effective potential energy. For a circular orbit E is a minimum, $dV'/dr = 0 \Rightarrow r_c = -l^2 / \mu k$, $v = \sqrt{-k / \mu r_c}$ and for the minimal value of the energy we have $E_{min} = -k^2 \mu / (2l^2) = k / (2r_c)$.

For the perihelion ($r_{min} = r_p$) and aphelion ($r_{max} = r_a$) distances, $\dot{r} = 0 \Rightarrow E = V'$, $E = l^2 / (2\mu r^2) + k / r$, then

$$\begin{aligned} \frac{1}{r_p} &= -\frac{\mu k}{l^2} + \sqrt{\frac{\mu^2 k^2}{l^4} + \frac{2\mu E}{l^2}} , \\ \frac{1}{r_a} &= -\frac{\mu k}{l^2} - \sqrt{\frac{\mu^2 k^2}{l^4} + \frac{2\mu E}{l^2}} . \end{aligned} \quad (3.19)$$

Now, we define and redefine some expressions for a better understanding: the angular momentum $\mathbf{H} = \mu \mathbf{r} \times \mathbf{v}$, and the semi-major axis $a = p/(1 - \epsilon^2)$. So, for the orbit of the object we have

$$\begin{aligned}\frac{p}{r(\varphi)} &= 1 + \epsilon \cos(\varphi - \varphi_0) , \\ \frac{1}{r_p} &= -\frac{\mu k}{l^2} + \sqrt{\frac{\mu^2 k^2}{l^4} + \frac{2\mu E}{l^2}} , \\ \frac{1}{r_a} &= -\frac{\mu k}{l^2} - \sqrt{\frac{\mu^2 k^2}{l^4} + \frac{2\mu E}{l^2}} .\end{aligned}\tag{3.20}$$

where $A = \sqrt{(\mu^2 k^2)/l^4 + (2\mu E)/l^2}$, φ_0 is an arbitrary constant.

An orbit for which $\epsilon \geq 1$ is unbound, since $r \rightarrow \infty$ as $(\varphi - \varphi_0) \rightarrow \arccos(-1/\epsilon)$; the orbit forms a hyperbola if $\epsilon > 1$ and a parabola if $\epsilon = 1$. Also, the object's asymptotic speed v_0 as $r \rightarrow \infty$ is related to ϵ and l . Orbits for which $\epsilon < 1$ are bound, r is finite for all values of φ . Furthermore, r is now a periodic function of φ with period 2π , so the object returns to its original radial coordinate after exactly one revolution in φ . Thus these orbits are closed, and they form ellipses with the attracting center at one focus.

To construct the position vector \mathbf{r} we use the fact that $\mathbf{r} = r\mathbf{e}_r$, where \mathbf{e}_r is the unit vector onto the radial direction. For our case \mathbf{e}_r is defined as

$$\mathbf{e}_r = (\cos \Omega \cos \Theta - \sin \Omega \sin \Theta \cos i, \cos \Theta \sin \Omega + \sin \Theta \cos \Omega \cos i, \sin \Theta \sin i), \tag{3.21}$$

where Ω is the longitude of the ascending node, $\Theta = \omega + f$, ω is the argument of periapsis (as an angle measured from the ascending node to the pericenter/periapsis), $f = 2\Delta\varphi$ is the true anomaly, and i is the inclination with respect to the reference plane, measured at the ascending node (where the orbit passes upward through the reference plane). It is easy to prove that the minimal distance q is given by $f = 0$,

$r_p = a(1 - \epsilon) \equiv q$. The angles in Eq. (3.21) can be found by using (Klačka 2004)

$$\begin{aligned} \sin \Omega \sin i &= \frac{H_x}{|\mathbf{H}|}, \quad -\cos \Omega \sin i = \frac{H_y}{|\mathbf{H}|}, \quad i = \arccos \left(\frac{H_z}{|\mathbf{H}|} \right), \\ \sin \Theta \sin i &= \frac{z}{r}, \quad \cos \Theta \sin i = \frac{yH_x - xH_y}{r|\mathbf{H}|}. \\ \sin(\Theta - \omega) &= \frac{\mathbf{v} \cdot \mathbf{e}_r}{\epsilon \sqrt{G(M+m)/p}}, \quad \cos(\Theta - \omega) = \frac{\mathbf{v} \cdot \mathbf{e}_t}{\epsilon \sqrt{G(M+m)/p}} - \frac{1}{\epsilon}, \end{aligned} \quad (3.22)$$

where \mathbf{v} is the velocity of the object given by the radial ($v_r = \sqrt{G(M+m)/p} \epsilon \sin f$) and transversal ($v_t = \sqrt{G(M+m)/p}(1 + \epsilon \cos f)$) components,

$$\mathbf{v} = v_r \mathbf{e}_r + v_t \mathbf{e}_t, \quad (3.23)$$

and \mathbf{e}_t is the unit vector onto the transversal direction

$$\mathbf{e}_t = (-\cos \Omega \sin \Theta - \sin \Omega \cos \Theta \cos i, -\sin \Omega \sin \Theta + \cos \Omega \cos \Theta \cos i, \cos \Theta \sin i). \quad (3.24)$$

By finding the angles in previous equations one can build the object's position vector \mathbf{r} . We focus on two special positions, for an initial time (all used parameters with index zero, 0) and for the time when the object passes the perihelion (all used parameters with index p). For initial conditions $\mathbf{r}_0 = (x_0, y_0, z_0)$, $\mathbf{v}_0 = (v_{x,0}, v_{y,0}, v_{z,0}) \Rightarrow \mathbf{H}_0 \equiv (H_{x,0}, H_{y,0}, H_{z,0})$, $\mathbf{H}_0 = \mu \mathbf{r}_0 \times \mathbf{v}_0$, the angle i_0 is computed as

$$i_0 = \arccos \left(\frac{H_{z,0}}{|\mathbf{H}_0|} \right), \quad (3.25)$$

the previous relation is a number given by initial conditions. Since we know i_0 , in Eqs. (3.22) we have two equations by which we are able to find Ω_0 ,

$$\sin \Omega_0 = \frac{H_{x,0}}{|\mathbf{H}_0| \sin i_0}, \quad \cos \Omega_0 = -\frac{H_{y,0}}{|\mathbf{H}_0| \sin i_0}. \quad (3.26)$$

To choose the right angle quadrant, and therefore the right angle, we have to know the signs of the right sides in previous equations. Since we find these problems in several parts of this Thesis, we show a table (which can be used as algorithm) to choose the

right (quadrant) angle. Let

$$\begin{aligned}\cos \vartheta &= A, \\ \sin \vartheta &= B,\end{aligned}\tag{3.27}$$

where A and B are known numbers computed from the right sides of given equations. These numbers can be positive or negative, then we need to know which quadrant the angle belongs. It is recommended to remember where $\sin \vartheta$, $\cos \vartheta$ and $\tan \vartheta$ are positive (or negative). Table 3.1 allows us to solve problems as the given in Eq. (5.16).

	$\sin \vartheta > 0$	$\sin \vartheta < 0$	$\sin \vartheta = 0$
$\cos \vartheta > 0$	$\vartheta = \arccos A$	$\vartheta = 2\pi - \arccos A$	$\vartheta = 0$
$\cos \vartheta < 0$	$\vartheta = \arccos A$	$\vartheta = 2\pi - \arccos A$	$\vartheta = \pi$
$\cos \vartheta = 0$	$\vartheta = \pi/2$	$\vartheta = 3\pi/2$	

Table 3.1: Choosing the right angle.

Doing the same, from Eqs. (3.22), Θ_0 is computed as

$$\sin \Theta_0 = \frac{z_0}{r_0 \sin i_0}, \quad \cos \Theta_0 = \frac{y_0 H_{x,0} - x_0 H_{y,0}}{r_0 |\mathbf{H}_0| \sin i_0}.\tag{3.28}$$

In Eq. (3.28) we have the same problem as before with the right side signs, and for this we use Table 3.1. Until now we should know from previous Equations i_0, Ω_0 and Θ_0 . The last angle which we have to find is ω_0 , and doing the same as before where in Eqs. (3.22) we also have two equations,

$$\sin(\Theta_0 - \omega_0) = \frac{\mathbf{v}_0 \cdot \mathbf{e}_{r,0}}{\epsilon \sqrt{G(M+m)/p}}, \quad \cos(\Theta_0 - \omega_0) = \frac{\mathbf{v}_0 \cdot \mathbf{e}_{t,0}}{\epsilon \sqrt{G(M+m)/p}} - \frac{1}{\epsilon},\tag{3.29}$$

the right angle is found by using the same way, by Table 3.1. i_0, Ω_0, Θ_0 and ω_0 are now known values which help us to build the unit radial and transversal vectors, Eq. (3.21) and Eq. (3.24), respectively. And hence it helps us to construct the position and velocity vectors. In Eq. (3.29) \mathbf{v}_0 and $\mathbf{e}_{r,0}$ may be found from initial conditions or just by using the known values of the angles as $\mathbf{e}_{t,0}$ is found. Now, for the perihelion (all used parameters with index p) distance $f = 0$ and $|\mathbf{r}_p| = |(x_p, y_p, y_p)| = a(1 - \epsilon) \equiv q$, then the perihelion vector of position is easily computed from $\mathbf{r}_p = r_p \mathbf{e}_{r,p}$. The point

here is to calculate (x_p, y_p, z_p) , and we carry this out by using Eq. (3.21) and the values of angles from Eqs(3.25 - 3.29). Hence

$$\begin{aligned} x_p &= r_p(\cos \Omega_0 \cos \Theta_p - \sin \Omega_0 \sin \Theta_p \cos i_0), \\ y_p &= r_p(\cos \Theta_p \sin \Omega_0 + \sin \Theta_p \cos \Omega_0 \cos i_0), \\ z_p &= r_p \sin \Theta_p \sin i_0 . \end{aligned}$$

In the previous equation r_p , Ω_0 , i_0 are known and since $f_p = 0$ (for the perihelion), $\Theta_p = \omega_0$, then the perihelion position vector \mathbf{q} is definitely given by

$$\mathbf{q} \equiv \mathbf{r}_p = (x_p, y_p, z_p) = \begin{cases} x_p &= r_p(\cos \Omega_0 \cos \omega_0 - \sin \Omega_0 \sin \omega_0 \cos i_0), \\ y_p &= r_p(\cos \omega_0 \sin \Omega_0 + \sin \omega_0 \cos \Omega_0 \cos i_0), \\ z_p &= r_p \sin \omega_0 \sin i_0 . \end{cases} \quad (3.30)$$

As we can see, the perihelion position vector \mathbf{q} for the two-body problem is given by Eq. (3.30). The angles, which allow us to build the position vector, are computed from Eqs.(3.25), (3.26), (3.28) and from Eq. (3.29).

Chapter 4

Galactic tide

In this chapter we choose our reference frame in the galactic center (GC). In addition to the gravitational influence of the Sun, we consider that the object is perturbed by the gravitational effects of the Galaxy. As before we focus on the relative motion of the object with respect to the Sun. Global galactic gravitational field influences the relative motion of two close bodies in the form of galactic tide.

4.1 Model of Galaxy

A spiral galaxy like the Milky Way (Galaxy) has three basic components to its visible matter: the disk (containing the spiral arms), the halo, and the nucleus or central bulge [7]. Simple models can be constructed by neglecting spiral structure of the Galaxy. There are several galactic models, as of Dauphole [3], which considers spherical symmetry for galactic bulge and halo and cylindrical symmetry for galactic disk [3]. Drawback of this model is that it does not yield values of Oort constants corresponding to $A = (14.2 \pm 0.5) \text{ km s}^{-1} \text{ kpc}^{-1}$ and $B = (-12.4 \pm 0.5) \text{ km s}^{-1} \text{ kpc}^{-1}$. Another disadvantage is that the model cannot be used as a realistic model of Galaxy for galactocentric distances larger than 40 kpc, since the model produces a decreasing rotation curve for these distances.

We consider the model given in [19], better consistent with values of the Oort constants and with flat rotation curve of the Galaxy. This model considers galactic

bulge (index b) of Dauphole [3] and its gravitational potential is

$$\begin{aligned}\Phi_b(r) &= -\frac{GM_b}{\sqrt{r^2 + b_b^2}}, \\ M_b &= 1.3955 \times 10^{10} M_\odot, \\ b_b &= 0.35 \text{ kpc},\end{aligned}\tag{4.1}$$

where G is the gravitational constant.

Galactic disk in this model [19, 7] is represented by mass density function given by

$$\varrho_d(R, z) = \varrho_0 \left[\exp\left(\frac{-R}{R_d}\right) \exp\left(\frac{-|z|}{h_d}\right) \right],\tag{4.2}$$

where $R_d = (3.5 \pm 0.5) \text{ kpc}$ is the scale length of the disk¹, $h_d = 330 \text{ pc}$ is the characteristic scale height for the lower-mass (older) objects in the disk and $h_d = 160 \text{ pc}$ for the gas-dust disk.

Finally, the simple model of galactic halo is given by a flat rotation curve. The rotation curve is given by circular speed $v_h(r)$ for spherical halo as

$$\begin{aligned}v_h^2(r) &= v_H^2 \left\{ 1 - \alpha \frac{a_H}{r} \arctan\left(\frac{r}{a_H}\right) - (1 - \alpha) \exp\left[-\left(\frac{r}{b_H}\right)\right] \right\} \\ v_H &= 220 \text{ km s}^{-1}, \\ \alpha &= 0.174, \\ a_H &= 0.04383 \text{ kpc}, \\ b_H &= 37.3760 \text{ kpc}.\end{aligned}\tag{4.3}$$

For more details about the model, see [19].

4.1.1 Motion in Galaxy near to the galactic equator

The model described in [19] considers an approximation when global galactic gravitational field is described by cylindrically symmetric potential $\Phi(R, z)$, where R is the distance from the axis of rotation and z the coordinate of a body above/below the galactic plane ($z = 0$ corresponds to the galactic equatorial plane; right-handed system

¹ Notice that at $R = 8 \text{ kpc}$ the Sun is in outer regions of the galactic disk

$x - y - z$ has its origin at the center of the Galaxy, z is positively oriented toward the north pole of the Galaxy; $R = \sqrt{x^2 + y^2}$). The galactic gravitational potential is generated by mass distribution within the Galaxy. Then, bulge, halo and disk contribute to the total gravitational field. The bulge contribution is computed from Eq. (4.1), for the disk contribution is given by the solution to the Poisson's equation with right side given in Eq. (4.2), and, finally for the halo is given by using Eq. (4.3). Acceleration of the body is found from the total gravitational field.

We focus on the relative motion of a object with respect to the Sun. The Sun is moving in a distance $R_\odot = 8 \text{ kpc}$ from the galactic center. Nowadays, the Sun is situated 30 pc above the galactic equatorial plane ($Z_\odot = 30 \text{ pc}$). The Sun has rotational motion with speed $(A - B)R_\odot$ and vertical (in the normal direction to the galactic plane) with speed 7.3 km/s. As we said, our system of coordinates is the galactic center. The position vector of the Sun is given by $(X_\odot, Y_\odot, Z_\odot)$, of the object by $(X_\star, Y_\star, Z_\star)$, and the relative position vector Sun - object by $\mathbf{r} = (\xi, \eta, \zeta)$.

The total action of all galactic components explained in [19], can be summarized in the following equations

$$\begin{aligned}
\frac{d^2 X_\star}{dt^2} &= - \frac{v_0^2}{R_\odot^2} \left\{ X_\odot + \xi + 2 \left(R_\odot \frac{v'_0}{v_0} - 1 \right) \left[\left(\frac{X_\odot}{R_\odot} \right)^2 \xi + \frac{X_\odot Y_\odot}{R_\odot^2} \eta \right] \right. \\
&\quad \left. - X_\odot [\Gamma_1(Z_\odot^2 + 2 Z_\odot \zeta) - \frac{1}{2} \Gamma_2(Z_\odot^4 + 4 Z_\odot^3 \zeta)] \right\}, \\
\frac{d^2 Y_\star}{dt^2} &= - \frac{v_0^2}{R_\odot^2} \left\{ Y_\odot + \eta + 2 \left(R_\odot \frac{v'_0}{v_0} - 1 \right) \left[\frac{X_\odot Y_\odot}{R_\odot^2} \xi + \left(\frac{Y_\odot}{R_\odot} \right)^2 \eta \right] \right. \\
&\quad \left. - Y_\odot [\Gamma_1(Z_\odot^2 + 2 Z_\odot \zeta) - \frac{1}{2} \Gamma_2(Z_\odot^4 + 4 Z_\odot^3 \zeta)] \right\}, \\
\frac{d^2 Z_\star}{dt^2} &= - \left\{ 4\pi G \left[\varrho_d \left(1 - \frac{u}{2} |Z_\star| \right) + \varrho_h \right] + 2(A^2 - B^2) \right\} Z_\star \\
&\quad - 4\pi G \left\{ \frac{X_\odot}{R_\odot} (X_\star - X_\odot) + \frac{Y_\odot}{R_\odot} (Y_\star - Y_\odot) \right\} \times \\
&\quad \times \left\{ \varrho'_d \left(1 - \frac{u}{2} |Z_\star| \right) + \varrho'_h \right\} Z_\star, \tag{4.4}
\end{aligned}$$

where higher order in ξ, η, ζ are neglected and $\varrho' = \varrho'_d + \varrho'_h$, $\varrho = \varrho_d + \varrho_h$. For the galactic plane $[v(R)]^2 = v_0^2 \{1 + 2(v'_0/v_0)(X_\odot \xi + Y_\odot \eta)/R_\odot\}$, where the prime denotes differentiation with respect to R , ($v_0 \equiv v_{R_0}$, $v'_0 \equiv [dv(R)/dR]_{R_0}$) and, again, higher orders in ξ and η are neglected. We dealing only with $|z| \ll 1 \text{ kpc}$.

Equations of motion for the relative motion of the object with respect to the Sun are in detail described, explained and deduced in [19]. From where we have

$$\begin{aligned}
\frac{d^2\xi}{dt^2} &= -\frac{G(M_\odot + m)}{r^3}\xi + (A - B)[A + B + 2A\cos(2\omega_0 t)]\xi \\
&\quad - 2A(A - B)\sin(2\omega_0 t)\eta + 2(A - B)^2(\Gamma_1 - \Gamma_2 Z_\odot^2)R_\odot Z_\odot \cos(\omega_0 t)\zeta, \\
\frac{d^2\eta}{dt^2} &= -\frac{G(M_\odot + m)}{r^3}\eta + (A - B)[A + B - 2A\cos(2\omega_0 t)]\eta \\
&\quad - 2A(A - B)\sin(2\omega_0 t)\xi - 2(A - B)^2(\Gamma_1 - \Gamma_2 Z_\odot^2)R_\odot Z_\odot \sin(\omega_0 t)\zeta, \\
\frac{d^2\zeta}{dt^2} &= -\frac{G(M_\odot + m)}{r^3}\zeta - 4\pi G\left\{\varrho\zeta - \varrho_d\frac{u}{2}[|Z_\odot + \zeta|(Z_\odot + \zeta) - |Z_\odot|Z_\odot]\right\} \\
&\quad - 2(A^2 - B^2)\zeta \\
&\quad - 4\pi G\left(\varrho' - \varrho'_d\frac{u}{2}|Z_\odot + \zeta|\right)(Z_\odot + \zeta)[\cos(\omega_0 t)\xi - \sin(\omega_0 t)\eta], \\
r &= \sqrt{\xi^2 + \eta^2 + \zeta^2}, \\
\omega_0 &= A - B,
\end{aligned} \tag{4.5}$$

where the first term in each equation (for each coordinate) represents the gravitational interaction between them, and for z coordinates (in application to the Sun and star –or gas cloud),

$$\begin{aligned}
\frac{d^2 Z_\odot}{dt^2} &= -\left\{4\pi G\left[\varrho_d\left(1 - \frac{u}{2}|Z_\odot|\right) + \varrho_h\right] + 2(A^2 - B^2)\right\}Z_\odot, \\
\frac{d^2 Z_\star}{dt^2} &= -\left\{4\pi G\left[\varrho_d\left(1 - \frac{u}{2}|Z_\star|\right) + \varrho_h\right] + 2(A^2 - B^2)\right\}Z_\star \\
&\quad - 4\pi G\left\{\frac{X_\odot}{R_\odot}(X_\star - X_\odot) + \frac{Y_\odot}{R_\odot}(Y_\star - Y_\odot)\right\} \times \\
&\quad \times \left\{\varrho'_d\left(1 - \frac{u}{2}|Z_\star|\right) + \varrho'_h\right\}Z_\star,
\end{aligned} \tag{4.6}$$

where $\varrho' = \varrho'_d + \varrho'_h$, $\varrho = \varrho_d + \varrho_h$, $X_\odot = R_\odot \cos(-\omega_0 t)$, $Y_\odot = R_\odot \sin(-\omega_0 t)$ ², G is the gravitational constant, M_\odot is the mass of the Sun and the numerical values of the

²Here, the sign minus at angular velocity ($-\omega_0$) denotes negative orientation of the galactic rotation (clockwise orientation/direction of the solar motion with respect to the center of the Galaxy)

used quantities are

$$\begin{aligned}
A &= 14.2 \text{ km s}^{-1} \text{ kpc}^{-1} , \\
B &= -12.4 \text{ km s}^{-1} \text{ kpc}^{-1} , \\
\Gamma_1 &= 0.124 \text{ kpc}^{-2} , \\
\Gamma_2 &= 1.586 \text{ kpc}^{-4} , \\
\varrho_d &= 0.126 M_{\odot} \text{ pc}^{-3} , \\
\varrho_h &= 0.004 M_{\odot} \text{ pc}^{-3} , \\
\varrho'_d &= -0.0360 M_{\odot} \text{ pc}^{-3} \text{ kpc}^{-1} , \\
\varrho'_h &= -0.0006 M_{\odot} \text{ pc}^{-3} \text{ kpc}^{-1} , \\
u &= 3.3 \text{ kpc}^{-1} .
\end{aligned} \tag{4.7}$$

In our computations it is important to consider two cases in the density: $u = 0 \text{ kpc}^{-1}$ and $u = 3.3 \text{ kpc}^{-1}$, and we expect better results for the second case. In next sections we solve the equations of motion for any value of u . As first step we analytically solve the equation for the Sun, which represents vertical motion.

4.1.2 Analytical solution to the solar equation of motion along the z-axis

In this subsection we give an analytical solution to the solar equation of motion for the z direction, which is given by

$$\frac{d^2 Z_{\odot}}{dt^2} = - \left\{ 4\pi G \left[\varrho_d \left(1 - \frac{u}{2} |Z_{\odot}| \right) + \varrho_h \right] + 2 (A^2 - B^2) \right\} Z_{\odot} , \tag{4.8}$$

which represents the solar anharmonic oscillations along the z -axis. Initial conditions for this equation are given by currently (at the time $t = 0$) observed values:

$$Z_{\odot}(0) = 30 \text{ pc}, \quad \dot{Z}_{\odot}(0) = 7.3 \text{ km s}^{-1} . \tag{4.9}$$

Eq. (4.8) can be written as

$$\frac{d^2 Z_{\odot}}{dt^2} = - \gamma_0^2 Z_{\odot} + \kappa |Z_{\odot}| Z_{\odot} , \tag{4.10}$$

where

$$\begin{aligned}\gamma^2 &= 4\pi G(\varrho_d + \varrho_h) + 2(A^2 - B^2) , \\ \kappa &= 2\pi G u \varrho_d .\end{aligned}\tag{4.11}$$

For $u = 0$, $\kappa = 0$, Eq. (4.8) describes the known simple harmonic oscillations. Taking into account the non-linear term ($u \neq 0$), we solve Eq. (4.10) considering the method of successive approximations [6, p. 102]. Here, we suppose a general solution in the form of

$$Z_{\odot}(t) = Z_{\odot}^{(1)}(t) + Z_{\odot}^{(2)}(t) ,\tag{4.12}$$

where initial conditions for $Z_{\odot}^{(1)}$ are given by Eq. (4.9) and $Z_{\odot}^{(2)}(0) = 0$ pc, and $\dot{Z}_{\odot}^{(2)}(0) = 0$ km s⁻¹ satisfy the general initial conditions, Eq. (4.9). Also, $|Z_{\odot}^{(2)}| \ll |Z_{\odot}^{(1)}|$, and functions $Z_{\odot}^{(1)}$ satisfy the non-perturbative equation

$$\frac{d^2 Z_{\odot}^{(1)}}{dt^2} + \gamma_0^2 Z_{\odot}^{(1)} = 0 .\tag{4.13}$$

Eq. (4.13) represents ordinary harmonic oscillations

$$Z_{\odot}^{(1)}(t) = a_{\odot} \cos(\gamma t + \phi_{\odot}) ,\tag{4.14}$$

where a_{\odot} and ϕ_{\odot} are found from initial conditions given by Eq. (4.9). Eq. (4.14) can be written as $Z_{\odot}^{(1)} = c_1 \cos(\gamma t) + c_2 \sin(\gamma t)$, then by using Eq. (4.9) we get $c_1 = Z_{\odot}(t=0)$ and $c_2 = \dot{Z}_{\odot}(t=0)/\gamma$. Also, it implies that $a_{\odot} = \sqrt{c_1^2 + c_2^2}$, $\cos \phi_{\odot} = c_1/a_{\odot}$ and $\sin \phi_{\odot} = -c_2/a_{\odot}$. The angle ϕ_{\odot} is then found by using the Tab. 3.1. We look for γ as $\gamma = \gamma_0 + \gamma^{(1)} + \dots$, and we write Eq. (4.10) in a convenient equivalent form for negative values of Z_{\odot} ³

$$\frac{\gamma_0^2}{\gamma^2} \ddot{Z}_{\odot} + \gamma_0^2 Z_{\odot} = -\kappa Z_0^2 - \left(1 - \frac{\gamma_0^2}{\gamma^2}\right) \ddot{Z}_{\odot} .\tag{4.15}$$

³ $|Z_{\odot}| = -Z_{\odot}$ for negative Z_{\odot}

The next step is to plug Eq. (4.12) into Eq. (4.15)

$$\begin{aligned}
LHS &= RHS , \\
LHS &\equiv \frac{\gamma_0^2}{\gamma^2} \ddot{Z}_\odot^{(1)} + \gamma_0^2 Z_\odot^{(1)} + \frac{\gamma_0^2}{\gamma^2} \ddot{Z}_\odot^{(2)} + \gamma_0^2 Z_\odot^{(2)} , \\
RHS &\equiv -\kappa \left(Z_\odot^{(1)} + Z_\odot^{(2)} \right)^2 - \left(1 - \frac{\gamma_0^2}{\gamma^2} \right) \left(\ddot{Z}_\odot^{(1)} + \ddot{Z}_\odot^{(2)} \right) . \quad (4.16)
\end{aligned}$$

Taking into account first order terms and needed derivatives of $Z_\odot^{(1)}$, we have

$$\ddot{Z}_\odot^{(2)} + \gamma_0^2 Z_\odot^{(2)} = -\kappa a_\odot^2 \cos^2(\gamma t + \phi_\odot) - \left(1 - \frac{\gamma_0^2}{\gamma^2} \right) \left(-a_\odot \gamma^2 \cos(\gamma t + \phi_\odot) \right) , \quad (4.17)$$

where $\gamma > 0$, $\cos^2(\gamma t + \phi_\odot) = 1/2 + [\cos(2\gamma t + 2\phi_\odot)]/2$, and $\gamma^2 - \gamma_0^2 \approx [\gamma^{(1)}]^2 + 2\gamma_0\gamma^{(1)}$. Neglecting second order terms, $\gamma^2 - \gamma_0^2 \approx 2\gamma_0\gamma^{(1)}$, we get

$$\ddot{Z}_\odot^{(2)} + \gamma_0^2 Z_\odot^{(2)} = -\frac{\kappa a_\odot^2}{2} - \kappa a_\odot^2 \cos(2\gamma t + 2\phi_\odot) + 2\gamma_0^2 \gamma^{(1)} \cos(\gamma t + \phi_\odot) . \quad (4.18)$$

We assume that there is no resonance, then the amplitude of $\cos(\gamma t + \phi_\odot)$ (on the right side) have to be zero, then for $\gamma^{(1)} = 0$, Eq. (4.18) gives

$$\ddot{Z}_\odot^{(2)} + \gamma_0^2 Z_\odot^{(2)} = -\frac{\kappa a_\odot^2}{2} - \kappa a_\odot^2 \cos(2\gamma t + 2\phi_\odot) , \quad \gamma = \gamma_0 , \quad (4.19)$$

with initial conditions given by $Z_\odot^{(2)}(0) = 0 \text{ pc}$, and $\dot{Z}_\odot^{(2)}(0) = 0 \text{ km s}^{-1}$. Eq. (4.19) is a nonhomogeneous second order linear equation. Recall that the general solution is given by $Z_\odot^{(2)} = Z_{0,h}^{(2)} + Z_{0,p}^{(2)}$, where $Z_{0,h}^{(2)}$ is the solution of the associated homogeneous equation (without right side) and $Z_{0,p}^{(2)}$ is a particular solution of Eq. (4.19).

Now, the solution of the homogeneous equation is well known and we look for it in the form of

$$Z_{0,h}^{(2)}(t) = A \cos(\gamma t + \phi') = c'_1 \cos(\gamma t) + c'_2 \sin(\gamma t) , \quad (4.20)$$

where A and ϕ' are found from initial conditions and can be computed by using $c'_{1,2}$ as $A = \sqrt{c_1'^2 + c_2'^2}$, $\cos \phi' = c'_1/A$ and $\sin \phi' = -c'_2/A$. The angle ϕ' may be computed by using the Tab. 3.1, or we just use the second expression of Eq. (4.20).

We guess the particular solution to be

$$Z_{0,p}^{(2)}(t) = b \cos(2\gamma t + 2\phi_{\odot}) + c. \quad (4.21)$$

Then, putting the previous equation and its respective derivatives into Eq. (4.19) we find b and c . For a better description of negative and positive values of Z_{\odot} , we define the parameter q as

$$q_{\odot} = \begin{cases} +1, & Z_{\odot} > 0 \\ -1, & Z_{\odot} < 0 \end{cases}$$

Hence, for both negative and positive values of Z_{\odot} , the particular solution of Eq. (4.19) is given by

$$Z_{0,p}^{(2)}(t) = -q_{\odot} \frac{\kappa a_{\odot}^2}{2\gamma_0^2} \left[\frac{\cos(2\gamma t + 2\phi_{\odot})}{3} - 1 \right] \quad (4.22)$$

As we wrote above, $Z_{\odot}^{(2)} = Z_{0,h}^{(2)} + Z_{0,p}^{(2)}$, then

$$Z_{\odot}^{(2)}(t) = c'_1 \cos(\gamma t) + c'_2 \sin(\gamma t) - q_{\odot} \frac{\kappa a_{\odot}^2}{2\gamma_0^2} \left[\frac{\cos(2\gamma t + 2\phi_{\odot})}{3} - 1 \right]. \quad (4.23)$$

As last step, we have to evaluate the solution in initial conditions to find c'_1 and c'_2

$$c'_1 = q_{\odot} \frac{\kappa a_{\odot}^2}{2\gamma^2} \left[\frac{\cos(2\phi_{\odot})}{3} - 1 \right], \quad c'_2 = -q_{\odot} \frac{\kappa a_{\odot}^2}{\gamma^2} \frac{\cos(2\phi_{\odot})}{3}. \quad (4.24)$$

Then,

$$\begin{aligned} Z_{\odot}^{(2)}(t) &= q_{\odot} \frac{\kappa a_{\odot}^2}{2\gamma^2} \left[\frac{\cos(2\phi_{\odot})}{3} - 1 \right] \cos(\gamma t) - q_{\odot} \frac{\kappa a_{\odot}^2}{\gamma^2} \frac{\cos(2\phi_{\odot})}{3} \sin(\gamma t) \\ &\quad - q_{\odot} \frac{\kappa a_{\odot}^2}{2\gamma_0^2} \left[\frac{\cos(2\gamma t + 2\phi_{\odot})}{3} - 1 \right]. \end{aligned} \quad (4.25)$$

Putting back Eq. (4.25) and Eq. (4.14) into Eq. (4.12) we get

$$\begin{aligned}
Z_{\odot} &= Z_{\odot}^{(1)} + Z_{\odot}^{(2)} , \\
&= Z_{\odot}(0) \cos(\gamma t) + \frac{\dot{Z}_{\odot}(0)}{\gamma} \sin(\gamma t) \\
&\quad + q_{\odot} \frac{\kappa a_{\odot}^2}{2\gamma^2} \left[\frac{\cos(2\phi_{\odot})}{3} - 1 \right] \cos(\gamma t) - q_{\odot} \frac{\kappa a_{\odot}^2}{\gamma^2} \frac{\cos(2\phi_{\odot})}{3} \sin(\gamma t) \\
&\quad - q_{\odot} \frac{\kappa a_{\odot}^2}{2\gamma_0^2} \left[\frac{\cos(2\gamma t + 2\phi_{\odot})}{3} - 1 \right] .
\end{aligned} \tag{4.26}$$

Previous equation represents anharmonic oscillations of the Sun along the z - axis across the galactic equator.

4.2 Simple model

For a better understanding we propose a simple model in the relative motion of the Sun-object, e.g. a star or an interstellar gas cloud. In this simple model we suppose a closest motion of the object with respect to the Sun and we do not consider gravitational interaction between these two bodies. Since we focus on the closest stars with respect to the Sun, it is a good approach to consider that the relative motion of the object with respect to the Sun depends linearly on time for x and y coordinates and that there are anharmonic oscillations along the z -axis. Then,

$$\begin{aligned}
\Delta X(t) &= \Delta \dot{X}_0(t_0) (t - t_0) + \Delta X_0(t_0) , \\
\Delta Y(t) &= \Delta \dot{Y}_0(t_0) (t - t_0) + \Delta Y_0(t_0) , \\
\Delta Z(t) &= Z_{\star}(t) - Z_{\odot}(t),
\end{aligned} \tag{4.27}$$

where initial conditions at t_0 , $\Delta X_0(t_0)$, $\Delta \dot{X}_0(t_0)$, $\Delta Y_0(t_0)$, $\Delta \dot{Y}_0(t_0)$, $\Delta Z_0(t_0)$ and $\Delta \dot{Z}_0(t_0)$ are given by observational data that we measure with respect to the Sun. For a given time t_0 , we have,

$$\begin{aligned}
\Delta X_0(t_0) &= X_{\star}(t_0 - r_0/c) - X_{\odot}(t_0) , \\
\Delta Y_0(t_0) &= Y_{\star}(t_0 - r_0/c) - Y_{\odot}(t_0) , \\
\Delta Z_0(t_0) &= Z_{\star}(t_0 - r_0/c) - Z_{\odot}(t_0) ,
\end{aligned} \tag{4.28}$$

and

$$\begin{aligned}
\Delta \dot{X}_0(t_0) &= \dot{X}_\star(t_0 - r_0/c) - \dot{X}_\odot(t_0) , \\
\Delta \dot{Y}_0(t_0) &= \dot{Y}_\star(t_0 - r_0/c) - \dot{Y}_\odot(t_0) , \\
\Delta \dot{Z}_0(t_0) &= \dot{Z}_\star(t_0 - r_0/c) - \dot{Z}_\odot(t_0) ,
\end{aligned} \tag{4.29}$$

where physics is respected. The speed of light, c , may play an important role for the signals coming from the studied object. For this reason we subtract the travelled time of the signal $|\mathbf{r}_0|/c$. $|\mathbf{r}_0| = r_0$ is the heliocentric distance of the object at the time t_0 .

For the motion along the z -axis we consider Eqs. (4.6). Since we consider objects which are close to the Sun, it is a good approach to describe the object's motion by the first part of the first equation in Eqs. (4.6) (the same equation as for the Sun, first equation in Eqs. (4.6), the difference lies in initial conditions, only). In reality, the approximation represented by Eqs. (4.27) is not required in general case.

4.2.1 Star's oscillation along the z -axis

In this subsection we describe the oscillations of the object along the z -axis, where we do not take into account the gravitational interaction Sun-object. As we said, we consider that the motion of the object is described by the same equation as for the Sun (first part of the second equation given in Eqs. (4.6)). Then,

$$\frac{d^2 Z_\star}{dt^2} = - \left\{ 4\pi G \left[\varrho_d \left(1 - \frac{u}{2} |Z_\star| \right) + \varrho_h \right] + 2(A^2 - B^2) \right\} Z_\star, \tag{4.30}$$

which represents the object's anharmonic oscillations along the z - axis. We get initial conditions from the third equation of (4.28) and of (4.29),

$$Z_\star(t_0 - r_0/c) = \Delta Z_0(t_0) + Z_\odot(t_0), \quad \dot{Z}_\star(t_0 - r_0/c) = \Delta \dot{Z}_0(t_0) + \dot{Z}_\odot(t_0). \tag{4.31}$$

where $\Delta Z_0(t_0)$ and $\Delta \dot{Z}_0(t_0)$ are known values from observations. Then, doing the same as for the solar motion along the z -axis, we get

$$\begin{aligned}
Z_\star(t) &= Z_\star^{(1)}(t) + Z_\star^{(2)}(t) , \\
&= Z_\star(0) \cos(\gamma t) + \frac{\dot{Z}_\star(0)}{\gamma} \sin(\gamma t) \\
&\quad + q_\star \frac{\kappa a_\star^2}{2\gamma^2} \left[\frac{\cos(2\phi_\star)}{3} - 1 \right] \cos(\gamma t) - q_\star \frac{\kappa a_\star^2 \cos(2\phi_\star)}{\gamma^2 3} \sin(\gamma t) \\
&\quad - q_\star \frac{\kappa a_\star^2}{2\gamma_0^2} \left[\frac{\cos(2\gamma t + 2\phi_\star)}{3} - 1 \right] . \tag{4.32}
\end{aligned}$$

where,

$$q_\star = \begin{cases} +1, & Z_\star > 0 \\ -1, & Z_\star < 0 \end{cases}$$

Homogeneous equation for the star, $Z_\star^{(1)} = a_\star \cos(\gamma t + \phi_\star)$, can be written as $Z_\star^{(1)} = c_1 \cos(\gamma t) + c_2 \sin(\gamma t)$, then by using initial conditions at $t = 0$ we get $c_1 = Z_\star(t = 0)$ and $c_2 = \dot{Z}_\star(t = 0)/\gamma$. Also, it implies that $a_\star = \sqrt{c_1^2 + c_2^2}$, $\cos \phi_\star = c_1/a_\star$ and $\sin \phi_\star = -c_2/a_\star$. The angle ϕ_\star is then found by using the Tab. 3.1.

In the next subsection we show the way how to obtain initial conditions, $Z_\star(0)$ and $\dot{Z}_\star(0)$, for the case when $u = 0$. We also show how to find these initial conditions for others values of u .

4.2.2 Initial conditions for the motion along the z -axis ($u = 0$)

Here, we show a way to find initial conditions for the motion along the z -axis when $u = 0$. From Eq. (4.32), the z -component of the star's position at $t_0 = 0$ is

$$Z_\star\left(-\frac{r_0}{c}\right) = Z_\star(0) \cos\left(\gamma \frac{r_0}{c}\right) - \frac{\dot{Z}_\star(0)}{\gamma} \sin\left(\gamma \frac{r_0}{c}\right) \tag{4.33}$$

and the z -component of the star's velocity at $t_0 = 0$ is

$$\dot{Z}_\star\left(-\frac{r_0}{c}\right) = Z_\star(0) \gamma \sin\left(\gamma \frac{r_0}{c}\right) + \dot{Z}_\star(0) \cos\left(\gamma \frac{r_0}{c}\right) \tag{4.34}$$

where, From Eq. (4.31) we compute the left side of Eq. (4.33) and of Eq. (4.34). Then, $Z_{\star}(-r_0/c)$ and $\dot{Z}_{\star}(-r_0/c)$ are given by

$$\begin{aligned} Z_{\star}\left(-\frac{r_0}{c}\right) &= \Delta Z_0(0) + Z_{\odot}(0) , \\ \dot{Z}_{\star}\left(-\frac{r_0}{c}\right) &= \Delta \dot{Z}_0(0) + \dot{Z}_{\odot}(0) . \end{aligned} \quad (4.35)$$

In Eqs. (4.35), $\Delta Z_0(0)$ and $\Delta \dot{Z}_0(0)$ are given from measured data, and, $Z_{\odot}(0)$ and \dot{Z}_{\odot} are known values from Eqs. (4.9), then $Z_{\star}(-r_0/c)$ and $\dot{Z}_{\star}(-r_0/c)$ are known values. Since in Eq. (4.33) and in Eq. (4.34) the unique unknown values are $Z_{\star}(0)$ and $\dot{Z}_{\star}(0)$, we have a nonhomogeneous system of equations. Putting to the right side all known values for the system, we get

$$\begin{aligned} Z_{\star}(0) \cos\left(\gamma \frac{r_0}{c}\right) - \frac{\dot{Z}_{\star}(0)}{\gamma} \sin\left(\gamma \frac{r_0}{c}\right) &= g_1 , \\ Z_{\star}(0) \gamma \sin\left(\gamma \frac{r_0}{c}\right) + \dot{Z}_{\star}(0) \cos\left(\gamma \frac{r_0}{c}\right) &= g_2 , \end{aligned} \quad (4.36)$$

where g_1 and g_2 are known values given by

$$g_1 = Z_{\star}\left(-\frac{r_0}{c}\right) , \quad (4.37)$$

$$g_2 = \dot{Z}_{\star}\left(-\frac{r_0}{c}\right) . \quad (4.38)$$

We rewrite Eqs. (4.36) as a matrix equation, $Ax = B$,

$$\begin{bmatrix} \cos(\gamma r_0/c) & -\sin(\gamma r_0/c)/\gamma \\ \gamma \sin(\gamma r_0/c) & \cos(\gamma r_0/c) \end{bmatrix} \begin{bmatrix} Z_{\star}(0) \\ \dot{Z}_{\star}(0) \end{bmatrix} = \begin{bmatrix} g_1 \\ g_2 \end{bmatrix} \quad (4.39)$$

Here, we look for $(Z_{\star}(0), \dot{Z}_{\star}(0))^t$. Since $\det(A) = \cos^2(\gamma r_0/c) + \sin^2(\gamma r_0/c) = 1 \neq 0$, the nonhomogeneous system of linear equations (4.36) has a unique non-trivial solution. Then, by using the Cramer's rule, we get

$$Z_{\star}(0) = \begin{vmatrix} g_1 & -\sin(\gamma r_0/c)/\gamma \\ g_2 & \cos(\gamma r_0/c) \end{vmatrix} , \quad (4.40)$$

$$\dot{Z}_\star(0) = \begin{vmatrix} \cos(\gamma r_0/c) & g_1 \\ \gamma \sin(\gamma r_0/c) & g_2 \end{vmatrix}. \quad (4.41)$$

Thus, the solution for the star's oscillations along the z -axis when $u = 0$ is then given by

$$Z_\star(t) = Z_\star(0) \cos(\gamma t) + \frac{\dot{Z}_\star(0)}{\gamma} \sin(\gamma t), \quad (4.42)$$

with initial conditions $Z_\star(0)$ and $\dot{Z}_\star(0)$, which are given by Eq. (4.40) and by Eq. (4.41), respectively, together with observational data represented by Eqs. (4.35).

4.2.3 Initial conditions for the object's motion along x , y and z directions ($u \neq 0$)

Because we already showed how to find initial conditions at $t_0 = 0$ for the motion of the object along the z -axis for the case when oscillations represent harmonic motion ($u = 0$), in this section we give an description to find initial conditions at t_0 for the object's motion along the x , y and z axis. From measurements we are able to know

$$\begin{aligned} \Delta X_0(t_0) &= X_\star(t_0 - r_0/c) - X_\odot(t_0), \\ \Delta Y_0(t_0) &= Y_\star(t_0 - r_0/c) - Y_\odot(t_0), \\ \Delta Z_0(t_0) &= Z_\star(t_0 - r_0/c) - Z_\odot(t_0), \end{aligned} \quad (4.43)$$

and

$$\begin{aligned} \Delta \dot{X}_0(t_0) &= \dot{X}_\star(t_0 - r_0/c) - \dot{X}_\odot(t_0), \\ \Delta \dot{Y}_0(t_0) &= \dot{Y}_\star(t_0 - r_0/c) - \dot{Y}_\odot(t_0), \\ \Delta \dot{Z}_0(t_0) &= \dot{Z}_\star(t_0 - r_0/c) - \dot{Z}_\odot(t_0). \end{aligned} \quad (4.44)$$

In right sides of previous equations are represented the differences that we measure from observational data (from equatorial coordinates). Now, in addition to the left sides of previous equations that are known from observational data, we suppose we know the coordinates of the Sun for the time t_0 . Then, we solve previous equation where the only unknown values are $X_\star(t_0)$, $Y_\star(t_0)$, $Z_\star(t_0)$, $\dot{X}_\star(t_0)$, $\dot{Y}_\star(t_0)$ and $\dot{Z}_\star(t_0)$. We also suppose

that the velocity and position vector of the object are infinitely differentiable in a neighborhood of t_0 , then, considering the Taylor expansion for these object's functions we get

$$\begin{aligned}\Delta X_0(t_0) &= X_\star(t_0) - X_\odot(t_0) - \dot{X}_\star(t_0)\frac{r_0}{c} + \frac{1}{2}\ddot{X}_\star(t_0)\left(\frac{r_0}{c}\right)^2 \dots, \\ \Delta Y_0(t_0) &= Y_\star(t_0) - Y_\odot(t_0) - \dot{Y}_\star(t_0)\frac{r_0}{c} + \frac{1}{2}\ddot{Y}_\star(t_0)\left(\frac{r_0}{c}\right)^2 \dots, \\ \Delta Z_0(t_0) &= Z_\star(t_0) - Z_\odot(t_0) - \dot{Z}_\star(t_0)\frac{r_0}{c} + \frac{1}{2}\ddot{Z}_\star(t_0)\left(\frac{r_0}{c}\right)^2 \dots, \end{aligned} \quad (4.45)$$

and

$$\begin{aligned}\Delta \dot{X}_0(t_0) &= \dot{X}_\star(t_0) - \dot{X}_\odot(t_0) - \ddot{X}_\star(t_0)\frac{r_0}{c} + \dots, \\ \Delta \dot{Y}_0(t_0) &= \dot{Y}_\star(t_0) - \dot{Y}_\odot(t_0) - \ddot{Y}_\star(t_0)\frac{r_0}{c} + \dots, \\ \Delta \dot{Z}_0(t_0) &= \dot{Z}_\star(t_0) - \dot{Z}_\odot(t_0) - \ddot{Z}_\star(t_0)\frac{r_0}{c} + \dots, \end{aligned} \quad (4.46)$$

where,

$$\begin{aligned}\mathbf{r}_0(t_0) &= [\Delta X_0(t_0), \Delta Y_0(t_0), \Delta Z_0(t_0)], \\ \mathbf{v}_0(t_0) &= [\Delta \dot{X}_0(t_0), \Delta \dot{Y}_0(t_0), \Delta \dot{Z}_0(t_0)], \\ \mathbf{r}_{\star\odot}(t_0) &= [X_\star(t_0) - X_\odot(t_0), Y_\star(t_0) - Y_\odot(t_0), Z_\star(t_0) - Z_\odot(t_0)], \\ \mathbf{v}_{\star\odot}(t_0) &= [\dot{X}_\star(t_0) - \dot{X}_\odot(t_0), \dot{Y}_\star(t_0) - \dot{Y}_\odot(t_0), \dot{Z}_\star(t_0) - \dot{Z}_\odot(t_0)]. \end{aligned} \quad (4.47)$$

From observational data we measure $\mathbf{r}_0(t_0)$ and $\mathbf{v}_0(t_0)$. $\ddot{X}_\star(t_0)$ and $\ddot{Y}_\star(t_0)$ are given by

$$\begin{aligned}
\ddot{X}_\star(t_0) &= -\frac{v_0^2}{R_\odot^2} \left\{ X_\odot(t_0) + \xi(t_0) + 2 \left(R_\odot \frac{v'_0}{v_0} - 1 \right) \times \right. \\
&\quad \times \left[\left(\frac{X_\odot(t_0)}{R_\odot} \right)^2 \xi(t_0) + \frac{X_\odot(t_0) Y_\odot(t_0)}{R_\odot^2} \eta(t_0) \right] \\
&\quad - X_\odot(t_0) [\Gamma_1(Z_\odot^2(t_0) + 2 Z_\odot(t_0) \zeta(t_0)) \\
&\quad \left. - \frac{1}{2} \Gamma_2(Z_\odot^4(t_0) + 4 Z_\odot^3(t_0) \zeta(t_0))] \right\}, \\
\ddot{Y}_\star(t_0) &= -\frac{v_0^2}{R_\odot^2} \left\{ Y_\odot(t_0) + \eta(t_0) + 2 \left(R_\odot \frac{v'_0}{v_0} - 1 \right) \times \right. \\
&\quad \times \left[\frac{X_\odot(t_0) Y_\odot(t_0)}{R_\odot^2} \xi(t_0) + \left(\frac{Y_\odot(t_0)}{R_\odot} \right)^2 \eta(t_0) \right] \\
&\quad - Y_\odot(t_0) [\Gamma_1(Z_\odot^2(t_0) + 2 Z_\odot(t_0) \zeta(t_0)) \\
&\quad \left. - \frac{1}{2} \Gamma_2(Z_\odot^4(t_0) + 4 Z_\odot^3(t_0) \zeta(t_0))] \right\}, \\
\ddot{Z}_\star(t_0) &= -\gamma^2 Z_\star(t_0) + \kappa Z_\star(t_0) |Z_\star(t_0)|, \tag{4.48}
\end{aligned}$$

where $\xi(t_0) = X_\star(t_0) - X_\odot(t_0)$, $\eta(t_0) = Y_\star(t_0) - Y_\odot(t_0)$, $\zeta(t_0) = Z_\star(t_0) - Z_\odot(t_0)$. The last equation is equivalent to Eqs. (4.5) without the two-body problem terms. To have a better understanding of the motion and to know the role of the light velocity it is important to find initial conditions for the motion along the x and y directions. Considering that measured values $\Delta \dot{X}_0(t_0)$, $\Delta \dot{Y}_0(t_0)$ and $\Delta \dot{Z}_0(t_0)$ are given by first and second derivatives (the first two terms of the Taylor expansion), we may neglect higher terms in Eqs. (4.46). Hence,

$$\begin{aligned}
\Delta \dot{X}_0(t_0) &= \dot{X}_\star(t_0) - \dot{X}_\odot(t_0) - \ddot{X}_\star(t_0) \left(\frac{r_0}{c} \right), \\
\Delta \dot{Y}_0(t_0) &= \dot{Y}_\star(t_0) - \dot{Y}_\odot(t_0) - \ddot{Y}_\star(t_0) \left(\frac{r_0}{c} \right), \\
\Delta \dot{Z}_0(t_0) &= \dot{Z}_\star(t_0) - \dot{Z}_\odot(t_0) - \ddot{Z}_\star(t_0) \left(\frac{r_0}{c} \right), \tag{4.49}
\end{aligned}$$

therefore, $\dot{X}_\star(t_0)$, $\dot{Z}_\star(t_0)$ and $\dot{Z}_\star(t_0)$ are given by

$$\begin{aligned}\dot{X}_\star(t_0) &= \Delta\dot{X}_0(t_0) + \dot{X}_\odot(t_0) + \ddot{X}_\star(t_0) \left(\frac{r_0}{c}\right), \\ \dot{Y}_\star(t_0) &= \Delta\dot{Y}_0(t_0) + \dot{Y}_\odot(t_0) + \ddot{Y}_\star(t_0) \left(\frac{r_0}{c}\right), \\ \dot{Z}_\star(t_0) &= \Delta\dot{Z}_0(t_0) + \dot{Z}_\odot(t_0) + \ddot{Z}_\star(t_0) \left(\frac{r_0}{c}\right).\end{aligned}\tag{4.50}$$

Putting back Eq. (4.50) into Eq. (4.45) we get

$$\begin{aligned}\Delta X_0(t_0) &= X_\star(t_0) - X_\odot(t_0) \\ &\quad - \left[\Delta\dot{X}_0(t_0) + \dot{X}_\odot(t_0) + \ddot{X}_\star(t_0) \left(\frac{r_0}{c}\right) \right] \frac{r_0}{c} \\ &\quad + \frac{1}{2} \ddot{X}_\star(t_0) \left(\frac{r_0}{c}\right)^2, \\ \Delta Y_0(t_0) &= Y_\star(t_0) - Y_\odot(t_0) \\ &\quad - \left[\Delta\dot{Y}_0(t_0) + \dot{Y}_\odot(t_0) + \ddot{Y}_\star(t_0) \left(\frac{r_0}{c}\right) \right] \frac{r_0}{c} \\ &\quad + \frac{1}{2} \ddot{Y}_\star(t_0) \left(\frac{r_0}{c}\right)^2, \\ \Delta Z_0(t_0) &= Z_\star(t_0) - Y_\odot(t_0) \\ &\quad - \left[\Delta\dot{Z}_0(t_0) + \dot{Y}_\odot(t_0) + \ddot{Z}_\star(t_0) \left(\frac{r_0}{c}\right) \right] \frac{r_0}{c} \\ &\quad + \frac{1}{2} \ddot{Z}_\star(t_0) \left(\frac{r_0}{c}\right)^2,\end{aligned}\tag{4.51}$$

then,

$$\begin{aligned}X_\star(t_0) &= \Delta X_0(t_0) + X_\odot(t_0) \\ &\quad + \left[\Delta\dot{X}_0(t_0) + \dot{X}_\odot(t_0) + \frac{1}{2} \ddot{X}_\star(t_0) \left(\frac{r_0}{c}\right) \right] \frac{r_0}{c}, \\ Y_\star(t_0) &= \Delta Y_0(t_0) + Y_\odot(t_0) \\ &\quad + \left[\Delta\dot{Y}_0(t_0) + \dot{Y}_\odot(t_0) + \frac{1}{2} \ddot{Y}_\star(t_0) \left(\frac{r_0}{c}\right) \right] \frac{r_0}{c}, \\ Z_\star(t_0) &= \Delta Z_0(t_0) + Y_\odot(t_0) \\ &\quad + \left[\Delta\dot{Z}_0(t_0) + \dot{Z}_\odot(t_0) + \frac{1}{2} \ddot{Z}_\star(t_0) \left(\frac{r_0}{c}\right) \right] \frac{r_0}{c}.\end{aligned}\tag{4.52}$$

Previous equations represent the initial conditions at time t_0 for the object's motion along the x , y and z directions. To describe the relative motion along x , y and z directions, we have to know the initial conditions for each motion. First, we find the initial conditions for the motion along z , then we put this into first and second equations of Eqs. (4.48), and therefore we put these two equations for $\ddot{X}_\star(t_0)$ and $\ddot{Y}_\star(t_0)$ into first and second equations of Eqs. (4.52). From this we get a system of two equations for $X_\star(t_0)$ and $Y_\star(t_0)$. By solving this system we find the initial conditions for the motion along x and y . Since in this Chapter we focus on the solar and star's motion along the z -axis, we give a complete expression for initial conditions of the motion along z . We solve the second order equation given by

$$a Z_\star^2(t_0) + b Z_\star(t_0) + c = 0 , \quad (4.53)$$

then, we get

$$Z_\star(t_0) = \frac{-b \pm \sqrt{b^2 - 4ac}}{2a} , \quad (4.54)$$

where,

$$\begin{aligned} a &= \left[\kappa \left(\frac{r_0}{c} \right)^2 + \frac{\kappa}{2} \left(\frac{r_0}{c} \right)^2 \right] = \frac{3\kappa}{2} \left(\frac{r_0}{c} \right)^2 , \\ b &= \left[1 + \gamma^2 \left(\frac{r_0}{c} \right)^2 - \frac{\gamma^2}{2} \left(\frac{r_0}{c} \right)^2 \right] = \left[1 + \frac{\gamma^2}{2} \left(\frac{r_0}{c} \right)^2 \right] , \\ c &= - \left[Z_\odot(t_0) + \dot{Z}_\odot(t_0) \left(\frac{r_0}{c} \right) + \Delta Z_0(t_0) + \Delta \dot{Z}_0(t_0) \left(\frac{r_0}{c} \right) \right] , \end{aligned} \quad (4.55)$$

are computed values from known parameters described in this chapter. To compute the initial condition of the velocity at t_0 we can use the third equation of Eqs. (4.50), from where we get

$$\dot{Z}_\star(t_0) = \Delta \dot{Z}_0(t_0) + \dot{Z}_\odot(t_0) + [-\gamma^2 Z_\star(t_0) + \kappa Z_\star(t_0) |Z_\star(t_0)|] \left(\frac{r_0}{c} \right) , \quad (4.56)$$

where we replaced the value of $\ddot{Z}_\star(t_0)$ by the third equation of Eqs. (4.48). Here, γ and κ are computed from Eqs. (4.11), r_0 , $\Delta Z_0(t_0)$, $\Delta \dot{Z}_0(t_0)$ are given from observational data by Eqs. (4.43,4.44), c is the speed of light, $Z_\odot(t_0)$ and $\dot{Z}_\odot(t_0)$ are given by Eqs. (4.9). As we explained in this chapter, we focus on the relative motion Sun-object, where objects are considered to be close to the Sun. In our computations we show results for

objects which are close to the Sun. Since at this moment the solar motion along the z -axis is oriented toward up, and in addition the Sun is situated 30 pc above the galactic equatorial plane, we focus our study on positive values of $Z_*(t_0)$. Also, in our work we carry out computations assuming that $t_0 = 0$.

4.2.4 The perihelion position vector

In this subsection we compute the perihelion position vector \mathbf{q} for this simple case. We proceed as for the non-interacting system. We minimize the following equation

$$r(t) = \sqrt{[\Delta X(t)]^2 + [\Delta Y(t)]^2 + [\Delta Z(t)]^2}, \quad (4.57)$$

where ΔX , ΔY and ΔZ are given in Eqs. (4.27). For $\Delta Z = Z_*(t) - Z_\odot(t)$ we get

$$\begin{aligned} \Delta Z(t) &= Z_*(t) - Z_\odot(t), \\ &= k_1 \sin(\gamma t) + k_2 \cos(\gamma t) - k_3 \cos(2\gamma t) \\ &\quad + k_4 \sin(2\gamma t) + k_5, \end{aligned} \quad (4.58)$$

where,

$$\begin{aligned} k_1 &= \frac{\dot{Z}_*(0) - \dot{Z}_\odot(0)}{\gamma} - [q_* a_*^2 \cos(2\phi_*) - q_\odot a_\odot^2 \cos(2\phi_\odot)] \frac{\kappa}{3\gamma^2}, \\ k_2 &= [Z_*(0) - Z_\odot(0)] + \left\{ q_* a_*^2 \left[\frac{\cos(2\phi_*)}{3} - 1 \right] - q_\odot a_\odot^2 \left[\frac{\cos(2\phi_\odot)}{3} - 1 \right] \right\} \frac{\kappa}{2\gamma^2}, \\ k_3 &= [q_* a_*^2 \cos(2\phi_*) - q_\odot a_\odot^2 \cos(2\phi_\odot)] \frac{\kappa}{6\gamma_0^2}, \\ k_4 &= [q_* a_*^2 \sin(2\phi_*) - q_\odot a_\odot^2 \sin(2\phi_\odot)] \frac{\kappa}{6\gamma_0^2}, \\ k_5 &= (q_* a_*^2 - q_\odot a_\odot^2), \end{aligned} \quad (4.59)$$

are known values. The point is easy, to find $(r)_{min} = r_{min}$, at first we look for $(t)_{min} = t_{min}$, and that is all. Minimizing Eq. (4.57), we find

$$\begin{aligned} 0 &= [\Delta \dot{X}_0(0) t + \Delta X_0(0)] \Delta \dot{X}_0(0) + [\Delta \dot{Y}_0(0) t + \Delta Y_0(0)] \Delta \dot{Y}_0(0) \\ &\quad + [k_1 \sin(\gamma t) + k_2 \cos(\gamma t) - k_3 \cos(2\gamma t) + k_4 \sin(2\gamma t) + k_5] \times \\ &\quad \times [\gamma k_1 \cos(\gamma t) - \gamma k_2 \sin(\gamma t) + 2\gamma k_3 \sin(2\gamma t) + 2\gamma k_4 \cos(2\gamma t)] . \end{aligned} \quad (4.60)$$

Previous equation may be written as

$$\begin{aligned}
0 = & \left[\Delta \dot{X}_0(0) t + \Delta X_0(0) \right] \Delta \dot{X}_0(0) + \left[\Delta \dot{Y}_0(0) t + \Delta Y_0(0) \right] \Delta \dot{Y}_0(0) \\
& + \sum_{i=1}^4 f_i \sin(i\gamma t) + \sum_{j=1}^4 h_j \cos(j\gamma t) .
\end{aligned} \tag{4.61}$$

Previous equation has to be solved numerically, but by using Taylor expansions for sine and cosine we can discover the role of higher terms. As a good approach, for short times, we can consider: $\sin(i\gamma t) \approx i\gamma t$ and $\cos(j\gamma t) \approx 1$, then

$$\begin{aligned}
0 = & \left\{ \left[\Delta \dot{X}_0(0) \right]^2 + \left[\Delta \dot{Y}_0(0) \right]^2 + \sum_{i=1}^4 i f_i \gamma \right\} t \\
& + \sum_{j=1}^4 h_j + \Delta X_0(0) \Delta \dot{X}_0(0) + \Delta Y_0(0) \Delta \dot{Y}_0(0) .
\end{aligned} \tag{4.62}$$

Now, the time t , corresponds to t_{min} , then

$$t_{min} = - \frac{\Delta X_0(0) \Delta \dot{X}_0(0) + \Delta Y_0(0) \Delta \dot{Y}_0(0) + \sum_{j=1}^4 h_j}{[\Delta \dot{X}_0(0)]^2 + [\Delta \dot{Y}_0(0)]^2 + \sum_{i=1}^4 i f_i \gamma} , \tag{4.63}$$

where,

$$\begin{aligned}
h_1 &= \left(\frac{k_2 k_4 + k_1 k_3}{2} + k_1 k_5 \right) \gamma , \\
h_2 &= (k_1 k_2 + 2 k_4 k_5) \gamma , \\
h_3 &= (2 k_2 k_4 - k_1 k_3) \frac{\gamma}{2} , \\
h_4 &= - \left(\frac{2 k_1 k_3 + k_2 k_4}{2} - 2 k_3 k_4 \right) \gamma ,
\end{aligned} \tag{4.64}$$

and

$$\begin{aligned}
f_1 &= \left(\frac{k_2 k_3 - k_1 k_4}{2} - k_2 k_5 \right) \gamma , \\
f_2 &= \left(\frac{k_1^2 - k_2^2}{2} + 2 k_3 k_5 \right) \gamma , \\
f_3 &= 3 (k_1 k_4 + k_2 k_3) \frac{\gamma}{2} , \\
f_4 &= (k_4^2 - k_3^2) \gamma .
\end{aligned} \tag{4.65}$$

Hence,

$$r(t_{min}) = \sqrt{[\Delta X(t_{min})]^2 + [\Delta Y(t_{min})]^2 + [\Delta Z(t_{min})]^2}, \quad (4.66)$$

represents the perihelion distance for this simple case assuming anharmonic oscillations along the z -axis. The perihelion position vector is given by Eq. (4.27), where for short times $t = t_{min}$ is a good approach, then

$$\mathbf{q} = (\Delta X(t_{min}), \Delta Y(t_{min}), \Delta Z(t_{min})) ,$$

$$t_{min} = - \frac{\Delta X_0(0)\Delta \dot{X}_0(0) + \Delta Y_0(0)\Delta \dot{Y}_0(0) + \sum_{j=1}^4 h_j}{[\Delta \dot{X}_0(0)]^2 + [\Delta \dot{Y}_0(0)]^2 + \sum_{i=1}^4 i f_i \gamma} . \quad (4.67)$$

Solving Eq. (5.28) numerically we obtain results not only for short times. As we said, we use observational data for our computations. These data are measured in equatorial coordinates, and since we focus on motions in the Galaxy, we will use the galactic coordinate system.

4.3 The Equatorial and galactic Coordinates

The most frequently used such system is the equatorial coordinate system which is still related to planet Earth and thus convenient for observers as is used in Eqs. (4.28, 4.29) and other equations in this Thesis. As we know the first coordinate in the equatorial system, corresponding to the latitude, is called Declination, δ , and is the angle between the position of an object and the celestial equator, and the longitudinal coordinate, called Right Ascension, α , that is the angle in degrees(or hours) measured from the Vernal Equinox along the celestial equator toward the east to the foot of the hour circle which passes through the object. Dealing with motions in the Galaxy, we will use the galactic coordinate system with the galactic longitude l and the galactic latitude b . We consider a spherical coordinate system, with its center being at the location of the Sun. The galactic plane is the plane of the galactic disk, i.e., it is parallel to the band of the Galaxy. The two galactic coordinates l and b are angular coordinates on the sphere. Here, b denotes the galactic latitude, the angular distance of a source from the galactic plane, with $b \in [-90^\circ, +90^\circ]$. The great circle $b = 0^\circ$ is then located in the plane of the galactic disk and denotes the North galactic Pole, while $b = -90^\circ$ marks

the direction to the South galactic Pole. The second angular coordinate is the galactic longitude l , with $l \in [0^\circ, 360^\circ]$. It measures the angular separation between the position of a source, projected perpendicularly onto the galactic disk, and the galactic center, which itself has angular coordinates $b = 0^\circ$ and $l = 0^\circ$. Given l and b for a source, its location on the sky is fully specified. In order to specify its three-dimensional location, the distance of that source from us is also needed. The conversion of the positions of sources given in equatorial coordinates (α, δ) to that in galactic coordinates is obtained from the rotation between these two coordinate systems, and is described by spherical trigonometry. In the next lines we give the necessary formulae to carry out this transformation.

The coordinates of a star at $t_0 = 0$ with respect to the Sun in the galactic coordinate system are

$$\begin{aligned}\Delta X_0(0) &= r \cos l \cos b, \\ \Delta Y_0(0) &= r \sin l \cos b, \\ \Delta Z_0(0) &= r \sin b,\end{aligned}\tag{4.68}$$

where l and b are computed from equatorial coordinates α and δ . The velocity of the star at $t_0 = 0$ with respect to the Sun in galactic coordinates is

$$\begin{aligned}\Delta \dot{X}_0(0) &= \dot{r} \cos l \cos b \\ &\quad - 4.74 r \{(\mu_l \cos b) \sin l + \mu_b \cos l \sin b\}, \\ \Delta \dot{Y}_0(0) &= \dot{r} \sin l \cos b \\ &\quad + 4.74 r \{(\mu_l \cos b) \cos l - \mu_b \sin l \sin b\}, \\ \Delta \dot{Z}_0(0) &= \dot{r} \sin b + 4.74 r \mu_b \cos b,\end{aligned}\tag{4.69}$$

where \dot{r} is the radial velocity and μ_l, μ_b are the proper motions in the galactic longitude and latitude, respectively. Since the units used in our calculations are $[v] = [\dot{r}] = km\ s^{-1}$, $[r] = pc$, $[\mu_l] = [\mu_b] = ''\ yr^{-1}$, the numerical factor in Eq. (7.3) is 4.74. To get Eq. (4.69) and Eq. (4.68) we have to know the proper motions in l and b directions, and, the galactic coordinates (l, b) . For this reason in the next subsections we show how to carry this out.

4.3.1 The conversion from (α, δ) to (l, b)

From observational data we know the equatorial coordinates (α, δ) , then the galactic coordinates (l, b) can be obtained from

$$\begin{aligned}\cos b \cos(l - l_0) &= \cos \delta \sin(\alpha - \alpha_0) , \\ \cos b \sin(l - l_0) &= \sin \delta \cos \delta_0 - \cos \delta \sin \delta_0 \cos(\alpha - \alpha_0) , \\ \sin b &= \sin \delta \sin \delta_0 + \cos \delta \cos \delta_0 \cos(\alpha - \alpha_0) ,\end{aligned}\tag{4.70}$$

where $l_0 = 33.932^\circ$, $\alpha_0 = 192.85948^\circ$, and $\delta_0 = 27.17825^\circ$ for the Epoch J2000.0. If α and δ are given, then Eqs. (4.70) offer

$$\begin{aligned}b &= \arcsin(\sin \delta \sin \delta_0 + \cos \delta \cos \delta_0 \cos(\alpha - \alpha_0)) , \\ \cos(l - l_0) &= \frac{1}{\cos b} \cos \delta \sin(\alpha - \alpha_0) , \\ \sin(l - l_0) &= \frac{1}{\cos b} \sin \delta \cos \delta_0 - \cos \delta \sin \delta_0 \cos(\alpha - \alpha_0) .\end{aligned}\tag{4.71}$$

In Eqs. (4.71): from the first equation we compute b , second and third equations allow us to calculate l by using Tab. 3.1.

4.3.2 Proper motions

Stars are moving relative to us or, more precisely, relative to the Sun. To study the kinematics of the Galaxy we need to be able to measure the velocities of stars. To know the components of the velocity in Eqs. (7.3), besides v_r which is a known value for each star, the values of proper motions $(\mu_l \cos b)$ and μ_b are also required. It is carried out by doing the transformation from equatorial to galactic coordinates. $(\mu_l \cos b)$ and μ_b are computed from

$$\begin{aligned}\mu_l \cos b &= \mu_\alpha \cos \delta \cos \psi + \mu_\delta \sin \psi , \\ \mu_b &= -\mu_\alpha \cos \delta \sin \psi + \mu_\delta \cos \psi .\end{aligned}\tag{4.72}$$

The angle ψ is found by using Tab. 3.1 from the $\sin \psi$ and $\cos \psi$ relations given in the following equations,

$$\begin{aligned}\cos b \sin \psi &= \cos \delta_0 \sin(\alpha - \alpha_0) , \\ \cos b \cos \psi &= \sin \delta_0 \cos(\alpha - \alpha_0) - \cos \delta_0 \sin \delta \cos(\alpha - \alpha_0) ,\end{aligned}\quad (4.73)$$

or just by replacing in Eqs. (4.72) the values of $\sin \psi$ and $\cos \psi$ given by

$$\begin{aligned}\sin \psi &= \frac{1}{\cos b} [\cos \delta_0 \sin(\alpha - \alpha_0)] , \\ \cos \psi &= \frac{1}{\cos b} [\sin \delta_0 \cos(\alpha - \alpha_0) - \cos \delta_0 \sin \delta \cos(\alpha - \alpha_0)] ,\end{aligned}\quad (4.74)$$

then, the proper motions in galactic coordinates to be used are:

$$\begin{aligned}\mu_l \cos b &= \mu_\alpha \cos \delta \frac{1}{\cos b} [\sin \delta_0 \cos(\alpha - \alpha_0) - \cos \delta_0 \sin \delta \cos(\alpha - \alpha_0)] \\ &\quad + \mu_\delta \frac{1}{\cos b} [\cos \delta_0 \sin(\alpha - \alpha_0)] , \\ \mu_b &= -\mu_\alpha \cos \delta \frac{1}{\cos b} [\cos \delta_0 \sin(\alpha - \alpha_0)] \\ &\quad + \mu_\delta \frac{1}{\cos b} [\sin \delta_0 \cos(\alpha - \alpha_0) - \cos \delta_0 \sin \delta \cos(\alpha - \alpha_0)] .\end{aligned}\quad (4.75)$$

Chapter 5

Summary of main equations

In this chapter we summarize the theoretical results to find the perihelion position vector \mathbf{q} and the impact parameter b . We show this in three cases: the non-interacting system, the two-body problem, and, the simple model, where in addition to the gravitational influence of the Sun, we consider that the object is perturbed by the gravitational effects of the Galaxy (the relative motion of the object with respect to the Sun depends linearly on time for x and y coordinates and that there are anharmonic oscillations along the z -axis). Here, equations for the perihelion position vector and for the impact parameter are computed from known observational data.

5.1 Observational data

In this section we describe what exactly is measured, and how it is transformed to carry out our computations. For a given star we know from observational data the equatorial coordinates (α, δ) , then by using next equation we find the galactic coordinates (l, b) ,

$$\begin{aligned} b &= \arcsin(\sin \delta \sin \delta_0 + \cos \delta \cos \delta_0 \cos(\alpha - \alpha_0)) , \\ \cos(l - l_0) &= \frac{1}{\cos b} \cos \delta \sin(\alpha - \alpha_0) , \\ \sin(l - l_0) &= \frac{1}{\cos b} \sin \delta \cos \delta_0 - \cos \delta \sin \delta_0 \cos(\alpha - \alpha_0) . \end{aligned} \quad (5.1)$$

The correct angle, l , is found by using Tab. 6.2. Once that is done, we are able to find

$$\begin{aligned}\Delta X_0(t_0) &= r_0 \cos l \cos b, \\ \Delta Y_0(t_0) &= r_0 \sin l \cos b, \\ \Delta Z_0(t_0) &= r_0 \sin b,\end{aligned}\tag{5.2}$$

which represents the position coordinates at $t_0 = 0$ and,

$$\begin{aligned}\Delta \dot{X}_0(t_0) &= \dot{r}_0 \cos l \cos b \\ &\quad - 4.74 r_0 \{(\mu_l \cos b) \sin l + \mu_b \cos l \sin b\}, \\ \Delta \dot{Y}_0(t_0) &= \dot{r}_0 \sin l \cos b \\ &\quad + 4.74 r_0 \{(\mu_l \cos b) \cos l - \mu_b \sin l \sin b\}, \\ \Delta \dot{Z}_0(t_0) &= \dot{r}_0 \sin b + 4.74 r_0 \mu_b \cos b,\end{aligned}\tag{5.3}$$

which allow us to compute the velocity at t_0 , r_0 is the heliocentric distance of the object, \dot{r}_0 is the radial velocity of the object with respect to the Sun, and μ_l , μ_b are the proper motions in the galactic longitude and latitude at $t_0 = 0$, respectively. The units used in our calculations are: $[v] = [\dot{r}] = km\ s^{-1}$, $[r] = pc$, $[\mu_l] = [\mu_b] = ''\ yr^{-1}$. Also, here we notice that

$$\begin{aligned}\mathbf{r}_0(t_0) &= [\Delta X_0(t_0), \Delta Y_0(t_0), \Delta Z_0(t_0)], \\ \mathbf{v}_0(t_0) &= [\Delta \dot{X}_0(t_0), \Delta \dot{Y}_0(t_0), \Delta \dot{Z}_0(t_0)],\end{aligned}\tag{5.4}$$

are the measured initial velocity and position vectors of the object with respect to the Sun, which we compute from equatorial coordinates. In the following sections we label (as we also did in the previous section) $\mathbf{r}_0 = (x_0, y_0, z_0)$ and $\mathbf{v}_0 = (v_{x,0}, v_{y,0}, v_{z,0})$.

5.2 Non-interacting system

From observational data we know $\mathbf{r}_0 = (x_0, y_0, z_0)$ and $\mathbf{v}_0 = (v_{x,0}, v_{y,0}, v_{z,0})$, which are the initial ($t = 0$) position and velocity vectors of the object with respect to the Sun.

The impact parameter is computed as

$$b = \frac{1}{v_0^2} \left\{ \begin{aligned} & \left[x_0 (v_{y,0}^2 + v_{z,0}^2) - (y_0 v_{y,0} + z_0 v_{z,0}) v_{x,0} \right]^2 \\ & + \left[y_0 (v_{x,0}^2 + v_{z,0}^2) - (x_0 v_{x,0} + z_0 v_{z,0}) v_{y,0} \right]^2 \\ & + \left[z_0 (v_{x,0}^2 + v_{y,0}^2) - (x_0 v_{x,0} + y_0 v_{y,0}) v_{z,0} \right]^2 \end{aligned} \right\}^{1/2}, \quad (5.5)$$

where $v_0^2 = v_{x,0}^2 + v_{y,0}^2 + v_{z,0}^2$. and the perihelion position vector is

$$\mathbf{q} = \mathbf{r}_b - \mathbf{r}_\odot = \mathbf{r}_0 + \mathbf{v}_0 t_b, \quad t_b = - \frac{x_0 v_{x,0} + y_0 v_{y,0} + z_0 v_{z,0}}{v_{x,0}^2 + v_{y,0}^2 + v_{z,0}^2}. \quad (5.6)$$

5.3 The two-body problem

Initial conditions $\mathbf{r}_0 = (x_0, y_0, z_0)$, $\mathbf{v}_0 = (v_{x,0}, v_{y,0}, v_{z,0}) \Rightarrow \mathbf{H}_0 \equiv (H_{x,0}, H_{y,0}, H_{z,0})$, $\mathbf{H}_0 = \mu \mathbf{r}_0 \times \mathbf{v}_0$ are given from observational data. The impact parameter, we get from

$$\begin{aligned} b &= \frac{G(M+m)}{v_\infty^2} \frac{1 + \cos \theta}{\sin \theta}, \\ &= \frac{G(m+M)}{v_\infty^2} \cot \left(\frac{\theta}{2} \right), \end{aligned} \quad (5.7)$$

where, $\theta = 2\pi - \varphi$, m is the mass of the object, M is the solar mass, and v_∞ is the magnitude of the velocity vector in the infinity that is found from conservation of energy and given by

$$v_\infty = \sqrt{\frac{2}{\mu} \left(\frac{\mu}{2} v_0^2 + \frac{k}{r_0} \right)}. \quad (5.8)$$

The perihelion position vector,

$$\mathbf{q} \equiv \mathbf{r}_p = (x_p, y_p, z_p) = \begin{cases} x_p &= r_p (\cos \Omega_0 \cos \omega_0 - \sin \Omega_0 \sin \omega_0 \cos i_0), \\ y_p &= r_p (\cos \omega_0 \sin \Omega_0 + \sin \omega_0 \cos \Omega_0 \cos i_0), \\ z_p &= r_p \sin \omega_0 \sin i_0. \end{cases} \quad (5.9)$$

where $|\mathbf{r}_p| \equiv |(x_p, y_p, z_p)| = a(1 - \epsilon)$, i_0 is computed from

$$i_0 = \arccos \left(\frac{H_{z,0}}{|\mathbf{H}_0|} \right), \quad (5.10)$$

Ω_0 from

$$\sin \Omega_0 = \frac{H_{x,0}}{|\mathbf{H}_0| \sin i_0}, \quad \cos \Omega_0 = -\frac{H_{y,0}}{|\mathbf{H}_0| \sin i_0}. \quad (5.11)$$

The correct value of Ω_0 is computed by using Tab. 6.2. Θ_0 is computed as

$$\sin \Theta_0 = \frac{z_0}{r_0 \sin i_0}, \quad \cos \Theta_0 = \frac{y_0 H_{x,0} - x_0 H_{y,0}}{r_0 |\mathbf{H}_0| \sin i_0}, \quad (5.12)$$

where, we also use Tab. 6.2 to find the right value of Θ_0 . And the last one, ω_0 , we compute from,

$$\sin(\Theta_0 - \omega_0) = \frac{\mathbf{v}_0 \cdot \mathbf{e}_{r,0}}{\epsilon \sqrt{G(M+m)/p}}, \quad \cos(\Theta_0 - \omega_0) = \frac{\mathbf{v}_0 \cdot \mathbf{e}_{t,0}}{\epsilon \sqrt{G(M+m)/p}} - \frac{1}{\epsilon}, \quad (5.13)$$

where as for the previous cases, here, we obtain the right angle by using Tab. 6.2. \mathbf{e}_r is defined as

$$\mathbf{e}_r = (\cos \Omega \cos \Theta - \sin \Omega \sin \Theta \cos i, \cos \Theta \sin \Omega + \sin \Theta \cos \Omega \cos i, \sin \Theta \sin i), \quad (5.14)$$

and, \mathbf{e}_t is the unit vector onto the transversal direction

$$\mathbf{e}_t = (-\cos \Omega \sin \Theta - \sin \Omega \cos \Theta \cos i, -\sin \Omega \sin \Theta + \cos \Omega \cos \Theta \cos i, \cos \Theta \sin i). \quad (5.15)$$

At initial time $t = 0$, $\mathbf{e}_{r,0}$ and $\mathbf{e}_{t,0}$ are given by angles i_0 , Ω_0 and by Θ_0 from equations (5.10), (5.11), (5.12), respectively. For the time when the object passes the perihelion position, Θ_0 changes its value to Θ_p , it means that we also need to know Θ_p , which can be computed assuming that $\Theta_0 = \omega_0$, and ω_0 is computed from Eq. (5.13). Here, v_0 , $\mathbf{e}_{r,0}$ and $\mathbf{e}_{t,0}$ are computed from initial conditions, since $\mathbf{e}_{r,0} = \mathbf{r}_0/|\mathbf{r}_0|$, or just by using equations (5.10), (5.11), (5.12).

5.3.1 Choosing the right angle

Let

$$\begin{aligned} \cos \vartheta &= A, \\ \sin \vartheta &= B, \end{aligned} \quad (5.16)$$

where A and B are known numbers computed from the right sides of given equations. These numbers can be positive or negative, then we need to know which quadrant the angle belongs. It is recommended to remember where $\sin \vartheta$, $\cos \vartheta$ and $\tan \vartheta$ are positive (or negative). Table 3.1 allows us to solve problems as the given in Eq. (5.16).

	$\sin \vartheta > 0$	$\sin \vartheta < 0$	$\sin \vartheta = 0$
$\cos \vartheta > 0$	$\vartheta = \arccos A$	$\vartheta = 2\pi - \arccos A$	$\vartheta = 0$
$\cos \vartheta < 0$	$\vartheta = \arccos A$	$\vartheta = 2\pi - \arccos A$	$\vartheta = \pi$
$\cos \vartheta = 0$	$\vartheta = \pi/2$	$\vartheta = 3\pi/2$	

Table 5.1: Choosing the right angle

5.4 Galactic tide

The third equations of Eqs. (5.2, 5.3) are important in equations given by

$$\begin{aligned} Z_{\star} \left(-\frac{r_0}{c} \right) &= \Delta Z_0(0) + Z_{\odot}(0) , \\ \dot{Z}_{\star} \left(-\frac{r_0}{c} \right) &= \Delta \dot{Z}_0(0) + \dot{Z}_{\odot}(0) . \end{aligned} \quad (5.17)$$

which permits us to find $Z_{\star}(0)$ and $\dot{Z}_{\star}(0)$ for the case when $u = 0$ given by

$$Z_{\star}(0) = \begin{vmatrix} g_1 & -\sin(\gamma r_0/c)/\gamma \\ g_2 & \cos(\gamma r_0/c) \end{vmatrix} , \quad (5.18)$$

$$\dot{Z}_{\star}(0) = \begin{vmatrix} \cos(\gamma r_0/c) & g_1 \\ \sin(\gamma r_0/c) & g_2 \end{vmatrix} , \quad (5.19)$$

where g_1 and g_2 are known values given by

$$g_1 = Z_{\star} \left(-\frac{r_0}{c} \right) , \quad g_2 = \dot{Z}_{\star} \left(-\frac{r_0}{c} \right) . \quad (5.20)$$

In Eqs. (5.17), $\Delta Z_0(0)$ and $\Delta \dot{Z}_0(0)$ are given from measured (observational) data, from Eqs. (5.2, 5.3), and, $Z_{\odot}(0)$ and \dot{Z}_{\odot} are given by

$$Z_{\odot}(0) = 30 \text{ pc}, \quad \dot{Z}_{\odot}(0) = 7.3 \text{ km s}^{-1}. \quad (5.21)$$

The initial conditions for the motion along the z -axis when $u \neq 0$, $Z_*(t_0)$, are given by

$$\begin{aligned} Z_*(t_0) &= \frac{-b \pm \sqrt{b^2 - 4ac}}{2a}, \\ \dot{Z}_*(t_0) &= \Delta\dot{Z}_0(t_0) + \dot{Z}_\odot(t_0) + [-\gamma^2 Z_*(t_0) + \kappa Z_*(t_0)|Z_*(t_0)|] \left(\frac{r_0}{c}\right), \end{aligned} \quad (5.22)$$

where,

$$\begin{aligned} a &= \left[\kappa \left(\frac{r_0}{c}\right)^2 + \frac{\kappa}{2} \left(\frac{r_0}{c}\right)^2 \right] = \frac{3\kappa}{2} \left(\frac{r_0}{c}\right)^2, \\ b &= \left[1 + \gamma^2 \left(\frac{r_0}{c}\right)^2 - \frac{\gamma^2}{2} \left(\frac{r_0}{c}\right)^2 \right] = \left[1 + \frac{\gamma^2}{2} \left(\frac{r_0}{c}\right)^2 \right], \\ c &= - \left[Z_\odot(t_0) + \dot{Z}_\odot(t_0) \left(\frac{r_0}{c}\right) + \Delta Z_0(t_0) + \Delta\dot{Z}_0(t_0) \left(\frac{r_0}{c}\right) \right], \end{aligned} \quad (5.23)$$

are computed values from known parameters described in the previous chapter. Here, γ and κ are computed from

$$\begin{aligned} \gamma^2 &= 4\pi G(\varrho_d + \varrho_h) + 2(A^2 - B^2), \\ \kappa &= 2\pi G u \varrho_d. \end{aligned} \quad (5.24)$$

r_0 , $\Delta Z_0(t_0)$, $\dot{Z}_0(t_0)$ are given from observational data, c is the speed of light, and, $Z_\odot(t_0)$ and $\dot{Z}_\odot(t_0)$ from Eqs. (5.21). As initial conditions for the star's motion along the z -axis we consider positive values, only. Now, we are able to compute $\Delta Z(t)$ for any value of u . To find the perihelion position vector we minimize

$$r(t) = \sqrt{[\Delta X(t)]^2 + [\Delta Y(t)]^2 + [\Delta Z(t)]^2}, \quad (5.25)$$

where ΔX , ΔY and ΔZ are given in Eqs. (4.27). For $\Delta Z = Z_*(t) - Z_\odot(t)$ we get

$$\begin{aligned} \Delta Z(t) &= Z_*(t) - Z_\odot(t), \\ &= k_1 \sin(\gamma t) + k_2 \cos(\gamma t) - k_3 \cos(2\gamma t) \\ &\quad + k_4 \sin(2\gamma t) + k_5, \end{aligned} \quad (5.26)$$

where,

$$\begin{aligned}
k_1 &= \frac{\dot{Z}_\star(0) - \dot{Z}_\odot(0)}{\gamma} - [q_\star a_\star^2 \cos(2\phi_\star) - q_\odot a_\odot^2 \cos(2\phi_\odot)] \frac{\kappa}{3\gamma^2}, \\
k_2 &= [Z_\star(0) - Z_\odot(0)] + \left\{ q_\star a_\star^2 \left[\frac{\cos(2\phi_\star)}{3} - 1 \right] - q_\odot a_\odot^2 \left[\frac{\cos(2\phi_\odot)}{3} - 1 \right] \right\} \frac{\kappa}{2\gamma^2}, \\
k_3 &= [q_\star a_\star^2 \cos(2\phi_\star) - q_\odot a_\odot^2 \cos(2\phi_\odot)] \frac{\kappa}{6\gamma_0^2}, \\
k_4 &= [q_\star a_\star^2 \sin(2\phi_\star) - q_\odot a_\odot^2 \sin(2\phi_\odot)] \frac{\kappa}{6\gamma_0^2}, \\
k_5 &= (q_\star a_\star^2 - q_\odot a_\odot^2), \tag{5.27}
\end{aligned}$$

are known values. Then we get

$$\begin{aligned}
0 &= \left[\Delta \dot{X}_0(0) t + \Delta X_0(0) \right] \Delta \dot{X}_0(0) + \left[\Delta \dot{Y}_0(0) t + \Delta Y_0(0) \right] \Delta \dot{Y}_0(0) \\
&+ \sum_{i=1}^4 f_i \sin(i\gamma t) + \sum_{j=1}^4 h_j \cos(j\gamma t). \tag{5.28}
\end{aligned}$$

Previous equation has to be solved numerically, but for short times we just consider the first terms of Taylor expansions for sine and cosine, then

$$\begin{aligned}
0 &= \left\{ \left[\Delta \dot{X}_0(0) \right]^2 + \left[\Delta \dot{Y}_0(0) \right]^2 + \sum_{i=1}^4 i f_i \gamma \right\} t \\
&+ \sum_{j=1}^4 h_j + \Delta X_0(0) \Delta \dot{X}_0(0) + \Delta Y_0(0) \Delta \dot{Y}_0(0). \tag{5.29}
\end{aligned}$$

Now, the time t , corresponds to t_{min} , then

$$t_{min} = - \frac{\Delta X_0(0) \Delta \dot{X}_0(0) + \Delta Y_0(0) \Delta \dot{Y}_0(0) + \sum_{j=1}^4 h_j}{[\Delta \dot{X}_0(0)]^2 + [\Delta \dot{Y}_0(0)]^2 + \sum_{i=1}^4 i f_i \gamma}, \tag{5.30}$$

where,

$$\begin{aligned}
h_1 &= \left(\frac{k_2 k_4 + k_1 k_3}{2} + k_1 k_5 \right) \gamma, \\
h_2 &= (k_1 k_2 + 2 k_4 k_5) \gamma, \\
h_3 &= (2 k_2 k_4 - k_1 k_3) \frac{\gamma}{2}, \\
h_4 &= - \left(\frac{2 k_1 k_3 + k_2 k_4}{2} - 2 k_3 k_4 \right) \gamma, \tag{5.31}
\end{aligned}$$

and

$$\begin{aligned}
f_1 &= \left(\frac{k_2 k_3 - k_1 k_4}{2} - k_2 k_5 \right) \gamma , \\
f_2 &= \left(\frac{k_1^2 - k_2^2}{2} + 2 k_3 k_5 \right) \gamma , \\
f_3 &= 3 (k_1 k_4 + k_2 k_3) \frac{\gamma}{2} , \\
f_4 &= (k_4^2 - k_3^2) \gamma .
\end{aligned} \tag{5.32}$$

Hence,

$$r(t_{min}) = \sqrt{[\Delta X(t_{min})]^2 + [\Delta Y(t_{min})]^2 + [\Delta Z(t_{min})]^2} , \tag{5.33}$$

represents the perihelion distance for this simple case assuming anharmonic oscillations along the z -axis. The perihelion position vector is then given by Eq. (4.27), where for short times $t = t_{min}$ is a good approach, then

$$\begin{aligned}
\mathbf{q} &= (\Delta X(t_{min}), \Delta Y(t_{min}), \Delta Z(t_{min})) , \\
t_{min} &= - \frac{\Delta X_0(0) \Delta \dot{X}_0(0) + \Delta Y_0(0) \Delta \dot{Y}_0(0) + \sum_{j=1}^4 h_j}{[\Delta \dot{X}_0(0)]^2 + [\Delta \dot{Y}_0(0)]^2 + \sum_{i=1}^4 i f_i \gamma} .
\end{aligned} \tag{5.34}$$

Solving Eq. (5.28) numerically we obtain results not only for short times.

Chapter 6

Applications

In this chapter we apply our results to specific stars. As we said, we focus on stars with close passages to the Sun. Studied stars were selected in [2] and some of them in [18]. Data from [2] are in Tab. 6.1. Computed perihelion distances by Garcia [18] may differ in more than 60 % from those given by [2]. Although [18] present results for two methods of calculations (integrated orbits and rectilinear motion), [2] does not present the method of calculation. The results presented in Table 2 by [18] show that both methods (integrated orbits and rectilinear motion) are consistent for almost all considered stars: the relative error is less than 1 % for many stars. The data published by [2] are used to compare with our results. In Tab. 6.2 we show all observed parameters

star	$ \mathbf{q}_{Dyb} $ [pc]
Gl 710	0.209
Gl 127.1A	0.803
Gl 445	1.071
Barnard's Star	1.146
Gl 217.1	1.316
Gl 729	1.988
GJ 2046	2.008
Gl 54.1	2.425
LP 816-60	2.485

Table 6.1: Computed perihelion distances by Dybczyński ($|\mathbf{q}|$)[2]

used in our calculations. These were taken from *ARICNS* [15], from *NStED Data Base* [20] and from *SIMBAD Data Base* [10]. Radial velocity measurements were obtained from the astronomical literature, in particular of Wilson (1953) [11], and from other

sources as [18, 15]. By using Table 6.2 we compute l, b, μ_b and $\mu_l \cos(b)$. These values

Star	α [°]	δ [°]	μ_α	μ_δ	r_0 [pc]	\dot{r}_0 [km/s]	m [M_\odot]
Gl 710	274.963	-1.990	-0.130	-0.05	19	-13.800	0.8
Gl 127.1A	47.629	-68.600	0.037	-0.103	10.118	33.8	0.63
Gl 445	176.922	78.691	0.744	0.478	5.396	-119	0.24
Barnard's Star	269.452	4.693	-0.799	10.277	1.834	-110.6	0.16
Gl 217.1	86.739	-14.822	-0.015	-0.001	21.5	22.35	2.0
Gl 729	282.456	-23.836	0.637	-0.192	2.97	-10.7	0.17
GJ 2046	88.518	-60.023	-0.052	-0.060	12.83	30	0.75
Gl 54.1	18.128	-16.999	1.209	0.641	3.7	28.2	0.085
LP 816-60	313.138	-16.975	-0.338	0.069	5.500	15.8	0.19

Table 6.2: Parameters of some nearest stars studied in this thesis.

are given in Table 6.3. These measurements allow us to compute the respective position and velocity vectors in galactic coordinates.

Star	l [°]	b [°]	μ_l	$\mu_l \cos(b)$
Gl 710	28.575	6.125	0.112	-0.053
Gl 127.1A	287.181	-43.781	0.160	0.053
Gl 445	127.85	37.998	-0.197	-0.222
Barnard's Star	31.996	14.061	1.654	9.095
Gl 217.1	220.381	-20.832	-0.013	0.005
Gl 729	12.316	-10.303	-0.528	-0.170
GJ 2046	269.797	-30.382	-0.005	0.069
Gl 54.1	277.271	-78.715	-1.855	-4.483
LP 816-60	31.197	-34.218	0.270	0.205

Table 6.3: Computed galactic coordinates

6.1 Non-interacting calculations

In this section we present results for the non-interacting system. We use equations described in Ch. 2. In Tables 6.4 we show the computed the perihelion position

star	$\mathbf{q} [10^{17} m]$	$ \mathbf{q} = b [10^{17} m]$
Gl 710	(2.366, -0.111, 2.821)	3.683
Gl 127.1A	(-0.312, 0.262, -0.601)	0.726
Gl 445	(0.033, 0.087, -0.051)	0.106
Barnard's Star	(0.011, 0.319, 0.094)	0.326
Gl 217.1	(0.211, 0.001, 0.350)	0.409
Gl 729	(0.262, -0.080, -0.466)	0.540
GJ 2046	(-0.535, -0.0796, -0.007)	0.541
Gl 54.1	(0.354, -0.287, -0.983)	1.083
LP 816-60	(0.073, -0.297, -0.403)	0.506

Table 6.4: Computed impact parameters and perihelion position vectors for the non-interacting system

vectors in SI units. Tab. 6.5 shows these calculations in parsecs. For this approach, we can see that the Gl 445 will have the closest approach. This results is totally different in comparison with results of Dybczyński (2006) [2]. Only computations for Barnard's, Gl 217.1, Gl 729 and for GJ 2046 are relatively similar to the presented by Dybczyński (2006) in [2].

star	$ \mathbf{q} = b [pc]$	r_0
Gl 710	11.936	19.000
Gl 127.1A	2.353	10.120
Gl 445	0.344	5.400
Barnard's Star	1.058	1.830
Gl 217.1	1.325	21.500
Gl 729	1.751	2.970
GJ 2046	1.753	12.830
Gl 54.1	3.512	3.700
LP 816-60	1.641	5.500

Table 6.5: Computed impact parameters and perihelion distances for the non-interacting system in parsecs, respectively. r_0 represents the initial distance of the object with respect to the Sun.

6.2 Two-body calculations

Here, Tab. 6.6 and Tab. 6.7 show computed perihelion position vectors, impact parameters and dispersion angles for selected nearest stars. These computations were carried out by using steps described in Ch. 3. As we expected, for the two-body system we

star	\mathbf{q} [$10^{17} m$]	$ \mathbf{q} $ [$10^{17} m$]	b [$10^{17} m$]	θ [$^\circ$]
Gl 710	(0.951, 0.288, 0.532)	1.127	3.226	58.088
Gl 127.1A	(0.012, -0.079, -0.125)	0.148	1.887	81.140
Gl 445	(0.020, -0.028, -0.025)	0.042	0.114	49.639
Barnard's Star	(0.249, 0.143, 0.070)	0.296	0.395	16.380
Gl 217.1	(0.006, 0.006, 0.005)	0.011	0.346	86.521
Gl 729	(0.016, 0.003, -0.004)	0.017	0.126	75.365
GJ 2046	(0.059, 0.014, 0.004)	0.061	1.147	83.981
Gl 54.1	(0.421, -0.300, -0.941)	1.073	1.309	11.298
LP 816-60	(0.001, 0.052, 0.051)	0.073	0.475	73.390

Table 6.6: Computed impact parameters, perihelion position vectors and dispersion angles for the two-body system

get smaller perihelion distances than for the system without interaction. Here, the star with the closest approach is Gl 217.1. Comparing with the results given in [2], only computations for Barnard's star are in agreement with [2], but this does not mean that our results are wrong. It is possible that in [2] and in other papers are taken into account others phenomena in addition to the two-body problem that we have not included in our computations. Another reason may be the values of used parameters to compute the initial conditions. In several sources (data bases) we found that for a parameter of the same star are given different values.

star	$ \mathbf{q} $ [pc]	b [pc]	θ [°]
Gl 710	3.652	10.045	58.088
Gl 127.1A	0.480	6.115	80.341
Gl 445	0.136	0.371	49.639
Barnard's Star	0.958	1.281	16.380
Gl 217.1	0.034	1.122	86.521
Gl 729	0.054	0.409	75.365
GJ 2046	0.197	3.719	83.981
Gl 54.1	3.477	4.241	11.298
LP 816-60	0.235	1.540	73.390

Table 6.7: Computed impact parameters, perihelion distances (in parsecs) and dispersion angles for the two-body system

6.3 Simple model

In this section we show and discuss results for the perihelion distance computed by using our proposed simple model. Results are given for $u = 0$, and for $u \neq 0$. Tab. 6.8 shows perihelion distances for zero value of u . As we already know, u represents anharmonic

star	$ \mathbf{q} $ [pc]
Gl 710	16.540
Gl 127.1A	6.460
Gl 445	2.735
Barnard's Star	1.567
Gl 217.1	18.112
Gl 729	1.241
GJ 2046	8.866
Gl 54.1	2.329
LP 816-60	2.720

Table 6.8: Computed perihelion distances (in parsecs) for our proposed simple model ($u = 0$)

oscillations along the z -axis, from where, we can say that this anharmonicity in the motion slightly acts on the computation of the perihelion distances, since the computed perihelion distances for nonzero u are slightly greater than for the case when $u = 0$. We get greater perihelion distances, because we have not taken into account the two-body problem, and we separately investigate the role of anharmonic oscillations along the z -axis. For a better approach it is really recommended to study the role of the galactic tide and the two-body interaction. This can be carry out by solving Eqs. (4.5).

star	$ \mathbf{q} $ [pc]
Gl 710	17.387
Gl 127.1A	8.394
Gl 445	3.237
Barnard's Star	1.830
Gl 217.1	20.375
Gl 729	1.925
GJ 2046	8.961
Gl 54.1	3.273
LP 816-60	5.490

Table 6.9: Computed perihelion distances (in parsecs) for our proposed simple model ($u \neq 0$)

Numerical computation may improve our presented results. Also, it is important to notice that our computations were done teoretically, and we used observational data to apply them, only. Note that anharmonic oscillations are not considered in the literature, and, this may be the reason of the difference in our values for the perihelion distances in comparison with results given in [2].

Chapter 7

The solar motion

*Note: In this Chapter we present part of a paper in preparation. This contribution was carried out with the participation of Klacka J., Nagy R., **Cayao J.**, Komar L. and M. Jurci.*

The kinematics of stars near to the Sun has long been known to provide crucial information regarding both the structure and evolution of the Milky Way [29]. That is the reason why we calculate the solar motion in the reference frame connected with the nearest stars. We identify series of N stars with heliocentric distances less than 100, 40, 15 pc and then determine the velocity of the Sun relative to the mean velocity of these stars. *The mean motion of all stars in the volume element considered is clearly the physically most meaningful when considered in the framework of the Galaxy. A point possessing this motion defines what is known as the Local Standard of Rest (LSR)* [8]. That is the LSR is a point in space that has a galactic velocity equal to the average velocity of stars in the solar neighborhood, including the Sun.

7.1 The solar motion

We consider a set of N stars. The coordinates of i -star in the equatorial coordinate system are $x_i = r_i \cos \alpha_i \cos \delta_i$, $y_i = r_i \sin \alpha_i \cos \delta_i$, $z_i = r_i \sin \delta_i$, where r_i is the heliocentric distance, α_i is the right ascension and δ_i is the declination of the i -star.

The velocity of the i -th star with respect to the Sun is

$$\mathbf{v}_i = \mathbf{V}_i - \mathbf{V}_S , \quad (7.1)$$

where \mathbf{V}_i and \mathbf{V}_S are the velocities of the i -th star and the Sun in the frame of the LSR. The velocities \mathbf{V}_i , \mathbf{V}_S and \mathbf{v}_i can be written as:

$$\begin{aligned} \mathbf{V}_S &= (X_S, Y_S, Z_S) , \\ \mathbf{V}_i &= (X_i, Y_i, Z_i) , \end{aligned} \quad (7.2)$$

and,

$$\begin{aligned} v_{x,i} &= \dot{r}_i \cos \alpha_i \cos \delta_i \\ &\quad - 4.74 r_i \{ (\mu_{\alpha,i} \cos \delta_i) \sin \alpha_i + \mu_{\delta,i} \cos \alpha_i \sin \delta_i \} , \\ v_{y,i} &= \dot{r}_i \sin \alpha_i \cos \delta_i \\ &\quad + 4.74 r_i \{ (\mu_{\alpha,i} \cos \delta_i) \cos \alpha_i - \mu_{\delta,i} \sin \alpha_i \sin \delta_i \} , \\ v_{z,i} &= \dot{r}_i \sin \delta_i + 4.74 r_i \mu_{\delta,i} \cos \delta_i , \end{aligned} \quad (7.3)$$

where \dot{r}_i is the radial velocity and $\mu_{\alpha,i}$, $\mu_{\delta,i}$ are the proper motions in the right ascension and declination. Since the units used in our calculations are $[v] = [\dot{r}] = km\ s^{-1}$, $[r] = pc$, $[\mu_\alpha] = [\mu_\delta] = ''\ yr^{-1}$, the numerical factor in Eq. (7.3) is 4.74.

Proper motions, radial velocities (calculated from redshift), and heliocentric distances (calculated from parallax) are observational data and can be used to describe the solar motion.

There are a few ways to calculate the solar motion with respect to the LSR. If we have all parameters of stars in our set, we will find the solar motion using direct calculation. Otherwise, we can approximate the solution using the least square method.

7.1.1 Determining \mathbf{V}_S by direct calculation

The LSR is given by

$$\sum_{i=1}^N \mathbf{V}_i = 0 , \quad (7.4)$$

where \mathbf{V}_i is given by Eq. (7.2). The average value of Eq. (7.1) is

$$\frac{1}{N} \sum_{i=1}^N \mathbf{v}_i = \frac{1}{N} \sum_{i=1}^N \mathbf{V}_i - \mathbf{V}_S . \quad (7.5)$$

Rewriting Eq. (7.5) by using Eq. (7.4) we get

$$\frac{1}{N} \sum_{i=1}^N \mathbf{v}_i = - \mathbf{V}_S , \quad (7.6)$$

or,

$$\begin{aligned} X_S &= - \frac{1}{N} \sum_{i=1}^N \dot{r}_i \cos \alpha_i \cos \delta_i \\ &\quad + 4.74 \frac{1}{N} \sum_{i=1}^N r_i (\mu_{\alpha,i} \cos \delta_i) \sin \alpha_i \\ &\quad + 4.74 \frac{1}{N} \sum_{i=1}^N r_i \mu_{\delta,i} \cos \alpha_i \sin \delta_i , \\ Y_S &= - \frac{1}{N} \sum_{i=1}^N \dot{r}_i \sin \alpha_i \cos \delta_i \\ &\quad - 4.74 \frac{1}{N} \sum_{i=1}^N r_i (\mu_{\alpha,i} \cos \delta_i) \cos \alpha_i \\ &\quad + 4.74 \frac{1}{N} \sum_{i=1}^N r_i \mu_{\delta,i} \sin \alpha_i \sin \delta_i , \\ Z_S &= - \frac{1}{N} \sum_{i=1}^N \dot{r}_i \sin \delta_i - 4.74 \frac{1}{N} \sum_{i=1}^N r_i \mu_{\delta,i} \cos \delta_i . \end{aligned} \quad (7.7)$$

Previous equations uniquely determine the solar motion in respect of the LSR.

7.1.2 Determining \mathbf{V}_S by Least square method

It is not immediately obvious from equations (7.1) and (7.3) how \mathbf{V}_S should be determined from a given body of data. We address this problem for the case of radial velocities and proper motions data. By using the Least square method we find \mathbf{V}_S as a generalization of the results presented by, e.g., [8, 17]. Let 3 N orthogonal unit vectors

$(i = 1, 2, \dots, N)$ are

$$\begin{aligned}\mathbf{e}_{\mathbf{r},i} &= (\cos \alpha_i \cos \delta_i, \sin \alpha_i \cos \delta_i, \sin \delta_i) , \\ \mathbf{e}_{\alpha,i} &= (-\sin \alpha_i, \cos \alpha_i, 0) , \\ \mathbf{e}_{\delta,i} &= (-\cos \alpha_i \sin \delta_i, -\sin \alpha_i \sin \delta_i, \cos \delta_i) ,\end{aligned}\tag{7.8}$$

where $\mathbf{e}_{\mathbf{r},i}$ are radial vectors and $\mathbf{e}_{\alpha,i}$, $\mathbf{e}_{\delta,i}$ are vectors in the direction of the right ascension and declination of the i -th star. We define the general unit vector:

$$\begin{aligned}\mathbf{e}_i &= \mathbf{e}_{\alpha,i} \cos \phi \sin \theta + \mathbf{e}_{\delta,i} \sin \phi \sin \theta + \mathbf{e}_{\mathbf{r},i} \cos \theta , \\ \phi &\in \langle 0, 2\pi \rangle , \quad \theta \in \langle 0, \pi \rangle .\end{aligned}\tag{7.9}$$

The projection of the vector \mathbf{v}_i onto the direction of the vector \mathbf{e}_i is given by $\mathbf{v}_i \cdot \mathbf{e}_i = (\mathbf{V}_i - \mathbf{V}_S) \cdot \mathbf{e}_i$. Therefore, using Eqs. (7.3) we get:

$$(\mathbf{V}_i - \mathbf{V}_S) \cdot \mathbf{e}_i = \dot{r}_i \cos \theta + 4.74 r_i [(\mu_{\alpha,i} \cos \delta_i) \cos \phi + \mu_{\delta,i} \sin \phi] \sin \theta .\tag{7.10}$$

We know

$$\begin{aligned}(\mathbf{V}_i - \mathbf{V}_S) \cdot \mathbf{e}_i &= (X_i - X_S) (-\sin \alpha_i \cos \phi \sin \theta \\ &\quad - \cos \alpha_i \sin \delta_i \sin \phi \sin \theta + \cos \alpha_i \cos \delta_i \cos \theta) \\ &\quad + (Y_i - Y_S) (\cos \alpha_i \cos \phi \sin \theta \\ &\quad - \sin \alpha_i \sin \delta_i \sin \phi \sin \theta + \sin \alpha_i \cos \delta_i \cos \theta) \\ &\quad + (Z_i - Z_S) (\cos \delta_i \sin \phi \sin \theta + \sin \delta_i \cos \theta) .\end{aligned}\tag{7.11}$$

From equations (7.10) and (7.11) follows

$$\begin{aligned}
p_i \equiv & \dot{r}_i \cos \theta + 4.74 r_i [(\mu_{\alpha,i} \cos \delta_i) \cos \phi + \mu_{\delta,i} \sin \phi] \sin \theta \\
& - (X_i - X_S) (-\sin \alpha_i \cos \phi \sin \theta - \cos \alpha_i \sin \delta_i \sin \phi \sin \theta \\
& + \cos \alpha_i \cos \delta_i \cos \theta) \\
& - (Y_i - Y_S) (\cos \alpha_i \cos \phi \sin \theta - \sin \alpha_i \sin \delta_i \sin \phi \sin \theta \\
& + \sin \alpha_i \cos \delta_i \cos \theta) \\
& - (Z_i - Z_S) (\cos \delta_i \sin \phi \sin \theta + \sin \delta_i \cos \theta) ,
\end{aligned} \tag{7.12}$$

where p_i is the residual and $p_i = 0$, exactly. But we admit $p_i \neq 0$ and we use the Least square method for finding X_S, Y_S, Z_S . Defining the sum of squared residuals

$$S(X_S, Y_S, Z_S) = \sum_{i=1}^N [p_i]^2 , \tag{7.13}$$

we minimize it:

$$\frac{\partial S}{\partial X_S} = \frac{\partial S}{\partial Y_S} = \frac{\partial S}{\partial Z_S} = 0 . \tag{7.14}$$

We assume

$$\langle \mathbf{V}_i \cos^k \alpha_i \sin^l \alpha_i \cos^m \delta_i \sin^n \delta_i \rangle = 0 \tag{7.15}$$

for arbitrary k, l, m, n [8]. We denote

$$\begin{aligned}
\Gamma_i \equiv & \dot{r}_i \cos \theta + 4.74 r_i (\mu_{\alpha,i} \cos \delta_i \cos \phi + \mu_{\delta,i} \sin \phi) \sin \theta \\
& - X_S (\sin \alpha_i \cos \phi \sin \theta + \cos \alpha_i \sin \delta_i \sin \phi \sin \theta - \cos \alpha_i \cos \delta_i \cos \theta) \\
& + Y_S (\cos \alpha_i \cos \phi \sin \theta - \sin \alpha_i \sin \delta_i \sin \phi \sin \theta + \sin \alpha_i \cos \delta_i \cos \theta) \\
& + Z_S (\cos \delta_i \sin \phi \sin \theta + \sin \delta_i \cos \theta) .
\end{aligned} \tag{7.16}$$

Then rewriting Eq. (7.15) by using Eqs. (12), (13), (7.16)- (7.17) we get:

$$\begin{aligned}
\frac{\partial S}{\partial X_S} &= 2 \sum_{i=1}^N \Gamma_i (-\sin \alpha_i \cos \phi \sin \theta - \cos \alpha_i \sin \delta_i \sin \phi \sin \theta \\
&\quad + \cos \alpha_i \cos \delta_i \cos \theta) = 0 , \\
\frac{\partial S}{\partial Y_S} &= 2 \sum_{i=1}^N \Gamma_i (\cos \alpha_i \cos \phi \sin \theta - \sin \alpha_i \sin \delta_i \sin \phi \sin \theta \\
&\quad + \sin \alpha_i \cos \delta_i \cos \theta) = 0 , \\
\frac{\partial S}{\partial Z_S} &= 2 \sum_{i=1}^N \Gamma_i (\cos \delta_i \sin \phi \sin \theta + \sin \delta_i \cos \theta) = 0 . \tag{7.17}
\end{aligned}$$

ϕ, θ are arbitrary angles, $\phi \in \langle 0, 2\pi \rangle$, $\theta \in \langle 0, \pi \rangle$. Therefore, coefficients of the same combination of $(\sin \phi, \cos \phi, \sin \theta, \cos \theta)$ are equal to zero for each equation in (??). From this we get six independent linear systems of three equations in unknowns (X_S, Y_S, Z_S) . These systems are used to determine the solar motion using the Least square method and they are presented in Appendix A (Eqs. A1-A6).

Eqs. (A1) represent the way how to calculate the solar motion by using only the proper motions in right ascension. However, they allow us to determine the solar motion only in the X_S, Y_S directions. The system of equations Eqs. (A1) is similar to the type of Eqs. (7.5-7.13)-(7.5-7.14) by [8]. The system of equations Eqs. (A5) is similar to the type of Eqs. (7.5-7.10)-(7.5-7.12) in [8]. Suprising is the following formulation in [8]: “Finally, if we add equations (7.5-7.10) to (7.5-7.13) and (7.5-7.11) to (7.5-7.14) to utilize the proper motion information as fully as possible, we obtain three equations of their form ...” (equations for X_S, Y_S, Z_S). However, the access of the authors yield result not consistent with our system represented by Eqs. (A.2).

Eqs. (A.2)-(A.6) provide a complete information about the solar motion (X_S, Y_S, Z_S) . Thus, we determine the solar motion for each system. In this Chapter, up to now we have used equatorial coordinate system with the right ascension α and the declination δ . Dealing with motions in Galaxy, we will use galactic coordinate system with the galactic longitude l and the galactic latitude b . Those transformations are done as is described in Sec. 4.3.

7.2 Results

We selected stars from the database SIMBAD [10]. At first, we chose stars with the heliocentric distance less than 100 pc , but only stars with complete observational data (radial velocities, proper motion, parallax). The number of stars to that distance was 24167. Then we selected stars with the best quality index (A) in parallax, proper motions and radial velocities. This selection reduced the number of stars to 769. These stars are used in our calculations of the solar motion. We remind that Eqs. (7.3), (7.7) and (??) are given in the equatorial coordinates, but the results are shown in the galactic coordinates.

7.2.1 For $r_i < 100$ pc

For the set of 769 stars with $r_i < 100$ pc we compute the solar motion presented in Table 7.1.

Method	X_S [km/s]	Y_S [km/s]	Z_S [km/s]	$ \mathbf{V}_S $ [km/s]
Eqs. (7.7)	7.63	16.65	7.43	19.76
Eqs. (A.2)	74.7	-34.0	159.5	179.4
Eqs. (A.3)	76.2	106.6	-0.7	131.1
Eqs. (A.4)	59.3	-53.4	38.5	88.6
Eqs. (A.5)	8.82	17.64	8.07	21.31
Eqs. (A.6)	10.59	17.86	6.90	21.88

Table 7.1: The solar motion in the galactic coordinates for our sample of stars with $r_i < 100$ pc calculated using the direct method (Eqs. (7.7)) and the Least square method (Eqs. (A.2)-(A.6)).

Table 7.1 shows that the results $\{ Z_S, V_S \equiv |\mathbf{V}_S| \}$ from the direct method (without approximations) for this case are in accord with the standard solar motion presented by [10] (see Table 7.4). The solar motions calculated from Eqs. (A.1), (A.5)-(A.6) are similar to results of the direct method. The rest of equations deduced from the Least square method (Eqs. A.2-A.4) give quite different solutions (see Table 7.1) from the direct calculation. Thus, these equations are useless in determining the solar motion.

7.2.2 For $r_i < 40$ pc

Here we consider stars with $r_i < 40$ pc. This set contains 360 stars. Calculated values of the solar motion in the galactic coordinates are shown in Table 7.2.

Method	X_S [km/s]	Y_S [km/s]	Z_S [km/s]	$ \mathbf{V}_S $ [km/s]
Eqs. (7.7)	7.09	18.53	7.70	21.28
Eqs. (A.2)	11.5	10.0	50.5	52.8
Eqs. (A.3)	150.9	-10.7	-49.1	159.1
Eqs. (A.4)	1678.8	-1314.3	-142.4	2136.9
Eqs. (A.5)	5.92	18.28	10.53	21.91
Eqs. (A.6)	13.18	20.95	4.37	25.13

Table 7.2: The solar motion in the galactic coordinates for our set of stars with $r_i < 40$ pc calculated using the direct method (Eqs. (7.7)) and the Least square method (Eqs. (A.2)-(A.6)).

The solutions of Eqs. (A.2)-(A.4) are quite different from the solar motion calculated by the direct method again. Eqs. (A.5) give correct absolute value of the velocity, but the components of the solar motion are slightly different from our direct calculations. The solution of Eqs. (A.6) is more different than the solution of Eqs. (A.5), but both of them are still good estimations of the solar motion.

7.2.3 For $r_i < 15$ pc

The nearest hundred stars in the solar neighborhood have the heliocentric distance less than 15 pc. Our results are presented in Table 7.3.

Method	X_S [km/s]	Y_S [km/s]	Z_S [km/s]	$ \mathbf{V}_S $ [km/s]
Eqs. (7.7)	14.16	17.59	7.09	23.68
Eqs. (A.2)	-8.3	15.7	30.4	35.2
Eqs. (A.3)	120.0	-43.7	25.3	130.2
Eqs. (A.4)	41.77	-56.5	20.75	73.3
Eqs. (A.5)	7.02	18.42	2.37	19.85
Eqs. (A.6)	24.08	20.58	3.77	31.9

Table 7.3: The solar motion in the galactic coordinates for our set of stars with $r_i < 15$ pc calculated using the direct method (Eqs. (7.7)) and the Least square method (Eqs. (A.2)-(A.6)).

The solutions of Eqs. (A.2)-(A.4) are useless in comparison with the direct method (Eqs. (7.7)). Eqs. (A.5) give relatively good approximation of the solar motion in respect of this LSR. But the solution of Eqs. (A.6) differ from the direct method (Eqs. (7.7)) especially in the absolute value of the velocity and Z_S component. However, these results may be influenced by using small solar neighborhood.

7.2.4 The solution of Eqs. (7.7) for different distances

Now we use the direct method (Eqs. (7.7)) to calculate the solar motion for the Solar neighborhoods with various radii. The results are presented in Table 7.4.

Distance [pc]	X_S [km/s]	Y_S [km/s]	Z_S [km/s]	$ \mathbf{V}_S $ [km/s]	Number of stars
10	12.57	15.36	6.14	20.77	44
20	12.10	17.51	6.98	22.41	165
30	8.18	17.41	7.28	20.57	273
40	7.08	18.53	7.70	21.28	360
50	9.34	18.38	7.59	21.97	445
60	9.11	18.03	7.61	21.59	532
70	8.53	18.09	7.44	21.34	603
80	7.91	17.52	7.64	20.69	669
90	7.57	16.99	7.43	20.04	725
100	7.63	16.65	7.43	19.77	769

Table 7.4: The solar motion calculated by direct method (Eqs. (7.7)) for different distances. Velocity components are given in galactic coordinates.

The relation between the velocity components of the solar motion and radius of the solar neighborhood is illustrated in Fig. 7-1.

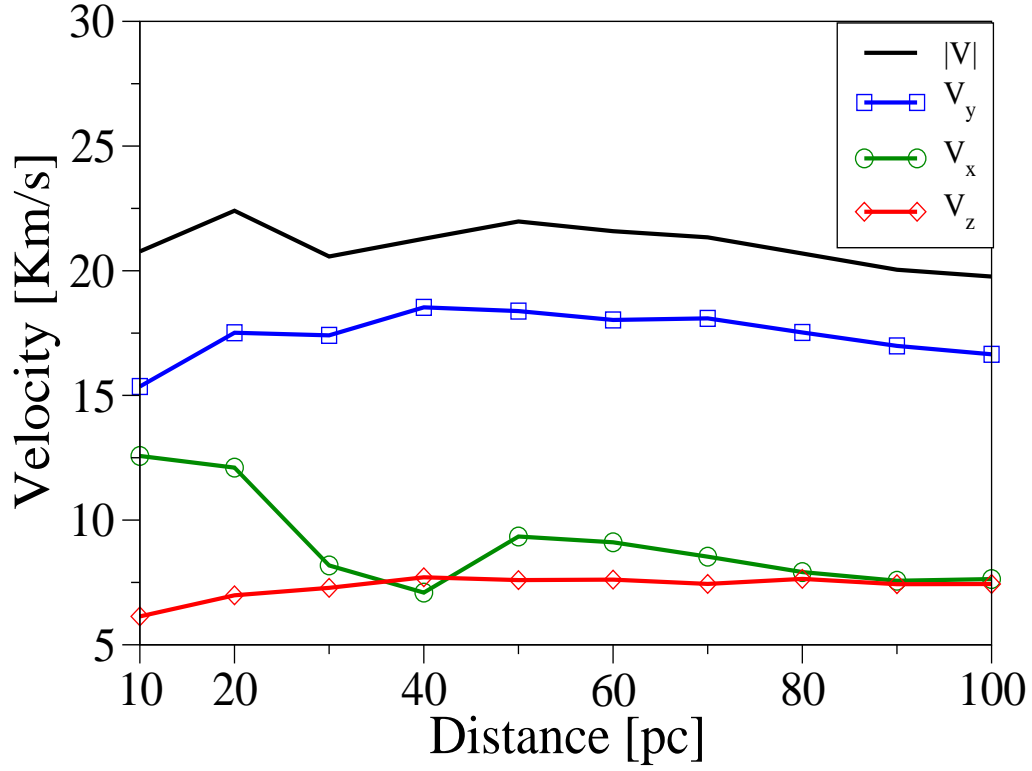


Figure 7-1: The relation between the velocity components of the solar motion and radius of the solar neighborhood.

7.3 Application

The knowledge of the solar motion, especially Z_S component, allows us to calculate the solar oscillations in direction perpendicular to the galactic equator. In this case, we can use solar equation of motion presented in Klačka (2009) [19]:

$$\ddot{z} = - [4\pi G\rho(z) + 2(A^2 - B^2)] z \quad (7.18)$$

where A , B are the Oort constants and ρ is the mass density ($z = 0$ in the galactic equatorial plane) in a galactocentric distance equal to the galactocentric distance of

the Sun. The relevant values are:

$$\begin{aligned}
A &= 14.2 \text{ km s}^{-1} \text{ kpc}^{-1} , \\
B &= -12.4 \text{ km s}^{-1} \text{ kpc}^{-1} , \\
\rho &\equiv \rho(z=0) = 0.13 \text{ } M_{\odot} \text{ pc}^{-3} .
\end{aligned} \tag{7.19}$$

7.3.1 The solar oscillation – simple access

If the density $\rho(z)$ in Eq. (7.18) is a constant $\rho = \rho_{disk} + \rho_{halo}$, then Eq. (7.18) is the equation of motion of a linear harmonic oscillator with angular frequency ω . In our case $\omega^2 = 4\pi G\rho + 2(A^2 - B^2)$. The solution of Eq. (7.18) is:

$$\begin{aligned}
z &= C_1 \cos(\omega t) + C_2 \sin(\omega t) , \\
C_1 &= z(t=0) , \quad C_2 = \dot{z}(t=0)/\omega , \\
z_{max} &= \sqrt{[z(t=0)]^2 + [\dot{z}(t=0)/\omega]^2} ,
\end{aligned} \tag{7.20}$$

since the constants C_1, C_2 are given by initial conditions. Our results of the solar motion in z -direction are used for various initial values of $\dot{z}(t=0)$ and for $z(t=0) = 30 \text{ pc}$.

	$Z_S [km/s]$	$z_{max} [pc]$	P [Myrs]
min. value of Z_S	6.14	78.71	73.89
max. value of Z_S	7.70	96.06	73.89
average Z_S value	7.32 ± 0.15	91.79 ± 1.66	73.89

Table 7.5: Amplitude z_{max} and periods of the solar oscillations with the initial position $z(t=0) = 30 \text{ pc}$. Various initial velocities Z_S and constant mass density are used.

As we can see in Table 7.5, maximal distance of the Sun from the galactic equator relevantly depends on the z -component of the solar motion.

7.3.2 The solar oscillation – improved access

Using Z_S component and a better approximation of a mass density as a function of the coordinate z , $\rho(z) = \rho_{disk} (1 - u |z|) + \rho_{halo}$, $u = 3.3 \text{ kpc}^{-1}$ (Klačka 2009),

numerical calculation of the solar oscillations in the direction perpendicular to the galactic equator (Eq. 7.18) yields the results summarized in Table 7.6.

	$Z_S[km/s]$	$z_{max}[pc]$	P [Myrs]
minimum value of Z_S	6.14	81.8	77.0
maximum value of Z_S	7.70	101.1	77.9
average Z_S value	7.32	96.2	77.8

Table 7.6: Amplitude z_{max} and periods of the solar oscillations with the initial position $z(t = 0) = 30 pc$. Various initial velocities Z_S are used. Mass density as a function of z is considered.

7.3.3 The Oort constants

There are a couple of numbers A and B that describe the relative orbital motions of the Sun and stars in our neighborhood of the Galaxy. These are called Oort constants. The values of A and B can be calculated from the observational data based on radial velocities and proper motions.

The original results come back to Bottlinger, who derived the relevant equations in 1924-1925 (see [12]). Simplification of the Bottlinger's equations are known as the Oort equations containing the Oort's constants A and B . Since the Oort's equations hold only for galactic latitude $b = 0$, we will consider more general equations holding for arbitrary b .

The following subsections present the relevant equations for finding the values of A and B using various observational data. The subsections are based on the values of the observed radial velocities, proper motions in right ascension, and, proper motions in declination, respectively.

Radial velocities

The radial velocity for the i -th star is given by

$$v_{r,i} = A r \cos^2 b \sin(2 l) , \quad (7.21)$$

where A is the first Oort constant. By using Eq. (7.1) and the unit vector $\mathbf{e}_{r,i} = (\cos l_i \cos b_i, \sin l_i \cos b_i, \sin b_i)$ we project the vector velocity V_i to the radial direction

as

$$(\mathbf{v}_i + \mathbf{V}_S) \cdot \frac{\mathbf{r}_i + \mathbf{R}_S}{|\mathbf{r}_i + \mathbf{R}_S|} = A |\mathbf{r}_i + \mathbf{R}_S| \cos^2 B_i \sin(2 L_i) , \quad (7.22)$$

then

$$(\mathbf{v}_i + \mathbf{V}_S) \cdot (\mathbf{r}_i + \mathbf{R}_S) = 2A(\mathbf{r}_i + \mathbf{R}_S)_x(\mathbf{r}_i + \mathbf{R}_S)_y , \quad (7.23)$$

where \mathbf{r}_i , \mathbf{v}_i , and \mathbf{V}_S are known values. But $\mathbf{R}_S \neq 0$, in general. We will assume, as it is usual, that the LSR is at the Sun (the LSR has its origin at the Sun's location, [4]). Therefore $\mathbf{R}_S = 0$ and the unique unknown parameter is A . This constant is found by using the Least Square method.

Proper motions μ_l

Here we do the same steps as for the previous case. The velocity $v_{l,i}$ and the proper motion $\mu_{l,i}$ for the i -th star is given by

$$\begin{aligned} v_{l,i} &= 4.74 r_i \mu_{l,i} \cos b_i , \\ \mu_{l,i} &= 4.74^{-1} [A \cos(2 l_i) + B] , \\ v_{l,i} &= [A \cos(2 l_i) + B] r_i \cos b_i , \end{aligned} \quad (7.24)$$

where A and B are the Oort constants which we want to find. Also, the velocity $v_{l,i}$ can be found by using the projection of $\mathbf{v}_i + \mathbf{V}_S$ onto l as

$$v_{l,i} = (\mathbf{v}_i + \mathbf{V}_S) \cdot \mathbf{e}_{l,i} = (\mathbf{v}_i + \mathbf{V}_S)_x (-\sin l_i) + (\mathbf{v}_i + \mathbf{V}_S)_y (\cos l_i) , \quad (7.25)$$

where we used $\mathbf{e}_{l,i} = (-\sin l_i, \cos l_i, 0)$. From equations (7.24) and (7.25) we can calculate the Oort constants by using the Least Square method. Note that by using proper motions $\mu_{l,i}$ we can find A and B .

Proper motions μ_b

The velocity $v_{b,i}$ and the proper motion $\mu_{b,i}$ for the i -th star is given by

$$\begin{aligned} v_{b,i} &= 4.74 \, r_i \, \mu_{b,i} , \\ \mu_{b,i} &= -4.74^{-1} \, A \, \sin(2 \, l_i) \, \sin b_i \, \cos b_i , \\ v_{b,i} &= -\frac{1}{2} \, A \, r_i \, \sin(2 \, l_i) \, \sin(2 \, b_i) . \end{aligned} \quad (7.26)$$

The velocity $v_{b,i}$ is replaced by using the projection of $\mathbf{v}_i + \mathbf{V}_S$ onto b as

$$v_{b,i} = (\mathbf{v}_i + \mathbf{V}_S) \cdot \mathbf{e}_{b,i} , \quad (7.27)$$

where $\mathbf{e}_{b,i} = (-\cos l_i \sin b_i, -\sin l_i \sin b_i, \cos b_i)$ is the unit vector on the b direction. From equations (7.26) and (7.27) we can find A by using the Least Square method.

7.3.4 Oort cloud of comets

As we have already presented in sections 7.3.1 and 7.3.2, the found values of Z_S lead to various values of maximal distance between the Sun and the galactic equatorial plane. The result suggests that Z_S may play an important role in orbital evolution of comets of the Oort cloud. As a consequence, the uncertainty in Z_S generates an uncertainty in the mass of the Oort cloud.

The standard model of the Oort cloud considers that the Sun is situated in the galactic equatorial plane and $Z_S \equiv 0$. Let us consider, as an example, that a comet is characterized by the following initial orbital elements: semi-major axis $a_{in} = 5 \times 10^4 \, AU$, eccentricity $e_{in} \approx 0$, inclination to galactic equatorial plane $i_{in} = 90$ degrees. The conventional models yield 6 returns of the comet into the inner part of the Solar System during the existence of the Solar System (see Fig. 2 in [21]- conventional models = standard or simple models). Using the physical model by [19], we obtain the following number of returns (see also Fig. 7-2):

- 9 for $Z_S = 7.70 \, km/s$,
- 12 for $Z_S = 6.14 \, km/s$.

Thus, the frequency of cometary returns into the inner part of the Solar System is

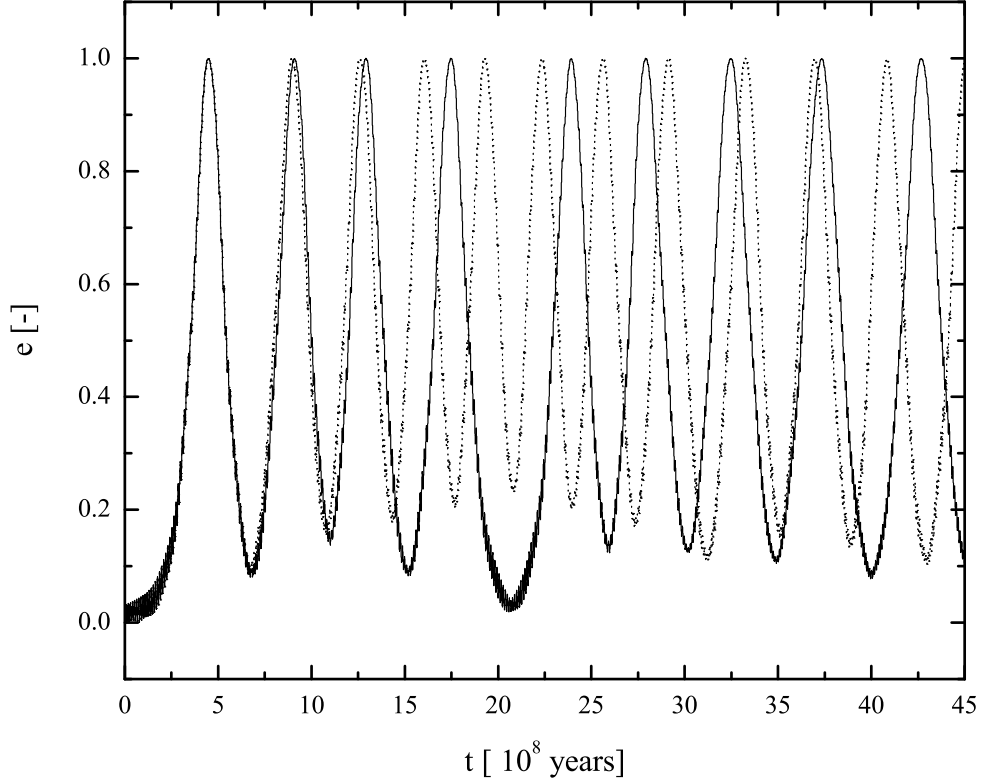


Figure 7-2: Evolution of eccentricity under the action of gravity of the Sun and Galaxy. The model by [19] is used. Two values of Z_S are used: the dotted line holds for $Z_S = 6.14 \text{ km/s}$, the solid line holds for $Z_S = 7.70 \text{ km/s}$.

2-times greater than the frequency of the conventional models (6 returns for the conventional models, see [21], if the effect of the Sun and Galaxy are considered.

7.4 Discussion

The presented method of determining \mathbf{V}_S by the least square method is based on the definition of a new general unit vector defined in Eq. (7.9). Various values of ϕ and θ produce six independent systems of linear equation determining components of the vector \mathbf{V}_S . None of the systems, represented by Eqs. (A.1)-(A.6), contains the set of quantities $\{\dot{r}_i, \mu_{\alpha i}, \mu_{\delta i}\}$ simultaneously. One, or maximally two of the components of the set $\{\dot{r}_i, \mu_{\alpha i}, \mu_{\delta i}\}$ are present in each of the final systems. This can be explained by the usage of the least square method. The exponent in Eq. (7.14) equals to 2. If

the exponent would be equal to 3, 4, ..., then also a set of equations with all three measured quantities \dot{r}_i , $\mu_{\alpha i}$, $\mu_{\delta i}$ would exist.

Mihalas and McRae Routly [8, p. 97] state that “Finally, if we add equations (7.5-7.10) to (7.5-7.13) and (7.5-7.11) to (7.5-7.14) to utilize the proper motion information as fully as possible, we obtain three equations of their form ...” (equations for X_S , Y_S , Z_S). This access of the authors yield result not consistent with our Eqs. (A.2). It is not possible to combine various equations in an arbitrary manner unless the equations are exact. Our access represented by Eqs. (7.8)-(7.16) yields combination of the measured quantities \dot{r}_i , $\mu_{\alpha i}$, $\mu_{\delta i}$ in a unique way.

As Tables 7.1- 7.3 show, the systems of equations Eqs. (A.2) - (A.4) do not yield results consistent with the direct method represented by Eqs. (7.6)-(7.7).

On the other side, the systems of Eqs. (A.1), (A.5) and (A.6) produce results which are much better consistent with the direct method. As Tables 7.1- 7.3 show, the error is less than 90%. If we compare Eqs. (A.1)-(A.6), then we can find one important property. Eqs. (A.1), (A.5)-(A.6) contain parts where all the terms of the sums are of the same sign for all stars. Thus, these terms dominate in Eqs. (A.1), (A.5)-(A.6). Moreover, these terms ensure that the systems (A.1), (A.5)-(A.6) can produce Eqs. (7.7) [a simple addition of the j -th equations of the systems produces the j -th equation of Eqs. (7.7), $j = 1, 2, 3$]. Nothing like this exists for Eqs. (A.2)-(A.4). This could explain the poor consistency of the results of Eqs. (A.2)-(A.4) with the direct method represented by Eqs. (7.7), and, a much better consistency of the results of Eqs. (A.1), (A.5)-(A.6) with the direct method. In any case, our results show that the Least square method is not a good method for finding the solar motion.

The results for the direct method are summarized in Table 7.4. On the basis of Table 7.4 we obtain the following results:

$$\begin{aligned} Z_S &= (7.32 \pm 0.15) \text{ kms}^{-1} , \\ V_S &= (21.04 \pm 0.26) \text{ kms}^{-1} . \end{aligned} \tag{7.28}$$

Our values correspond to the standard solar motion. The value of Z_S is consistent with the results published by other authors (see values in Table 7.7). However, our value of V_S is greater than the values of other authors and presented in Table 7.7. Especially

the value presented by Binney and Merrifield [17, p. 624–628] and Dehnen and Binney [29] is very small.

source:	SM1	SM2	SM3	SM4
$Z_S [km/s]$	7.3	6.0	7.17 ± 0.09	7.2 ± 0.4
$ \mathbf{V}_S [km/s]$	19.5	15.4	13.4	13.4

Table 7.7: The solar motion. SM1 corresponds to the standard motion presented by [8, 4]. SM2 corresponds to the basic motion presented by [8]. SM3 is presented by [29]. SM4 is presented by [17] and [1].

7.4.1 More on the Least square method

We have already discussed the approach of the Least square method. We have pointed out errors of the results for the systems represented by Eqs. (A.1), (A.5)-(A.6). Moreover, Eqs. (A.2)-(A.4) do not yield satisfactory results. In general, we can conclude that one should not use the Least square method. However, let us look in a more detail into the method. The fundamental approach is given by Eqs. (7.9)-(7.15) and the result is represented by Eqs. (A.1)-(A.6). While Eqs. (A.2)-(A.4) yield completely incorrect results, Eqs. (A.1), (A.5)-(A.6) yield results with errors less than $\approx 100\%$. So, the idea is that we do not need to solve the complete systems (A1), (A.5)-(A.6), but it is sufficient to take into account the most important parts on the right-hand sides of Eqs. (A.1), (A.5)-(A.6). In doing this, we can substitute the terms at X_S , Y_S and Z_S of the right-hand sides of Eqs. (A.1), (A.5)-(A.6) by the the average values of the type

$$\begin{aligned} \frac{1}{N} \sum_{i=1}^N \sin^k \alpha_i \cos^l \alpha_i \cos^m \delta_i \sin^n \delta_i &\rightarrow \frac{1}{4\pi} \int_{4\pi} \sin^k \alpha \cos^l \alpha \cos^m \delta \sin^n \delta d\Omega, \\ d\Omega &= \cos \delta d\delta d\alpha, \\ \alpha &\in \langle 0, 2\pi \rangle, \quad \delta \in \langle -\frac{\pi}{2}, +\frac{\pi}{2} \rangle. \end{aligned} \quad (7.29)$$

Eqs. (A.1) reduce to

$$X_S = 2 \frac{1}{N} 4.74 \sum_{i=1}^N r_i (\mu_{\alpha,i} \cos \delta_i) \sin \alpha_i, \quad (7.30)$$

$$Y_S = -2 \frac{1}{N} 4.74 \sum_{i=1}^N r_i (\mu_{\alpha,i} \cos \delta_i) \cos \alpha_i . \quad (7.31)$$

Eqs. (A.5) reduce to

$$X_S = 6 \frac{1}{N} 4.74 \sum_{i=1}^N r_i \mu_{\delta,i} \sin \delta_i \cos \alpha_i , \quad (7.32)$$

$$Y_S = 6 \frac{1}{N} 4.74 \sum_{i=1}^N r_i \mu_{\delta,i} \sin \delta_i \sin \alpha_i , \quad (7.33)$$

$$Z_S = -\frac{3}{2} \frac{1}{N} 4.74 \sum_{i=1}^N r_i \mu_{\delta,i} \cos \delta_i , \quad (7.34)$$

and, Eqs. (A.6) reduce to

$$X_S = -3 \frac{1}{N} \sum_{i=1}^N \dot{r}_i \cos \alpha_i \cos \delta_i , \quad (7.35)$$

$$Y_S = -3 \frac{1}{N} \sum_{i=1}^N \dot{r}_i \sin \alpha_i \cos \delta_i , \quad (7.36)$$

$$Z_S = -3 \frac{1}{N} \sum_{i=1}^N \dot{r}_i \sin \delta_i . \quad (7.37)$$

Eqs. (7.30)-(7.37) can be considered as a more straightforward approximation to the direct calculation represented by Eqs. (7.7). Numerical calculations for the set of our stars with $r_i < 100 \text{ pc}$, $i = 1$ to N , yield the following results in the galactic coordinates: X_S (Eq. 7.32) = 8.48 km/s , Y_S (Eq. 7.33) = 17.42 km/s , Z_S (Eq. 7.34) = 6.89 km/s , with the value $V_S = 20.56 \text{ km/s}$, and,

X_S (Eq. 7.35) = 10.08 km/s , Y_S (Eq. 7.36) = 17.87 km/s , Z_S (Eq. 7.37) = 8.54 km/s with the value $V_S = 22.22 \text{ km/s}$.

Of course, one may take various combinations of X_S , Y_S and Z_S in calculating $V_S = \sqrt{X_S^2 + Y_S^2 + Z_S^2}$. The values of the X_S , Y_S and Z_S components can be considered to be consistent with the correct values given in Table 7.1 (Eq. (7.7) in Table 7.1). The found values of V_S are greater than the values of Dehnen and Binney [29], Binney and Merrifield [17, p. 628] and Mihalas and McRae Routly [8, p. 101]. However, the values of V_S are less than the speed of the neutral interstellar gas [24, 23]. In any case,

the systems of Eqs. (A.1), (A.5)-(A.6) yields that the most probable values should be averaged in the following form:

$$\begin{aligned} X_S &= (1/2) X_S \text{ (Eq. 7.30)} + (1/6) X_S \text{ (Eq. 7.32)} + (1/3) X_S \text{ (Eq. 7.35)}, \\ Y_S &= (1/2) Y_S \text{ (Eq. 7.31)} + (1/6) Y_S \text{ (Eq. 7.33)} + (1/3) Y_S \text{ (Eq. 7.36)}, \\ Z_S &= (2/3) Z_S \text{ (Eq. 7.34)} + (1/3) Z_S \text{ (Eq. 7.37)}. \end{aligned}$$

7.4.2 More on the real motion of the Sun

We have dealt with the solar motion. We have considered it in the conventional way, i.e., the solar motion has meant the motion of the Sun with respect to the surrounding stars, with respect to the LSR. Now, we have in disposal another approach. Interplanetary probes found flux of interstellar dust and gas streaming into the Solar System.

The direct method for finding solar motion yields that the direction of the solar motion is characterized by the ecliptic longitude $\lambda_{solar\ motion} = 277.5^\circ$ and latitude $\beta_{solar\ motion} = 60.3^\circ$. Eqs. (7.32)-(7.34) yield $\lambda_{solar\ motion} = 265.2^\circ$ and $\beta_{solar\ motion} = 58.4^\circ$. Eqs. (7.35)-(7.37) yield $\lambda_{solar\ motion} = 258.2^\circ$ and $\beta_{solar\ motion} = 56.1^\circ$. The solar motion was determined by the motion of the Sun with respect to the surrounding stars. The obtained direction may be compared with the direction of the interstellar gas streaming into the Solar System: $\lambda_0 = 259^\circ$ and $\beta_0 = 8^\circ$ [22]. Similarly, the flow of interstellar grains arrives from the direction with heliocentric ecliptic longitude 259° and heliocentric ecliptic latitude $+8^\circ$ [5]. It is wise to stress that the motion of the surrounding stars with respect to the Sun is given by the direction $\lambda = \lambda_{solar\ motion} - 180^\circ$ and $\beta = -\beta_{solar\ motion}$. The result [$\lambda_{solar\ motion} = 277.5^\circ$, $\beta_{solar\ motion} = 60.3^\circ$] significantly differs from the direction of motion of the interstellar gas and dust [$\lambda_0 = 259^\circ$, $\beta_0 = 8^\circ$].

The interplanetary dust and gas are coming from the direction $\lambda_0 = 259^\circ$ and $\beta_0 = 8^\circ$. This direction corresponds to the values of the galactic latitude $l_0 = 8.9^\circ$ and the galactic latitude $b_0 = 13.5^\circ$. Thus, the velocity components of the Sun with respect to the dust and gas are given by the equations $V_x = V_S \cos l_0 \cos b_0$, $V_y = V_S \sin l_0 \cos b_0$, $V_z = V_S \sin b_0$ and the values are presented in Table 7.8. The values significantly differ from the values presented in Table 7.8 and from the conventional values presented in Table 7.7. Only z -component of the solar motion is characterized by a consistency among the results obtained from various approaches, $V_z \equiv Z_S \in \langle 6.1 \text{ km/s}, 7.7 \text{ km/s}$

\rangle (direct method; another presented result is Z_S (Eq. 7.37) = 8.54 km/s) .

$V_S[km/s]$	$V_x[km/s]$	$V_y[km/s]$	$V_z[km/s]$
26.0	25.0	3.9	6.1
28.0	26.9	4.2	6.5

Table 7.8: Velocity components of the Sun with respect to the surrounding interstellar gas and dust. Two values of the speed V_S are considered. The components are measured in galactic coordinates.

Let us consider that the dust and gas components of matter are situated in the galactic disk. We can determine the motion of the Sun with respect to these two components. This is the relevant solar motion in the direction normal to the galactic equatorial plane. So, also on the basis of the values presented in Table 7.8, we can obtain an orbital evolution of a comet from the Oort cloud as it is presented in Fig. 7-1. However, the lower value of V_z has to be preferred, i.e. $Z_S \approx 6.1 \text{ km/s}$ and not $Z_S \approx 7.7 \text{ km/s}$.

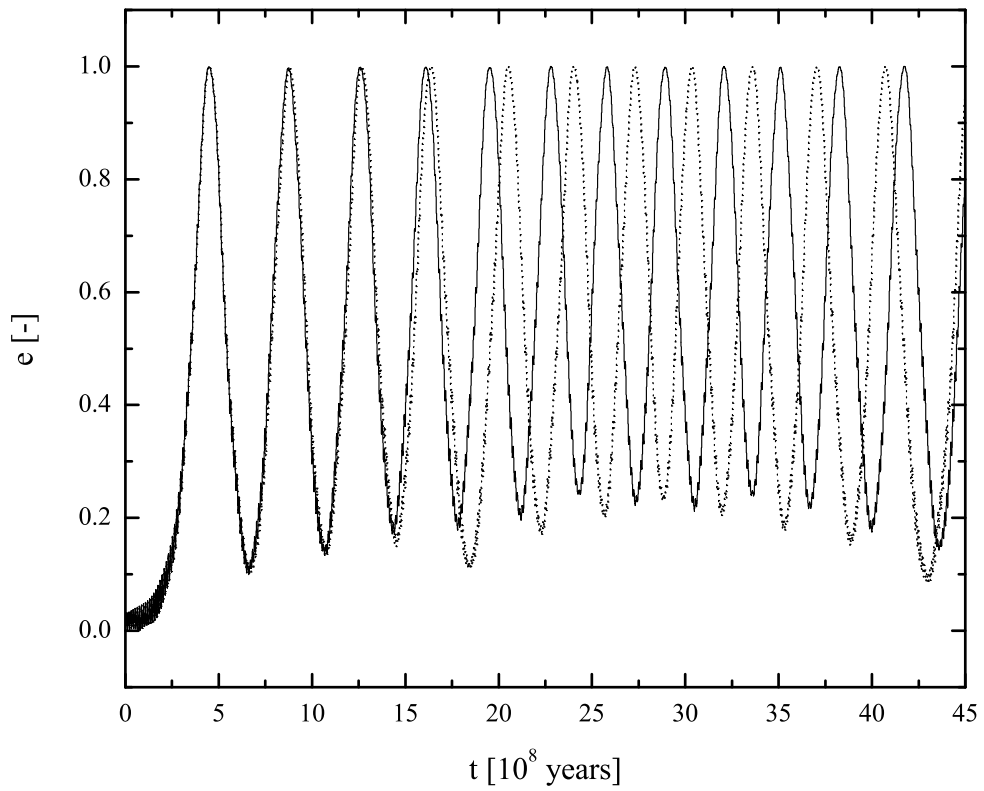


Figure 7-3: Evolution of eccentricity under the action of gravity of the Sun and Galaxy. The model by Klačka (2009) is used. Two values of Z_S are used: the dotted line holds for $Z_S = 6.14 \text{ km/s}$, the solid line holds for $Z_S = 7.70 \text{ km/s}$.

Chapter 8

Zhrnutie diplomovej práce

V tejto diplomovej práci sme skúmali metódy na počítanie perihéliových vzdialeností a zámerných vzdialeností pre vybrané blízke hviezdy. Tiež sme sa venovali výskumu pohybu Slnka. Naše teoretické výsledky boli aplikované na blízke hviezdy študované v [2, 18]. Observačné dáta sme získali z rôznych zdrojov ako *ARICNS* [15], *NStED Data Base* [20], *SIMBAD Data Base* [10], a z [11]. V nasledujúcich sekciách vysvetľujeme, čo sme robili v jednotlivých kapitolách tejto diplomovej práci.

8.1 Systém bez interakcie

V tomto prípade sme počítali perihéliovú vzdialenosť pre hviezdu, ktorá sa pohybuje po priamke vzhľadom na inerciálnu sústavu a neinteraguje so Slnkom. V kapitole 2 sme opísali náš postup, kde sme minimalizovali rovnicu (2.1). Po malej úprave sme dostali vzťah (2.6), ktorý reprezentuje perihéliovú vzdialenosť a čas, za ktorý sa hviezda do takej polohy dostane. Pre neinteragujúci systém platí, že perihéliová vzdialenosť a zámerná vzdialenosť nadobúdajú tie isté hodnoty.

8.2 Problém dvoch telies

Na výpočet perihéliovej vzdialenosti tu uvažujeme hviezdu pohybujúcu sa v gravitačnom potenciáli Slnka. Čiže skúmame problém dvoch telies. Pre presný postup odporúčame pozrieť sa do kapitoly 3. Výsledné vzťahy sú dané rovnicami (3.3) (na počítanie zámernej vzdialenosti) a (3.30) (na počítanie perihéliovej vzdialenosti). Tu, tak ako

sme očakávali, sme dostali menšie perihéliové vzdialenosti ako v systéme bez interakcie. Nasvedčuje to tomu, že počítame fyzikálne korektne.

8.3 Galaktické slapy

Cieľom kapitoly 4 je tiež počítať perihéliovú vzdialenosť pre vybranú hviezdu blízko Slnka. Na relatívny pohyb Slnko-hviezda v tomto prípade pôsobia gravitačné efekty Galaxie. Uvažujeme oscilačné pohyby Slnka a hviezdy vzhľadom na galaktický rovník, vrátane anharmonických oscilácií. Žiadne z takýchto oscilácií sa doteraz neuvažovali.

8.3.1 Oscilácie Slnka a hviezdy

Riešime analytickú rovnicu pohybu Slnka a hviezdy v z - smere, kde sa predpokladá, že Slnko i hviezda oscilujú okolo galaktického rovníka. Teražšia poloha (30 pc) a rýchlosť (7.3 km/s) sú údaje z literatúry. Riešenie je dané rovnicou 4.26.

8.3.2 Jednoduchý model

Pre uľahčenie našich výpočtov sme navrhli jednoduchý model, ktorý je založený na tom, že relatívny pohyb v smeroch x a y (rovina galaktického rovníka) rovnomerne závisí od času a v z konajú vo všeobecnosti anharmonické oscilácie. Tieto predpoklady sú opísané v rovniciach (4.27). V počiatočných podmienkach pohybu uvažujeme aj konečnú rýchlosť svetla.

8.4 Pohyb Slnka

V tejto časti sme analyzovali pohyb Slnka. Porovnávali sme rozličné metódy na výpočet slnečného pohybu vzhľadom na blízke hviezdy (vzhľadom na LSR -Local Standard of Rest: Miestny štandard pokoja-) priamou metódou (Subsec. 7.1.1) a metódou najmenších štvorcov (7.1.2).

Vedomosti o pohybe Slnka nám umožňujú skúmať dynamiku Galaxie. Slnečné oscilácie môžu mať svoje dôsledky pôsobenia na Oortov oblak, čiže kad informácia o takých osciláciách je dôležitá. Pri orčovaní pohybu Slnka sme vybrali hviezdy do vzdialenosti 100 pc. Použili sme databázu SIMBAD [10]. Hviezdy boli vybrané len

tak, aby mali všetky známe parametre s najvyššou kvalitou. Využitých bolo 769 hviezd. Na výpočet metódou najmenších štvorcov sme použili zjednodušenie dané v [8], ale náš prístup je všeobecnejší ako v [8]. Získali sme 6 nezávislých lineárnych sústav s tromi rovnicami.

Metódy boli aplikované na hviezdy v slnečnom okolí do 100, 40 a 15 pc. Konzistentné výsledky s priamou metódou sú tie, kde vystupuje v_r a μ_δ . Rovnice s kombinovaným v_r , μ_δ , a μ_α nedávajú výsledky konzistentné s priamou metódou. Tiež sme ukázali existujúcu závislosť rýchlosti slnečného pohybu vzhľadom na LSR od veľkosti slnečného okolia (z priamej metódy). Výsledné rýchlosti sú v intervale od 6,1 po 7,7 km/s. Porovnaním s literatúrou vidíme, že to, čo sa normálne používa ako rýchlosť v z - smere sa nachádza v nami nájdenom intervale.

Presnejšie modely galaktickej dynamiky by mali obsahovať aj oscilácie Slnka v rovine kolmej na rovinu galaktického rovníka, ak chceme uvažovať aj vplyv galaktických slapov na Oortov oblak. V závislosti na tom, či uvažujeme harmonické alebo anharmonické oscilácie, a rôzne počiatočné rýchlosti, dostaneme rôzne amplitúdy oscilácií. A keď to aplikujeme na kométy, tak dostaneme rozdielny vývoj orbitálnych elementov komét. Počet návratov kométy do slnečnej sústavy za dobu jej existencie: pre rýchlosť 6,1 km/s máme 12 návratov, pre 7,7 km/s máme 9 návratov, a pre nulovú rýchlosť len 6 návratov. Z toho vychádza, že hmotnosť Oortovho oblaku je (15-60)-krát menšia ako sa predpokladá. V dodatku A sú rovnice získané metódou najmenších štvorcov.

Appendix A

Equations deduced from the Least square method

For arbitrary choice of ϕ , and θ , we get

Coefficients at $\sin^2 \theta \cos^2 \phi$

$$\begin{aligned} 4.74 \sum_{i=1}^N r_i (\mu_{\alpha,i} \cos \delta_i) \sin \alpha_i &= X_S \sum_{i=1}^N \sin^2 \alpha_i \\ &\quad - Y_S \sum_{i=1}^N \cos \alpha_i \sin \alpha_i , \\ - 4.74 \sum_{i=1}^N r_i (\mu_{\alpha,i} \cos \delta_i) \cos \alpha_i &= - X_S \sum_{i=1}^N \sin \alpha_i \cos \alpha_i \\ &\quad + Y_S \sum_{i=1}^N \cos^2 \alpha_i . \end{aligned} \tag{A.1}$$

Coefficients at $\sin^2 \theta \sin \phi \cos \phi$

$$\begin{aligned}
LHS(2,1) &= RHS(2,1) , \\
LHS(2,1) &= 4.74 \sum_{i=1}^N r_i (\mu_{\alpha,i} \cos \delta_i) \cos \alpha_i \sin \delta_i \\
&\quad + 4.74 \sum_{i=1}^N r_i \mu_{\delta,i} \sin \alpha_i , \\
RHS(2,1) &= 2 X_S \sum_{i=1}^N \sin \alpha_i \cos \alpha_i \sin \delta_i \\
&\quad + Y_S \sum_{i=1}^N (\sin^2 \alpha_i - \cos^2 \alpha_i) \sin \delta_i \\
&\quad - Z_S \sum_{i=1}^N \sin \alpha_i \cos \delta_i , \\
LHS(2,2) &= RHS(2,2) , \\
LHS(2,2) &= - 4.74 \sum_{i=1}^N r_i (\mu_{\alpha,i} \cos \delta_i) \sin \alpha_i \sin \delta_i \\
&\quad + 4.74 \sum_{i=1}^N r_i \mu_{\delta,i} \cos \alpha_i , \\
RHS(2,2) &= - X_S \sum_{i=1}^N (\sin^2 \alpha_i - \cos^2 \alpha_i) \sin \delta_i \\
&\quad + 2 Y_S \sum_{i=1}^N \sin \alpha_i \cos \alpha_i \sin \delta_i \\
&\quad - Z_S \sum_{i=1}^N \cos \alpha_i \cos \delta_i , \\
4.74 \sum_{i=1}^N r_i (\mu_{\alpha,i} \cos \delta_i) \cos \delta_i &= X_S \sum_{i=1}^N \sin \alpha_i \cos \delta_i \\
&\quad - Y_S \sum_{i=1}^N \cos \alpha_i \cos \delta_i . \tag{A.2}
\end{aligned}$$

Coefficients at $\sin \theta \cos \theta \sin \phi$

$$\begin{aligned}
LHS(3,1) &= RHS(3,1) \\
LHS(3,1) &= - \sum_{i=1}^N \dot{r}_i \cos \alpha_i \sin \delta_i \\
&\quad + 4.74 \sum_{i=1}^N r_i \mu_{\delta,i} \cos \alpha_i \cos \delta_i \\
RHS(3,1) &= 2 X_S \sum_{i=1}^N \cos^2 \alpha_i \sin \delta_i \cos \delta_i \\
&\quad + 2 Y_S \sum_{i=1}^N \sin \alpha_i \cos \alpha_i \sin \delta_i \cos \delta_i \\
&\quad + Z_S \sum_{i=1}^N (\sin^2 \delta_i - \cos^2 \delta_i) \cos \alpha_i , \\
LHS(3,2) &= RHS(3,2) \\
LHS(3,2) &= - \sum_{i=1}^N \dot{r}_i \sin \alpha_i \sin \delta_i \\
&\quad + 4.74 \sum_{i=1}^N r_i \mu_{\delta,i} \sin \alpha_i \cos \delta_i \\
RHS(3,2) &= 2 X_S \sum_{i=1}^N \sin \alpha_i \cos \alpha_i \sin \delta_i \cos \delta_i \\
&\quad + 2 Y_S \sum_{i=1}^N \sin^2 \alpha_i \sin \delta_i \cos \delta_i \\
&\quad + Z_S \sum_{i=1}^N (\sin^2 \delta_i - \cos^2 \delta_i) \sin \alpha_i , \\
\sum_{i=1}^N \dot{r}_i \cos \delta_i + 4.74 \sum_{i=1}^N r_i \mu_{\delta,i} \sin \delta_i &= - X_S \sum_{i=1}^N (\cos^2 \delta_i - \sin^2 \delta_i) \cos \alpha_i \\
&\quad - Y_S \sum_{i=1}^N (\cos^2 \delta_i - \sin^2 \delta_i) \sin \alpha_i \\
&\quad - 2 Z_S \sum_{i=1}^N \sin \delta_i \cos \delta_i . \tag{A.3}
\end{aligned}$$

Coefficients at $\sin \theta \cos \theta \cos \phi$

$$\begin{aligned}
LHS(4,1) &= RHS(4,1) \\
LHS(4,1) &= - \sum_{i=1}^N \dot{r}_i \sin \alpha_i \\
&\quad + 4.74 \sum_{i=1}^N r_i (\mu_{\alpha,i} \cos \delta_i) \cos \alpha_i \cos \delta_i \\
RHS(4,1) &= 2 X_S \sum_{i=1}^N \sin \alpha_i \cos \alpha_i \cos \delta_i \\
&\quad + Y_S \sum_{i=1}^N (\sin^2 \alpha_i - \cos^2 \alpha_i) \cos \delta_i \\
&\quad + Z_S \sum_{i=1}^N \sin \alpha_i \sin \delta_i , \\
LHS(4,2) &= RHS(4,2) \\
LHS(4,2) &= \sum_{i=1}^N \dot{r}_i \cos \alpha_i \\
&\quad + 4.74 \sum_{i=1}^N r_i (\mu_{\alpha,i} \cos \delta_i) \sin \alpha_i \cos \delta_i \\
RHS(4,2) &= X_S \sum_{i=1}^N (\sin^2 \alpha_i - \cos^2 \alpha_i) \cos \delta_i \\
&\quad - 2 Y_S \sum_{i=1}^N \sin \alpha_i \cos \alpha_i \cos \delta_i \\
&\quad - Z_S \sum_{i=1}^N \cos \alpha_i \sin \delta_i , \\
4.74 \sum_{i=1}^N r_i (\mu_{\alpha,i} \cos \delta_i) \sin \delta_i &= X_S \sum_{i=1}^N \sin \alpha_i \sin \delta_i \\
&\quad - Y_S \sum_{i=1}^N \cos \alpha_i \sin \delta_i . \tag{A.4}
\end{aligned}$$

Coefficients at $\sin^2 \theta \sin^2 \phi$

$$\begin{aligned}
4.74 \sum_{i=1}^N r_i \mu_{\delta,i} \cos \alpha_i \sin \delta_i &= X_S \sum_{i=1}^N \cos^2 \alpha_i \sin^2 \delta_i \\
&+ Y_S \sum_{i=1}^N \sin \alpha_i \cos \alpha_i \sin^2 \delta_i \\
&- Z_S \sum_{i=1}^N \cos \alpha_i \sin \delta_i \cos \delta_i , \\
4.74 \sum_{i=1}^N r_i \mu_{\delta,i} \sin \alpha_i \sin \delta_i &= X_S \sum_{i=1}^N \sin \alpha_i \cos \alpha_i \sin^2 \delta_i \\
&+ Y_S \sum_{i=1}^N \sin^2 \alpha_i \sin^2 \delta_i \\
&- Z_S \sum_{i=1}^N \sin \alpha_i \sin \delta_i \cos \delta_i , \\
- 4.74 \sum_{i=1}^N r_i \mu_{\delta,i} \cos \delta_i &= - X_S \sum_{i=1}^N \cos \alpha_i \sin \delta_i \cos \delta_i \\
&- Y_S \sum_{i=1}^N \sin \alpha_i \sin \delta_i \cos \delta_i \\
&+ Z_S \sum_{i=1}^N \cos^2 \delta_i . \tag{A.5}
\end{aligned}$$

Coefficients at $\cos^2 \theta$

$$\begin{aligned}
- \sum_{i=1}^N \dot{r}_i \cos \alpha_i \cos \delta_i &= X_S \sum_{i=1}^N \cos^2 \alpha_i \cos^2 \delta_i + Y_S \sum_{i=1}^N \sin \alpha_i \cos \alpha_i \cos^2 \delta_i \\
&+ Z_S \sum_{i=1}^N \cos \alpha_i \sin \delta_i \cos \delta_i , \\
- \sum_{i=1}^N \dot{r}_i \sin \alpha_i \cos \delta_i &= X_S \sum_{i=1}^N \sin \alpha_i \cos \alpha_i \cos^2 \delta_i \\
&+ Y_S \sum_{i=1}^N \sin^2 \alpha_i \cos^2 \delta_i + Z_S \sum_{i=1}^N \sin \alpha_i \sin \delta_i \cos \delta_i , \\
- \sum_{i=1}^N \dot{r}_i \sin \delta_i &= X_S \sum_{i=1}^N \cos \alpha_i \sin \delta_i \cos \delta_i + Y_S \sum_{i=1}^N \sin \alpha_i \sin \delta_i \cos \delta_i \\
&+ Z_S \sum_{i=1}^N \sin^2 \delta_i . \tag{A.6}
\end{aligned}$$

Bibliography

- [1] Choudhuri A. *Astrophysics for Physicists*. Cambridge University Press, Cambridge, pp. 490, 2010.
- [2] Dybczyński P. A. Simulating observable comets. *Astronomy and Astrophysics*, 449:1233–1242, 2005.
- [3] Dauphole B., Colin J., Geffert M., Odenkirchen M., and Tucholke H.J. The mass distribution of the milky way deduced from globular cluster dynamics. In *Unsolved Problems of the Milkyway*, 1996.
- [4] Ryden B. and Peterson B. M. *Foundations of Astrophysics*. Addison-Wesley, San Francisco, pp. 596, 2010.
- [5] Frisch P. C., Dorschner J. M., Geiss J., Mayo Greenberg J., Grun E., Landgraf M., Hoppe P., Jones A. P., Kratschmer W., Linde T. J., Morfill G. E., Reach W., Slavin J. D., Svestka J., Witt A. N., and Zank G. P. Dust in the local interstellar wind. *The Astrophysical Journal*, 525(1):492–516, 1999.
- [6] Landau L. D. and Lifshitz E.M. *Mechanics (Course of Theoretical Physics)*. Butterworth-Heinemann, Oxford, pp. 198, 1998.
- [7] Maoz D. *Astrophysics in a Nutshell*. Princeton University Press, Princeton, 2007.
- [8] Mihalas D. and McRae-Routly P. *Galactic Astronomy*. W. H. Freeman and Company, San Francisco, pp. 257, 1968.
- [9] Strauch D. *Classical Mechanics: An Introduction*. Springer-Verlag, Berlin, pp. 405, 2009.
- [10] Centre de Données astronomiques de Strasbourg. *SIMBAD Astronomical Database*, 2010. <http://simbad.u-strasbg.fr/simbad/>.

- [11] Wilson R. E. General catalogue of stellar radial velocities. *DC: Carnegie Institute of Washington*, 1953.
- [12] Kulikovskij P. G. *Stellar Astronomy (in Russian)*. Nauka, Moscow, pp. 272, 1985.
- [13] Luther G. G. and Towler W. R. Redetermination of the newtonian gravitational constant g . *Phys. Rev. Lett.*, 48(3):121–123, 1982.
- [14] Oort J. H. The structure of the cloud of comets surrounding the solar system and a hypothesis concerning its origin. *Bull. Astron. Inst. Neth.*, 11:91–110, 1950.
- [15] Astronomisches Rechen-Institut Heidelberg. *ARICNS Ari Data Base for Nearby Stars*, 2010. <http://www.ari.uni-heidelberg/datenbanken/aricns/>.
- [16] Collins G. W. II. *The Foundations of Celestial Mechanics*. Pachart Foundation dba, pp. 145, 2004.
- [17] Binney J. and Merrifield M. *Galactic Astronomy*. Princeton University Press, Princeton, pp. 796, 1998.
- [18] Garcia-Sanchez J., Preston R. A., Jones D. L., Weissman P. R., Lestrade J. F., Latham D. W., and Stefanik R. P. Stellar encounters with the oort cloud based on hipparcos data. *The Astronomical Journal*, 117:1042–1055, 1999.
- [19] Klačka J. Galactic tide. *arXiv:0912.3112v2[astro-ph.GA]*, 2009.
- [20] Stauffer J., Tanner A. M., Bryden G., Ramirez S., Berriman B., Ciardi D. R., Kane S. R., Mizusawa T., Payne A., P. Plavchan, von Braun K., Wyatt P., and Kirkpatrick J. D. Accurate coordinates and 2mass cross identifications for (almost) all gliese catalog star. *The Astronomical Society of the Pacific*, 122:885–897, 2010.
- [21] Komar L., Klacka J., and Pastor P. Galactic tide and orbital evolution of comets. *arXiv: 0912. 3447v2[astro-ph. EP]*, 2009.
- [22] Landgraf M. Modeling the motion and distribution of interstellar gas inside the heliosphere. *J. Geophys. Res.*, 105:10303–10316, 2000.
- [23] Witte M., Banaszkiewicz M., and Rosenbauer H. Recent results on the parameters of the interstellar helium from the Ulysses/gas experiment. *Space Science Reviews*, 78:289–296, 1996.

- [24] Lallement R. Relations between ism inside and outside the heliosphere. *Space Science Reviews*, 78:361–374, 1996.
- [25] Martin B. R. *Nuclear and Particle Physics: An Introduction*. John Wiley & Sons, Chichester, pp. 453, 2009.
- [26] Symon K. R. *Mechanics*. Addison-Wesley, Reading, Massachusetts, pp. 551, 1970.
- [27] Taylor J. R. *Classical Mechanics*. University Science Books, Sausalito, pp. 786, 2005.
- [28] Liang-Cheng Tu, Qing Li, Qing-Lan Wang, Cheng-Gang Shao, Shan-Qing Yang, Lin-Xia Liu, Qi Liu, and Jun Luo. New determination of the gravitational constant g with time-of-swing method. *Phys. Rev. D*, 82(2):022001, 2010.
- [29] Dehnen W. and Binney J. Local stellar kinematics from hipparcos data. *Mon. Not. R. Astron. Soc.*, 298:387–394, 1998.